FRP Dowels for Concrete Pavements

By

Darren Eddie, EIT

A Thesis
Presented to the University of Manitoba
in Partial Fulfillment of the
Requirements for the Degree of

Master of Science

Department of Civil and Geological Engineering
University of Manitoba
Winnipeg, Manitoba
March 31, 1999

THE UNIVERSITY OF MANITOBA

FACULTY OF GRADUATE STUDIES

*****

COPYRIGHT PERMISSION PAGE

FRP DOWELS FOR CONCRETE PAVEMENTS

BY

DARREN EDDIE

A Thesis/Practicum submitted to the Faculty of Graduate Studies of The University of Manitoba in partial fulfillment of the requirements of the degree

of

MASTER OF SCIENCE

Abstract

Steel dowels currently used for highway pavement could cause severe deterioration of concrete highway pavements due to the expansion of steel during the corrosion process. A corrosion-free alternative, such as Fiber Reinforced Polymer (FRP) dowels, could provide a promising solution to extend the service life of concrete pavements.

FRP materials have exceptionally high tensile strength in the direction of the fibers, however, it has a relatively low strength in the perpendicular direction. In order to study the behaviour of FRP dowels and compare their behaviour to conventional epoxy-coated steel dowels, an experimental program was undertaken at the University of Manitoba. A total of twelve full-scale models representing a section of highway pavement slab were tested. The specimens included two dowels of either Glass Fibre Reinforced Polymer (GFRP) dowels or conventional epoxy-coated steel dowels. The slab/joint system was placed on a simulated base that provides two levels of stiffness conditions. The joint was tested under an equivalent AASHTO half axle truck load.

The specimens were tested under static and cyclic loading conditions using a servohydraulic MTS loading system. Nine slabs were tested to determine the joint effectiveness under static loads while the remaining three slabs were tested under cyclic loading to examine the behaviour under repeated loads. The dowel materials within the slab/joint systems were epoxy-coated steel, as well as two products of Glass FRP. This thesis summarizes the test setup, test results, and the recommendation for the use of GFRP dowels for concrete pavements including a discussion on the first in field application of GFRP dowels in Canada.

Acknowledgements

This project would not have been possible without the help of certain key individuals. I would like to thank Dr. S. Rizkalla, Department of Civil Engineering at the University of Manitoba and President of ISIS Canada, for proposing the project, and for providing his assistance and direction throughout the project. Two other important individuals, Mr. S. Kass and Mr. S. Hilderman, both from the Manitoba Department of Highways and Transportation, were instrumental in initiating this project. The funding provided by the Canadian Network Centre of Excellence on Intelligent Sensing for Innovative Structures, ISIS Canada and Manitoba Department of Highways and Transportation are greatly appreciated.

There were many others that have helped providing ideas and guidance throughout this testing program. I wish to thank Dr. A. Shalaby, Department of Civil Engineering at the University of Manitoba, and Dr. A. Abdelrahman, Post-Doctoral Fellow at the University of Manitoba, for all the time they took with me during their busy schedules. I would like to thank Mr. Moray McVey, ISIS Canada technician at the University of Manitoba, for providing the insight, ingenuity, and manpower necessary to complete all phases of this testing program. I also thank Scott Sparrow, Structural Engineering lab technician, for all his time and patience.

The final phase of this project would not have been possible without the work of a determined undergraduate student, Mike Stoyko. Mike not only helped me with a large portion of the final phase but also used the data gathered to create his own undergraduate thesis. Some of my fellow graduate students also need to be recognized for all their

efforts during the project, from help during multiple castings to recording data during tests. These students are Ryan Morphy, Haney Louka, David Donald, Alieu Jawara, and Brea Williams. There have also been a few undergraduate students who worked in the structural lab during the summers that need to be thanked. These students are: Natalie Rizkalla, Bart Flisak, and Grant Horezce.

I would also like to express my loving thanks to my wife, Trina Mathison, whose support during this process was invaluable. She was there at every step providing me with encouragement even whilst completing her own studies in medicine and bringing a child into this world.

Table of Contents

List of Figures

List of Tables

Chapter 1 Introduction

1.1 General

Joints are used in concrete pavements in order to control cracking due to thermal and environmental conditions. Joints may be parallel to traffic, longitudinal joints, or perpendicular to traffic, transverse joints. There are three types of transverse joints that are typically used in concrete pavements: contraction joints, construction joints, and expansion or isolation joints. Contraction and construction joints are very similar in their function of controlling the crack patterns in concrete pavement. Expansion and isolation joints are generally used to isolate the slab from adjacent structures such as bridge abutments and manholes.

Dowels are commonly used to transfer load from one slab to an adjacent slab and to provide vertical and horizontal alignment. Currently, smooth epoxy coated steel dowels are placed across a transverse joint to transfer load and to allow for longitudinal thermal expansion and contraction.

Corrosion of steel dowels causes severe deterioration of the concrete highway pavement due to the expansion of steel during the corrosion process. Expansion of the steel dowels induces significant stresses in the concrete around the dowel at the joint and therefore inhibits joint movement. This 'freezing' or 'binding' of the joint can create large stresses, sufficient to cause cracking and spalling of the concrete. This also causes a reduction of the load that the joint can transfer. In an attempt to reduce the effect of de-icing salts on dowels, epoxy coated steel dowels are used. The thin layer of epoxy is effective only if there are no nicks, cracks, or other abrasions in the coating.

Construction practices require careful handling and storage of the coated dowels. Small defects inevitably occur in the epoxy coat. Thus, corrosion remains a problem with the epoxy coated steel dowels and therefore, a better solution must be found.

Fiber reinforced polymer (FRP) dowels could provide an alternative solution to steel dowels due to their corrosion-free characteristics. There are several manufacturers in the United States and Canada that produce glass FRP at a comparative cost with epoxy-coated steel. FRP material is known for its high ultimate tensile strength in the direction of the fibers, however, it has a relatively low strength perpendicular to the fibers. An experimental study was conducted at the University of Manitoba to provide data on the behaviour and performance of FRP dowels for concrete highway pavement joints.

1.2 Objective

The objective of this research was to investigate the behaviour of FRP dowels for transverse construction joints of a concrete highway pavement under the effect of typical traffic loading conditions. The behaviour of glass fiber reinforced polymer (GFRP) dowels is compared to that of epoxy coated steel dowels. Two different types of GFRP dowels are used in this investigation; Glasform dowels produced by Glasform Inc. in San Jose, California and FiberDowels produced by RJD Industries in Laguna Hills, California.

1.3 Scope

This research encompasses testing of GFRP and steel dowels using a scaled model of a concrete pavement slab section subjected to static and cyclic loads. The

scaled model represents a portion of a full thickness, 254 mm (10 in.), concrete pavement slab with a limited length, 2440 mm (8 ft.), and width, 610 mm (2 ft.). A simulated half axle truck load was applied on one side of the joint until failure.

The research program consisted of testing twelve slab specimens. The first nine were tested under monotonic load whereas the final three slabs were tested under cyclic loading conditions. The first nine slabs are divided into two phases, three slabs in the first phase and six in the second. Considered in this program are the level of subgrade support and the type of dowel material.

Chapter 2 Literature Review

2.1 Highway pavements

Highway pavement should provide the best combination of ride quality, strength, durability, and economy. Casting concrete pavements directly on the subgrade causes severe deterioration and leads to failure at an early stage. The use of a stiffer subbase system placed on top of the properly compacted subgrade provides a stable support for concrete pavement. Within the pavement, joints are provided to control thermal cracking at designated locations. At these locations, dowels are used to provide the necessary load transfer and rigidity of the joints.

2.1.1 Concrete and Jointing

Typically, plain concrete has been used for highway pavements in Manitoba. The strength of the concrete is generally in the range of 30 MPa (4350 psi) with a maximum aggregate size of approximately 16 mm (5/8 in). The specified slump is 60 mm (2.4 in) and since the pavement is not reinforced, the workability or flow of the concrete is not as important as the case of reinforced concrete structures.

The depth of pavements may range from 200 mm to 350 mm (8 in to 14 in) depending on the projected traffic loads on the highway. The width of the traffic lane may vary from 3.5 m to 4.5 m (11.5 ft to 15 ft), resulting in a total width of the pavement ranging from 7 m to 9 m (23 ft to 30 ft) wide.

During the curing process of concrete pavements, stresses created by thermal gradients experienced from the environment as well as the concrete hydration, can create random cracking of the concrete. In order to control and reduce the randomness of the

cracking, joints are introduced into the pavement. Joints are generally placed in both the longitudinal and the transverse directions of the pavement.

Joints can be created in a number of ways: providing a groove, saw cutting, or butting. The most commonly used method is the saw cut. Cutting through one third of the slab thickness creates the concrete pavement joint. During the curing process, the joint behaves as a controlled crack location and the crack initiated by the cut propagates through the remainder of the slab under shrinkage and thermally induced stresses as shown in Figure 2-1.

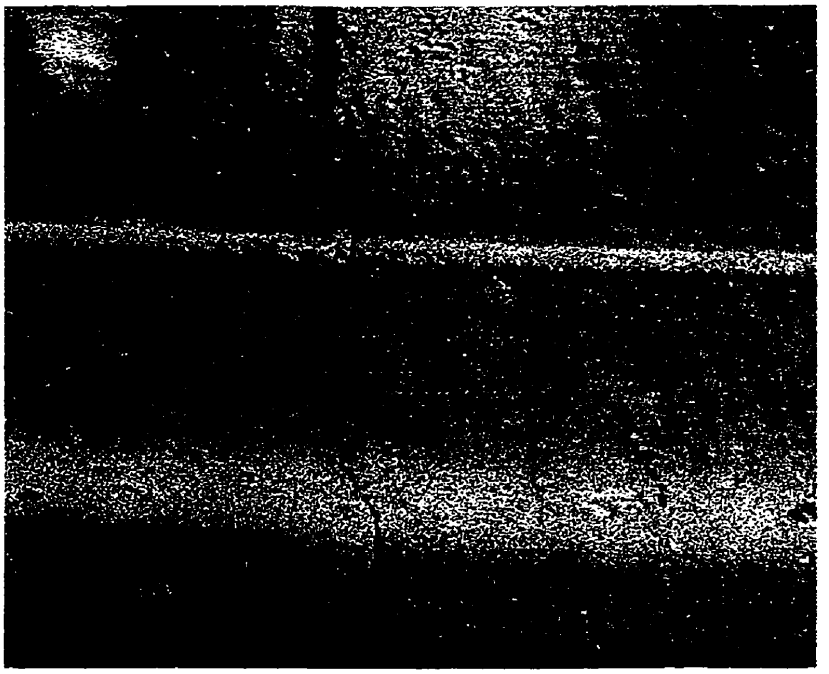

Figure 2-1: Crack propagation leading from saw cut

For classification purposes, joints are divided into four types depending upon their primary function. The classifications are: transverse contraction joints, transverse construction joints, longitudinal joints, and isolation or expansion joints. The type and function of each joint is described briefly in the following sections and illustrated in Figure 2-2.

2.1.1.1 Transverse Contraction Joints

Contraction joints are constructed by cutting a third of the depth of the concrete slab, perpendicular to the traffic flow. The primary function is to supply a stress relief point where cracking will occur due to thermal stresses during curing. During service life, their main function is to transfer load from one side of the joint to the other, and to provide alignment of the slab. Load transfer is accomplished by using dowels and aggregate interlock of the remaining two-thirds of the concrete slab depth.

2.1.1.2 Transverse Construction Joints

The functions of these types of joints are the same as the transverse contraction joints, to transfer load across the joint. The main difference in this type of joint is the way in which it is produced. Construction joints are only created when casting is interrupted for a prolonged period of time, for example, overnight. A board, or sheet metal, is placed to create a smooth surface on which the concrete cast later would be butted against. Another alternative is to cast concrete past the location of the joint and to cut through the depth of concrete prior to the new cast therefore creating a smooth surface. This joint does not develop aggregate interlock and is dependent only upon the dowels located across the joint. The best location to make a construction joint is where a transverse contraction joint is already planned, thus maintaining desired joint spacing.

2.1.1.3 Longitudinal Joints

Longitudinal joints are parallel to the direction of traffic flow. They provide a separation of the traffic lanes along a highway. Their function is to control longitudinal cracking by providing stress relief and to provide alignment and connection between highway lanes. These joints can either be doweled with smooth or deformed bars, or

contain a concrete key system to transfer load. In most cases a combination of a keyed joint with deformed rebars are used to provide the necessary alignment and load transfer.

2.1.1.4 Isolation and Expansion Joints

Isolation joints are placed to isolate one structure from another. The objective is to protect adjacent structures from being damaged by large compressive forces. Isolation joints are normally 12 mm to 25 mm (1/2 in to 1 in) wide to allow for large horizontal and vertical movements.

Expansion joints have a different function from isolation joints but the two are commonly grouped together. They are especially useful when casting takes place at low temperatures and eventual expansion is expected.

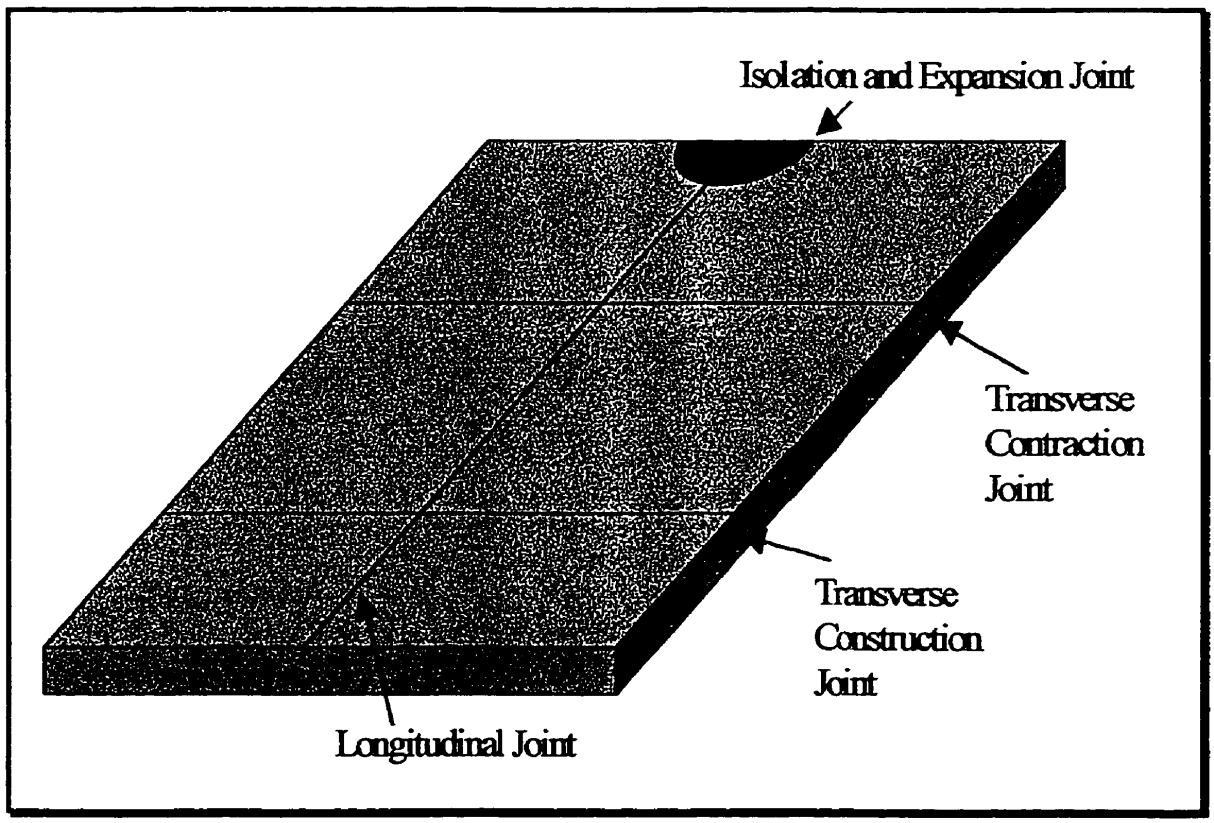

Figure 2-2: Joint types and arrangement

2.1.1.5 Joint Spacing

Joint spacing is based upon crack patterns that have been experienced and observed over the past 50 years of highway pavement construction. Currently, transverse joints are placed at 3 m to 6 m (10 ft to 20 ft) apart. Some highway agencies use different joint configurations. The Manitoba Department of Highways and Transportation uses an alternating spacing of 4 m (13 ft), 5.2 m (17 ft), 5.5 m (18 ft), and 3.7 m (12 ft). Another alteration that some departments use is the skewing of the joint from the perpendicular. The dowel alignment is still parallel to the direction of travel but the ride harmonics for the travelling vehicles are changed and most importantly, the simultaneous wheel loading at the joint is eliminated. Recent studies have shown that there are no real advantages in joint effectiveness when using skewed joints.

2.1.1.6 Joint Movement

Concrete pavements experience many cycles of temperature changes during their service life. The joints created within the concrete pavement control cracking due to temperature changes. To determine the change in length of a concrete slab due to a change in temperature, Equation 2-1 may be used.

$$\Delta L = CL(\alpha \Delta T + \varepsilon) \qquad \text{Equation 2-1}$$

where C is the frictional restraint (normally 0.65 for stabilized material, 0.80 for granular), L is slab length, α is the thermal expansion coefficient of Portland Cement Concrete in the range of $10\text{-}12 \times 10^{-6}$ $(C°)^{-1}$, ΔT is the maximum temperature change, and ε is the shrinkage strain in the range of 200×10^{-6}.

2.1.1.7 Joint Effectiveness

The American Concrete Paving Association (ACPA) provides information on concrete pavements used for street and highway construction. In order to determine the usefulness of a concrete highway joint, ACPA uses Joint Effectiveness to measure the performance of the joints. If a joint is 100 percent effective, the deflections on both sides of the joint are equal due to the sharing of the applied load. Zero percent effectiveness means the unloaded side is experiencing no deflection at any specific load level. The measure of Joint Effectiveness is based upon the measured deflections of the loaded and unloaded side of the joint as given in Equation 2-2.

$$E = \frac{2d_u}{d_l + d_u} \times 100 \qquad \text{Equation 2-2}$$

where E is the joint effectiveness, d_u is the deflection on the side of the joint without the direct application of load or the unloaded deflection, and d_l is the deflection on the loaded side. A joint is considered adequate if the effectiveness is 75 percent or greater.

2.1.2 Loading

The size and weight regulations are determined by government bodies to ensure safety of highway and bridge operations. Some of these agencies and their codes are: American Association of State Highway and Transportation Officials (AASHTO), Regional Transportation Association of Canada (RTAC), and the Ontario Bridge Code (OBC). In Table 2-1, the current maximum axle loads, maximum single tire or half axle loads, and their tire contact areas are given for each agency.

Table 2-1: Weight and area requirements for tire loadings

Agency	Maximum Axle Load kN (kips)	Maximum 1/2 Axle Load kN (kips)	Tire Area m^2 (in^2)
AASHTO	214 (48)	107 (24)	
RTAC	90 (20)	45 (10)	
OBC	200 (45)	100 (22.5)	0.15 (240)

2.1.2.1 Load frequency

Pavement design requires information on axle loads and frequency. The Manitoba Department of Highways and Transportation regularly places counters and weigh scales at key locations of their highway network. These counters are able to record the number of times that tires cross over a pneumatic tube. To complete this data, the breakdown between multi-axle vehicles and dual-axle vehicles needs to be determined. These values are then compiled and are accessible to the public and could also be obtained from the homepage of the University of Manitoba Transportation Information Group (UMTIG).

2.1.2.2 Load Transfer

The load transfer is based upon the effectiveness with which a joint can transfer the applied load to an adjacent slab. Under ideal conditions, one half of the applied load are assumed to be transferred. Poor joints, providing inadequate alignment, experience cracking and consequently, will have a less effective load transfer. The transfer of loads is shared between the dowels and aggregate interlock.

2.1.2.3 Aggregate Interlock

Aggregate interlock is based upon the friction and bearing of aggregates against each other as a shearing force is attempting to propagate a crack. Rough aggregates, like

crushed stone, have high friction coefficients and provide good interlock. In contrast, natural gravel, or those that have been weathered and have polished surfaces, are not as effective in providing interlocking characteristics.

Aggregate interlock becomes ineffective when the space between joint surfaces is large enough that the aggregates are no longer in contact with each other. This is the case when a concrete joint experiences tensile or contraction stresses that reduce the joints capabilities for load transfer. It is also ineffective when the aggregates are not interlocked as in the case of construction joints.

2.1.2.4 Dowel Action

Dowel action is the mechanism by which the dowels transfer load. In the presence of a separation or gap between the two structures, the dowel has the ability to move when stress is applied. The three modes of the mechanism that can develop at the joint are flexure, shear, and kinking as shown in Figure 2-3.

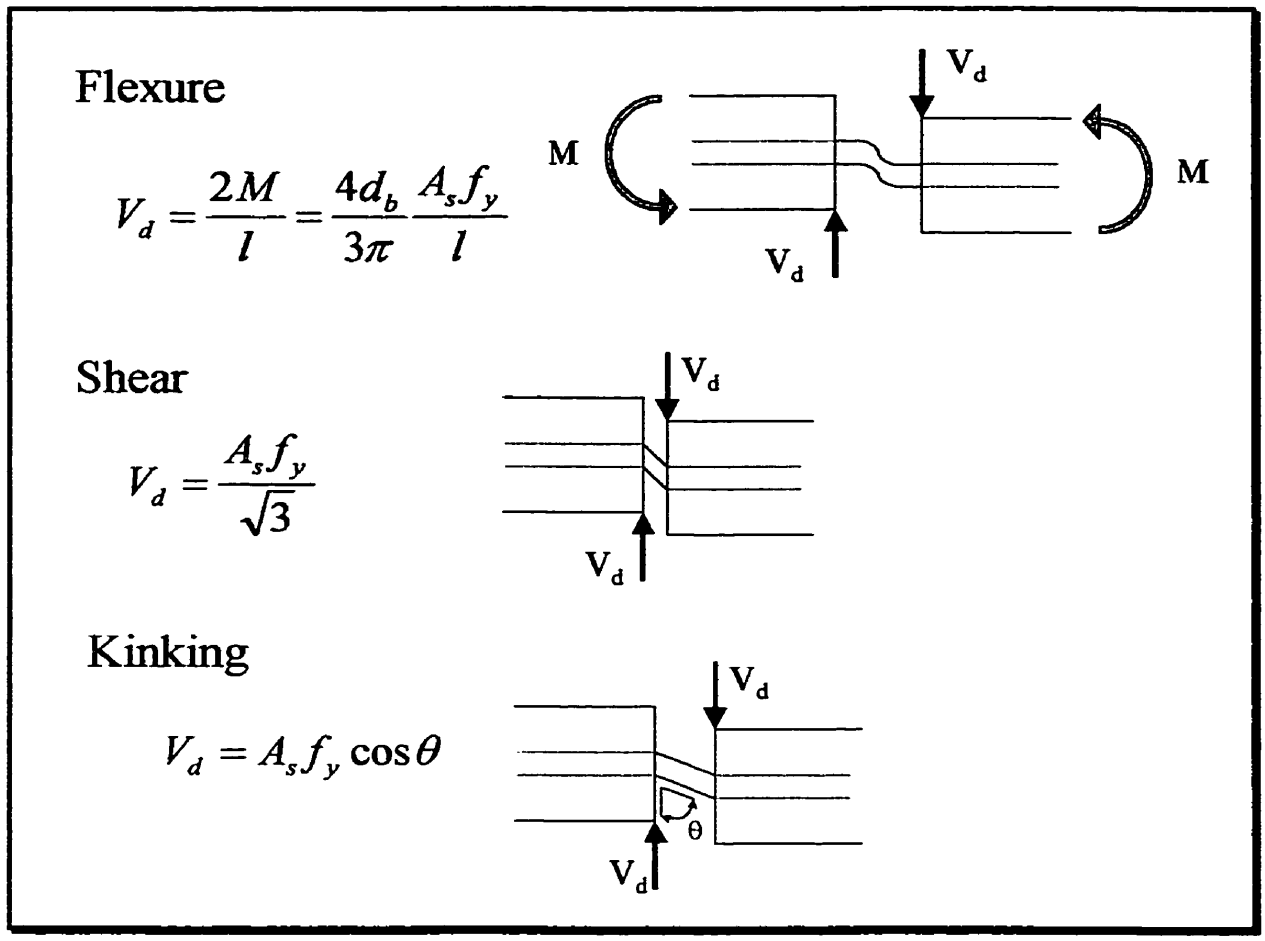

Figure 2-3: Dowel Action Mechanisms

where V_d is the shear strength of the dowels, M is the plastic moment of the dowel, l is the length of the joint gap, d_b is the dowel diameter, A_s is the total area of the steel crossing the shear plane, f_y is the yield strength of the steel, and θ is the kinking angle.

2.1.3 Road Base

In order to reduce the cost of highway construction, a compacted base is normally used to transfer the traffic loads to the subgrade and reduce the thickness of the concrete pavement. Therefore, by providing a rigid and stable base for the pavement, cracking,

deformations, and deterioration could be reduced. It was found that the more stable the subbase, the more stable the concrete pavement, thereby prolonging its life.

A compacted base is placed upon the subgrade to provide a buffer between the applied load and the weaker subgrade material. The base allows for the stress to be spread over a larger bearing area of the subgrade. Typically, the Manitoba Department of Highways and Transportation provide a base system, as shown in Figure 2-4, consisting of: 100 mm (4 in) 'A Base', and 200 mm (8 in) 'C Base'. Each layer is compacted during the construction process. Initially the subgrade will be compacted to 20 MPa (2900 psi), then the 'C Base' will be applied and compacted to 200 MPa (29 ksi), followed by the final topping of 'A Base' compacted as well to 200 MPa (29 ksi). (Hilderman 1997)

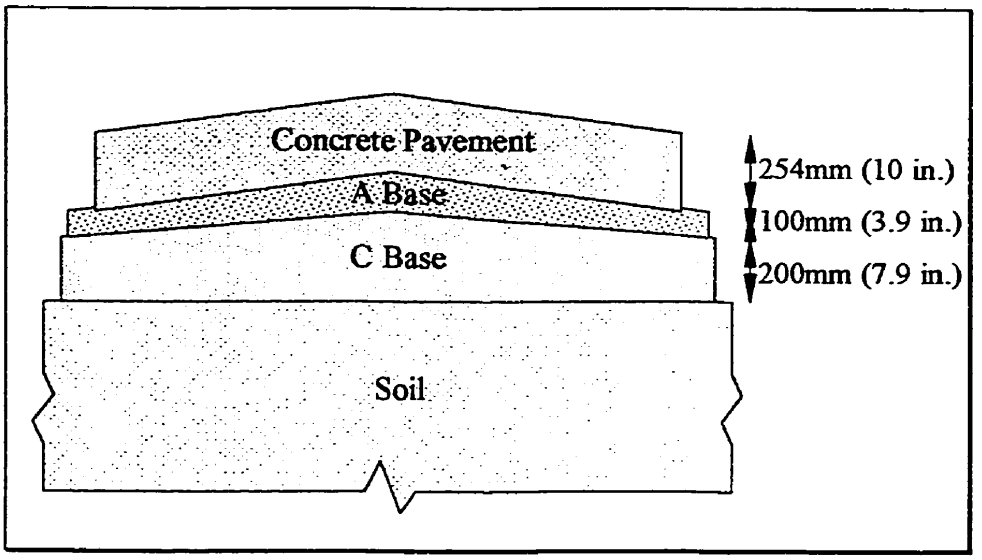

Figure 2-4: Soil and base layers underneath the concrete pavement

Compaction is required to stabilize the material and is accomplished by passing vibrating or static rollers and watering trucks over the base material. Water is added to the base material to provide lubrication and reach the optimum compaction level. It is better to add moisture to stabilize the material during construction than for the material to

attain moisture from the environment over time that could cause shrinkage or expansion of the material. Once the base material has been compacted, readings can be taken to determine the water content and the percent of compaction compared to a laboratory standard.

2.1.3.1 Subgrade Modulus

In order to model a subgrade, assumptions had to be made to determine whether soil behaved in a linear or non-linear elastic manner. Winkler (1867) provided a simple model of the linear elastic soil behaviour. A linear relationship between load and displacement using a stiffness modulus k, is given in Equation 2-3:

$$q = k\Delta \qquad \text{Equation 2-3}$$

where q is the stress applied to a point, Δ is the vertical deflection, and k is the subgrade modulus. Winkler's model considered that no displacement occurred outside the loaded area and therefore could be modeled with simple linear spring elements with k representing the spring constant over an area.

Winkler's model lacked the continuity at the boundary of the loaded area. Other models representing soil continuum behaviour were developed by Filoneko-Borodich (1940-45) and Hetenyi (1946). These models provided continuity between spring elements by modeling a type of membrane, plate, or beam element, which connects the spring elements together. This method provided a more representative soil deformation outside of the loaded area.

The common factor in the above models was the use of the modulus of subgrade reaction. This measure of subgrade stiffness allowed the designers to estimate the loading conditions that the soil could support. A study by Terzaghi (1955) provided

numerical values for *k*, which are still used in soil-structure interaction calculations, as given in Table 2-2. Terzaghi determined that *k* is not a unique characteristic of the soil itself. In performing many plate bearing tests, it was determined that plate size and shape, as well as the depth of embedment affected the calculated value of the subgrade modulus. It was also noted that the soil was subjected to irreversible deflections which illustrated a plastic deformation instead of the assumed elastic behaviour.

Table 2-2: Modulus of Subgrade Reaction (Terzaghi 1955)

Reference	Type of Soil	Loose [kN/m^3] [(tons/ft^3)]	Medium [kN/m^3] [(tons/ft^3)]	Dense [kN/m^3] [(tons/ft^3)]
Terzaghi (1955)	Dry or Moist Sand	6.3-18.9x10^3 (20-60)	18.9-94.3 x10^3 (60-300)	94.3-314.2 x10^3 (300-1000)
Miner and Seastone (1955)	Gravel and Gravelly soils			135-190x10^3 (430-605)

It was determined by Teller and Cashell (1958) that the expected load transfer efficiency will be reduced with an increase of the modulus of subgrade reaction. They suggested that "a dowel will show its highest effectiveness on a flexible subgrade where it is needed, and its lowest effectiveness on a stiff subgrade where it is not needed".

2.2 Dowels

Dowels are required to transfer the load across the joint and to provide alignment of concrete pavements. Dowels are used to provide load transfer and to provide a smooth and safer ride as shown in Figure 2-5.

Certain factors should be considered for the design of dowels in concrete pavements. Two of the important factors are spacing and diameter of the dowels. Each dowel should provide the ability to transfer load over its designated tributary area.

Because of flexibility of the subgrade, a group action develops and the load is transferred by multiple dowels. Adjacent dowels will contribute to the load transfer and this is referred to as dowel group action.

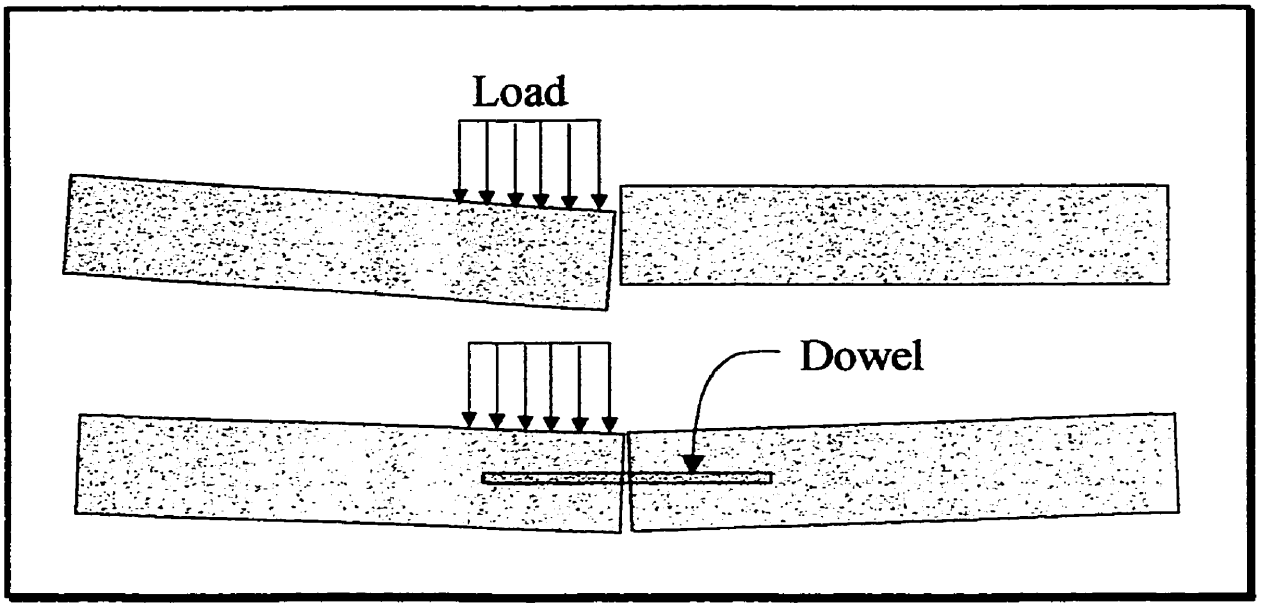

Figure 2-5: Positive effect of dowel load transfer

Another important factor affecting the overall behaviour of the joint is the embedment length of the dowels. The effect was studied by Timoshenko and Friberg (1938) using an infinite and finite bar surrounded by an elastic mass. Friberg showed that the moment in the dowel drops rapidly with the distance from the joint face therefore no dowel is required after the moments' second point of contraflexure. This is illustrated in Figure 2-6. Timoshenko introduced Equation 2-4, for the deflection of an elastic structure.

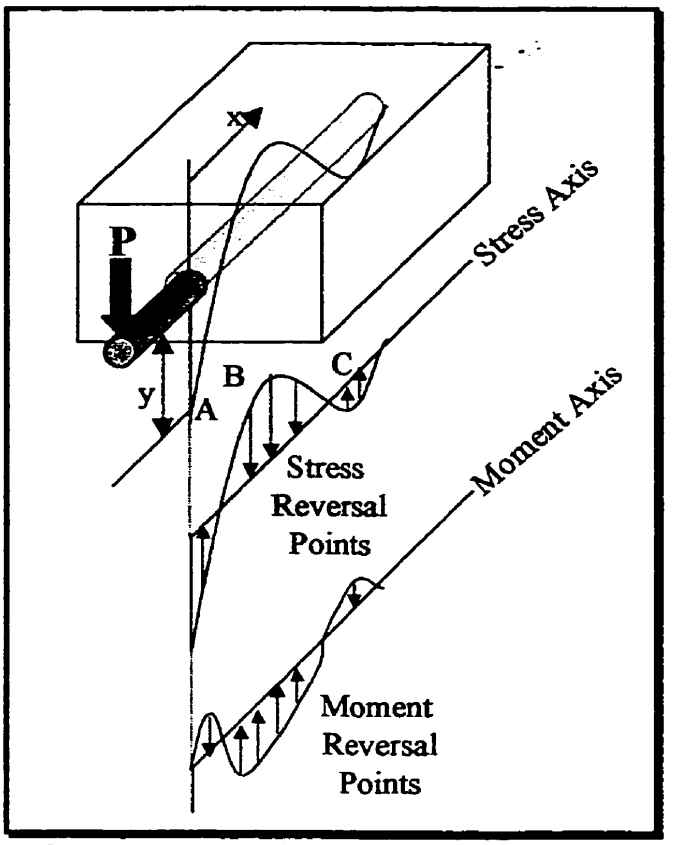

Figure 2-6: Contact stress and moment along a dowel within a slab

$$y = \frac{e^{-\beta x}}{2\beta^3 EI}\{P\cos\beta x - \beta M_o(\cos\beta x - \sin\beta x)\}$$ Equation 2-4

where x is distance along dowel from the face of the concrete, M_o is the bending moment at the face of the concrete, P is the transferred load, and EI is the flexural rigidity. β is the relative stiffness of the bar to the concrete and is given by Equation 2-5.

$$\beta = \left(\frac{kb}{4EI}\right)^{\frac{1}{4}}$$ Equation 2-5

where b is the diameter of the dowel, and k is the modulus of dowel support. The modulus of dowel support is defined as the pressure required to cause 25.4 mm (1 in) displacement in the support material.

During the construction process, it is important to note that the dowels remain in parallel alignment. If the dowels become non-parallel, the joint will 'freeze' or 'bind'. The joint must be free to expand and contract due to temperature and moisture changes. When the dowels are not in alignment stresses may be induced due to the imposed restraint and could cause cracking of the concrete pavement at the joint.

2.3 Research on the use of FRP Dowels

2.3.1 FRP Dowel Bars in Reinforced Concrete Pavements

Brown and Bartholomew, at Widener University in Chester, Pa., conducted an experimental program using 508 mm (20 in) wide, 914 mm (36 in) long, and 102 mm (4 in) thick slab with a 6.4 mm (1/4 in) joint at the mid-length. The diameter of the dowels used was 12.7 mm (1/2 in) to match 1/8th scale of the slab thickness. The dimensions of the specimens were controlled by the limitations of the testing facilities.

The slab was supported by a subgrade/subbase system without consideration of the field subgrade conditions. The system consisted of 200 mm (8 in) of expanded polystyrene foam for the subgrade, covered by 100mm (4 in) of 19 mm (3/4 in) crushed stone to act as subbase. This system was used throughout the testing program to compare the load transfer efficiency of the different materials used in the testing program.

The program included square and round GFRP bars as well as steel bars. The general mode of failure observed was the propagation of a crack within the concrete perpendicular to the joint. The failure load was approximately the same for the tested specimens regardless if the type of dowel were the grade 60 steel dowels or either type of the E-Glass dowels. The two types of E-Glass dowels contained either a vinyl ester resin or isopthalic polyester resin. Test results indicated that square GFRP dowels were less

efficient in comparison to round GFRP and steel bars. The researchers concluded that increasing the diameter of the GFRP dowels by 20 to 30 percent could match the same transfer efficiencies of steel bars.

2.3.2 GFRP Dowel Bars for Concrete Pavement

An experimental program was conducted at the University of Manitoba to investigate the feasibility of using GFRP in concrete pavements, Grieef (1996). The study concentrated on the strength characteristics of the GFRP material in comparison to steel and also a life cycle cost analysis to determine the benefits of using GFRP dowels.

One type of GFRP material was used and compared to the behaviour of steel. The dowels were produced by Pultrall Inc., in Thetford Mines, QC and is known commercially as Isorod. The Isorod dowels were 450 mm (18 in) long and had a diameter of 19 mm (3/4 in).

Concrete push-off specimens were designed to determine the dowels capacity in direct shear. The specimens consisted of two 'L'-shaped concrete panels orientated to apply direct single shear on the dowels as shown in Figure 2-7. The joint width, between the two concrete surfaces, was 12.7 mm (1/2 in). Two dowels, were used for each specimen to cross the joint. These dowels were placed perpendicular to the applied load and therefore were loaded in direct shear.

A total of eight specimens were tested in this program which included four specimens using Isorod GFRP dowels. Two of the four Isorod dowel specimens contained dowels that were partially bonded while the remaining two were not bonded.

The test results showed kinking behaviour at the dowels causing an inward movement of the panels toward each other. In comparison with the steel dowels, the

Isorod dowels carry about one third of the load of the steel before failure. It could be shown that bonding of one side of the dowels increased the load carrying capacity 3.8 percent for the steel dowels and 7 percent for the Isorod dowels. The displacement of the joints increased for the unbonded specimen, by 15 percent for the steel and 8 percent for the Isorod.

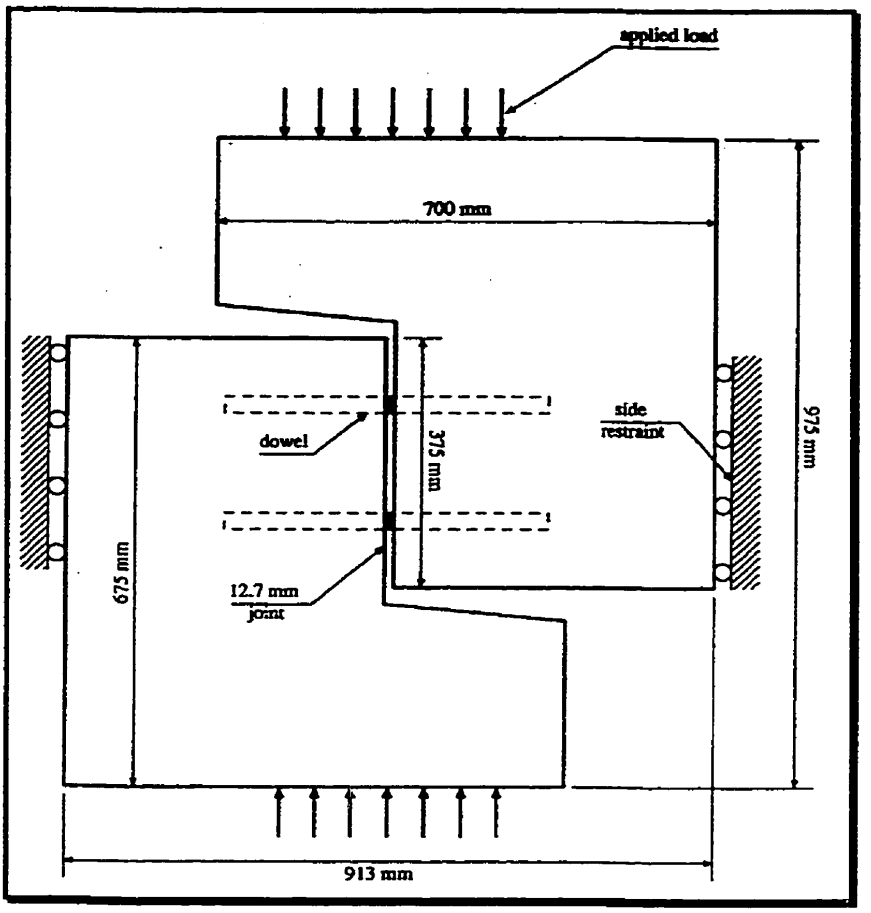

Figure 2-7: Push-off specimen

The conclusions of this experimental program stated that with the testing of push-off specimens, kinking occurred at lower load levels for Isorod dowels in comparison to steel dowels. It was also found that Isorod dowel stiffness is much lower than steel dowels. Bonding of one end of the dowels provided a strengthening as well as a

stiffening effect. It was also determined that by increasing the diameter of the GFRP dowel, similar strengths as steel could be achieved. It was also concluded that the use of GFRP dowels, specifically Isorod, would not be an economically viable alternative to steel.

2.3.3 Research at Iowa State University

Porter et al. (1993) at Iowa State University, investigated the use of FRP and steel dowels under laboratory and field conditions. The laboratory investigation included testing of full-scale slabs with one transverse joint, set on a simulated subgrade. The testing of the slabs included static, dynamic, and fatigue loading. The field investigation included placing FRP dowels in two joints of the westbound lane during the construction of U.S. Highway 30, east of Ames, Iowa, during the summer of 1992, for direct comparison to the behaviour of steel dowels located in adjacent joints.

The placement of FRP dowels in the new construction consisted of replacing 38 mm (1 1/2 in) steel dowels by 44.5 mm (1 3/4 in) GFRP dowels in two joints at a spacing of 203 mm (8 in) instead of the typical spacing of 305 mm (12 in). The dowels used in all the joints were 457 mm (18 in) in length. This placement is considered for long-term evaluation of the FRP dowel material. Due to the altered spacing and diameter of the dowels, placement and casting of concrete was a concern. The construction normally used basket system designed for the steel dowels which was altered to support the FRP dowels. A steel wire was used to hold the dowels in their appropriate locations. Problems arose during casting of the concrete, some of the dowels were pushed out of alignment. These dowels were straightened when observed by the construction crew.

The joints were tested using the Road Rating™ system to determine their effectiveness after approximately eight months. This system combines visual inspection with physical application of loads from which deflection measurements are recorded for comparison. The results from the field-testing were very promising and showed virtually no difference in behaviour between the steel and FRP dowels.

The laboratory setup consisted of a 300 mm (12 in) slab, 1830 mm (6 feet) wide and 3660 mm (12 feet) long, supported by steel I-beams to simulate the subgrade stiffness. Six beams, orientated across the width of the slab, were used to support the specimen during casting, curing, and testing. Each beam was instrumented with strain gauges that were calibrated to determine the load transfer efficiencies of the joints. The load transfer efficiency is the direct ratio of the unloaded side deflection divided by the loaded side deflection. Deflection measurements were also taken to compare to the calculated load transfers. Measurements were recorded to calculate the load transfer across the joint. Cyclic loading was applied by two actuators used to simulate traffic loads. Static loads were applied at a certain number of cycles to monitor the efficiency of the joint over the range of the test.

Conclusions of the experimental program stated that the FRP dowels achieved the same load carrying capacity as the steel dowels, even under cyclic loading. The average load transfer efficiency calculated for the FRP dowels was in the range of 44 percent compared to that of the steel dowels at 41 percent. A transfer efficiency of 50% would be the maximum that could be obtained assuming full load transfer. It was also noted that the deflections increased with the number of load cycles for both types of dowels.

Chapter 3 Experimental Program

3.1 General

The experimental program included testing of GFRP and steel dowels using a full-scale concrete slab thickness. Each slab contained two dowels to transfer the applied load across the joint. Epoxy coated steel dowels were also tested to provide control specimens to the GFRP specimens. The shear strength of the GFRP and steel dowels was also determined based on testing individual bars in double shear.

The experimental program was conducted at the McQuade Structural Laboratory at the University of Manitoba. The concrete pavement slabs were supported by two different subgrade conditions, a uniformly distributed steel spring system and a compacted 'A base' gravel to simulate the subgrade. These two conditions were used to simulate typical field conditions of highway subgrades.

The scope of the experimental program included testing of twelve specimens using three types of dowel material; Glasform GFRP, FiberDowel GFRP, and epoxy-coated steel. The first set, phase I, consisted of three specimen reinforced by the three types of material. A steel spring system of relatively low stiffness was used to support the concrete slab. This specimen included a gap of 3 mm (1/8 in) at the joint to simulate a typical thermal contraction of the concrete. The second set, phase II, consisted of six specimens containing the same dowel materials. There were two slabs of each type of dowel and the slabs were supported by a compacted 'A base' gravel mixture with a stiffness similar to field conditions. The slab joint systems were statically loaded on one side of the joint. The third set, phase III, consisted of three specimen supported also by

the 'A base' gravel mix and is subjected to 1 million load cycles at a load equivalent to the service load level.

3.2 Test Specimen

To simulate the behaviour of a highway pavement, the dimensions of the specimens were 610 mm (2 feet) wide and 254 mm (10 in) thick as shown in Figure 3-1. The selected width allowed the use of a loading area equivalent to AASHTO design truck tire of 600 x 254 mm (2 feet x 10 in). To determine the length of the specimen, finite element analysis was performed using Visual Analysis software. The computer analysis consisted of a beam resting on springs. The length of the specimen was determined as the length where all the supporting springs are in compression due to the applied load. The analysis indicated that a length of 1220 mm (4 feet) on either side of the joint would be sufficient for the test specimen. Therefore, the overall specimen dimensions selected were 610 x 254 x 2440 mm (2 feet x 10 in x 8 feet) as shown in Figure 3-1. Twelve specimens were cast, each containing two dowels crossing the joint as shown in Figure 3-1. Glasform GFRP of 38.1 mm (1 1/2 in) diameter, produced by Glasform Inc., were used in four specimens. FiberDowel of the same diameter, produced by RJD Industries, were also used in four specimens while 31.75 mm (1 1/4 in) epoxy coated steel dowels were used in the final four specimens. The entire lengths of the first three specimens were cast containing a sheet metal divider located at the mid-length of the specimen. The other nine specimens were cast using the same formwork and the same manufacturers dowels however each segment of the specimen were cast on two consecutive days. The first day the concrete was cast against the plywood separator which was removed after 24 hours before casting the concrete on the second day against the previous cast. This

guaranteed a smooth surface with no possibility of additional load being transferred by aggregate interlock.

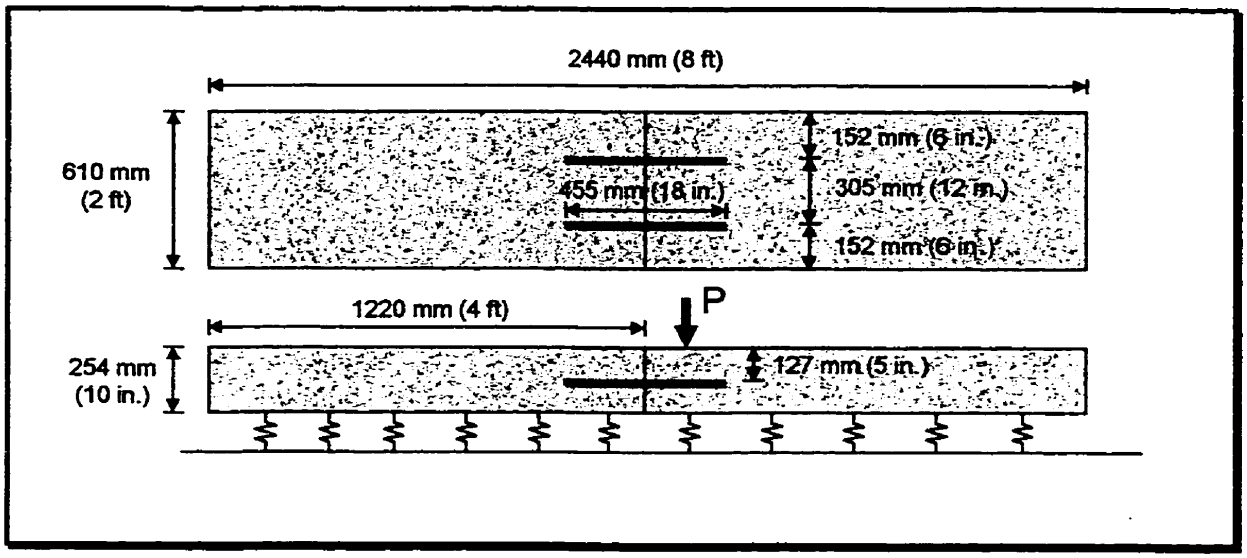

Figure 3-1: Slab and dowel dimensions

3.3 Material Properties

3.3.1 Concrete

All test specimens were cast using concrete provided by a local concrete company. For each concrete batch, six cylinders were cast to determine the average strength of the concrete. The compressive and tensile strengths of the concrete used for the three phases are given in Table 3-1. The cylinders and the slabs were tested at the same time to determine the strength of the concrete at the time of testing.

Table 3-1: Concrete Strengths

Specimen Type	Project Phase	Cast Date	Cylinder Compressive Failure Load [kN (kip)]	Average Compressive Strength [MPa (psi)]	Cylinder Split Test Failure Load [kN (kip)]	Average Tensile Strength [MPa (psi)]
Steel Dowel Specimen	1		792 (178) 783 (176) 770 (173)	44.2 (6400)	n/a	n/a
Glasform and FiberDowel Specimens	1		923 (207.5) 879 (197.5) 876 (197)	49.6 (7200)	165 (37) 240 (54) 251 (56.5)	3.1 (450)
All Specimens (First Set)	2	19/11/97 [unloaded side]	596(134) 587(132) 583(131)	33.3(4830)	178(40) 151(34) 133(30)	2.22 (320)
	2	21/11/97 [loaded side]	747(168) 818(184) 814(183)	44.9(6500)	267(60) 280(63) 236(53)	3.69 (535)
All Specimens (Second Set)	2	16/04/98 [unloaded side]	676(152) 667(150) 698(157)	38.5(5400)	236(53) 236(53) 258(58)	3.45 (485)
	2	17/04/98 [loaded side]	662(149) 613(138) 653(147)	36.5(5130)	218(49) 178(40) 245(55)	2.74 (425)
All Specimens	3	28/05/98 [unloaded side]	747(168) 755(170) 703(158)	41.4(5770)	222(50) 218(49) 200(45)	2.97 (420)
	3	29/05/98 [loaded side]	755(170) 729(164) 719(162)	41.5(5800)	191(43) 307(69) 142(32)	2.97 (420)

3.3.2 Dowels

The 455 mm (18 in) long dowels were placed in each specimen at 305 mm (12 in) centers, as shown in Figure 3-1. The diameter of the glass FRP dowels used was 38.1 mm (1 ½ in) which is larger than that of the epoxy coated steel dowels of 31.75 mm (1 ¼

in.). The larger diameter of the GFRP was selected to compensate for the lower strength of the GFRP perpendicular to the fibers.

The dowels were tested in double shear as illustrated in Figure 3-2. Following placement of the specimen in the shear test set up, the load was applied through a 25 mm (15/16 in.) section. The configuration of the shearer used to transfer the load to the dowel is a steel block with a half circle of the same diameter as the dowel. The dowel rests in a V-groove along the shearing block and is supported near the loading area by two shearing rests that also have the same diameter as the dowel.

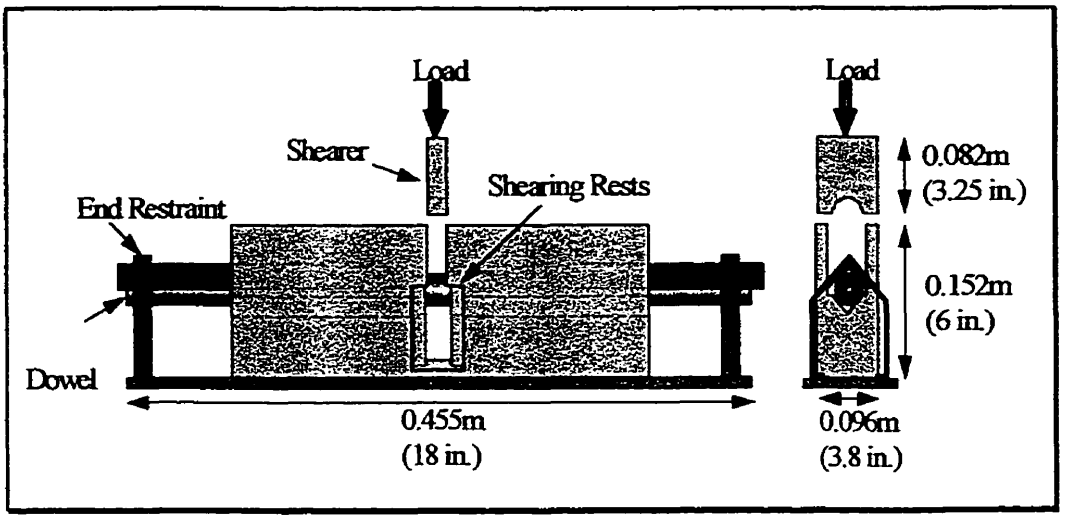

Figure 3-2: Apparatus for double shear test

The Manitoba Department of Highways and Transportation provided the epoxy coated steel dowels. Using the apparatus shown in Figure 3-2, the measured ultimate shear strength of the steel dowels was 570 MPa (82.6 ksi) based on a measured ultimate double shearing load of 901 kN (202.6 kips) and an area of 791.7 mm^2 (1.227 in^2). The measured values of the Glasform and FiberDowels were 150 MPa (21.8 ksi) and 107.0 MPa (15.5 ksi) based on measured ultimate double shearing loads of 343 kN (77.1 kips)

and 244 kN (54.9 kips) respectively. The area of both types of GFRP dowels was 1140.1 mm^2 (1.767 in^2). These values are summarized in Table 3-2. The GFRP were provided by Glasforms Inc. in San Jose, California and FiberDowel, by RJD Industries Inc., in Laguna Hills, California.

Table 3-2: Summary of Dowel Double Shear Tests

Dowels	Dowel Diameter mm (in)	Number of tests	Ultimate Double Shear Load kN (kips)	Ultimate Strength MPa (ksi)	Standard Deviation MPa (ksi)
Epoxy Coated Steel	31.75 (1.25)	3	901 (202.6)	570 (82.6)	14.2
FiberDowel	38.1 (1.5)	3	244 (54.9)	107.0 (15.5)	3.8
Glasform	38.1 (1.5)	3	343 (77.1)	150 (21.8)	21.4

3.3.2.1 Epoxy-Coated Steel

Manitoba highways and transportation provided the epoxy coated steel dowels directly from a stockpile. Standard dowels are grade 60 (ASTM A615) steel, coated initially with a thin layer of epoxy. The dowels and basket assemblies are coated with an ashphaltic substance to provide debonding from the concrete.

3.3.2.2 Glasforms

Glasforms Inc. produces glass fiber dowels in San Jose, California. At the time of receiving the dowels, the company did not have any commercially ready dowels but were very willing to participate in this research. From correspondence received, it was noted that the dowels consisted of fiberglass in a vinyl-ester resin matrix. The flexural modulus and the flexural strength is, 41.3×10^3 MPa (6 Msi) and 688.9 MPa (100 ksi) respectfully. Also, values of 55.1 MPa (8 ksi) for interlaminar shear and 1.9 for specific gravity were

given. As their product was relatively new, the tensile and shear strength were not available but may now be at the company's web site: www.glasforms.com.

3.3.2.3 FiberDowel

FiberDowel is produced by RJD Industries in Laguna Hills, California, and marketed as a "Corrosion Proof Dowel Bar System". The dowels may be ordered from their catalogue in varying diameters and lengths. Table 3-3 contains a summary of certified testing provided by the manufacturer and conducted by two testing agencies; Twinning Laboratories, Long Beach, California, and Smith Emery, Los Angeles, California both using the ASTM D3916 tensile testing criteria. The FiberDowels strength information can also be accessed from their homepage: www.rjdindustries.com.

Table 3-3: FiberDowel Certified Strength

FiberDowel Diameter mm (in)	Tensile Tests			Shear Tests	
	Average Load kN (kips)	Elongation %	Failure Mode	Average Load kN (kips)	Failure Mode
12.7 (0.5)	89.7 (20.2)	0.08	Tensile	29.8 (6.7)	Shear
19.0 (0.75)	173.9 (39.1)	0.09	Tensile	91.0 (20.5)	Shear
22.2 (0.875)	234.0 (52.6)	0.09	Tensile	113.7 (25.6)	Shear
25.4 (1.0)	286.5 (64.4)	0.08	Tensile	127.7 (28.7)	Shear
31.7 (1.25)	458.0 (103.0)	0.24	Tensile	131.1 (29.5)	Shear
38.1 (1.5)	630.4 (141.7)	0.39	Tensile	146.3 (32.9)	Shear
44.4 (1.75)	855.8 (192.4)	0.39	Tensile	192.6 (43.3)	Shear

From Table 3-3, the 38.1 mm (1.5 in.) dowel has a guarantied strength of 146.3 kN (32.9 kips). In comparison to the values in Table 3-2, the FiberDowels reached a load level of 244 kN (54.9 kips) in double shear performed at the University of Manitoba.

During the FiberDowel manufacturing process, quality checks are made continuously and random samples are sent for certification. Within the engineering

specifications supplied with the product, it was noted that RJD had comparatively tested the dowels in bond with concrete against steel dowels, both with and without an epoxy coat. It was reported that when a pull out test was conducted on dowels with a 305 mm (12") embedment length, the bond strength for a plain steel dowel is 1.52 MPa (220 psi), epoxy coated steel bar bond is 0.43 MPa (63 psi), and the FiberDowel is 0.1 MPa (15 psi). From these results, it was clear that the FiberDowel would not require any coatings for debonding.

3.3.3 Subgrade Simulation

Current construction practice of typical rigid highway pavements includes the preparation of a base on the top of existing or excavated soil as shown in Figure 2-4. The base consists of compacted soil typically to 20 MPa (2.9 ksi) followed by a layer of 200 mm (7.9 in) 'C base' compacted to 200 MPa (29.0 ksi) and by a layer of 100 mm (3.9 in) 'A base' also compacted to 200 MPa (29.0 ksi).

The appropriate determination of the subgrade modulus requires a good description of the material used for the subgrade and its compaction level. Since the subbase is densely packed limestone of different gradations, the characteristics can be found from tables provided by Terzaghi (1955) as given in Table 3-4. The data reflects a wide range of values exist for the subgrade modulus. A value of 204×10^3 kN/m^3 (650 tons/ft^3), which is the median dense value provided by Terzaghi, was used as the appropriate subgrade modulus. To further explain the development of the subgrade modulus an example is provided.

Table 3-4: Modulus of Subgrade Reaction

Reference	Type of Soil	Loose [kN/m^3] [(tons/ft^3)]	Medium [kN/m^3] [(tons/ft^3)]	Dense [kN/m^3] [(tons/ft^3)]
Terzaghi (1955)	Dry or Moist Sand	6.3-18.9x10^3 (20-60)	18.9-94.3 x10^3 (60-300)	94.3-314.2 x10^3 (300-1000)
Miner and Seastone (1955)	Gravel and Gravelly soils			135-190x10^3 (430-605)

The subgrade modulus, k, assuming a liquid foundation, can be determined based on the pressure, P, applied over an area and the vertical deflection, y, as follows.

$$k = P / y \qquad \text{Equation 3-1}$$

According to AASHTO code (1993) the maximum concentrated load of a half axle truck tire load is 100 kN (22.5 kips) spread over an area of 610 mm x 254 mm (2 feet x 10 in). The acceptable vertical deflection under this specified load level is normally in the range of 3 mm (1/8 in). Therefore, based on pressure P:

$$P = Q / A = 100/[(0.6)(0.25)]$$

$$= 666.67 \text{ kN/m}^2$$

the subgrade stiffness k:

$$k = P / y = 666.67 / 0.003$$

$$= 222 \times 10^3 \text{ kN/m}^3$$

The calculated subgrade modulus is within the range provided by Terzaghi. It should be noted that the modulus of subgrade reaction is a fictitious property that depends on the size of the loading plate and the load level as well as the load rate. The modulus is used to simplify the in-situ determination of soil structural support capacity.

3.3.3.1 Phase 1

The subgrade simulation for the first three specimens consisted of 36 steel springs used to support the concrete slabs as shown in Figure 3-3. The springs were 76 mm (3 in) diameter and spaced at 200 mm (8 in) centers.

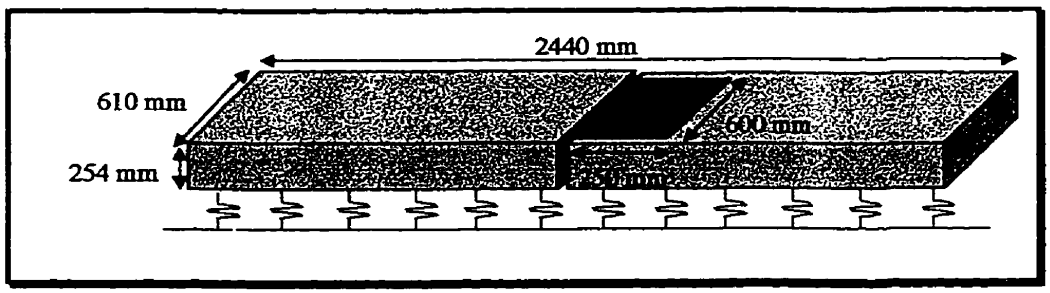

Figure 3-3: Slab on spring subgrade

For phase I, it was decided to provide a subgrade that simulates a possible failure of the subgrade close to the joint location. Failure of the subgrade would experience extreme deflections and subject the dowel to unusually high stress.

The average stiffness of the steel springs was 145.4 kN/m (830 lbs/in) and placed over an area of 200 x 200 mm (8 x 8 in.). This is corresponding to a stiffness of 3.6×10^3 kN/m^3 (752 lbs/in^3). Comparing this stiffness to the subgrade moduli in Table 3-4, of 204×10^3 kN/m^3 (13.3 lbs/in^3), it can be seen that the subgrade provided is approximately 3 percent of expected field conditions. Therefore, the test simulates a lower boundary condition for the subgrade.

3.3.3.2 Phase II & III

The subbase for the remaining specimens in phase II and III consisted of 330 mm (13 in) compacted 'A base' graded limestone. Manitoba Department of Highways and Transportation provided the specifications for base course material. From these

specifications, an appropriately graded 'A Base' was obtained. The gradation of the base material specified by the Highways Department and supplied by Inland Aggregates can be found in Table 3-5. This gradation is compared to the reduced gradation of a "C Base" limestone which is typically used in combination with "A Base" in a layered highway subbase system. The base material was built up in three layers each of 100 mm (4 in) and compacted using a 1.16 kN (260 lbs) plate compactor. After the third level was compacted, the box containing the base was topped off and compacted one final time.

Table 3-5: Base Course Specifications

Passing Sieve Size	Highways Specification		Inland Aggregates Limited Supplied "A Base"	
	Specified "A"	Specified "C"	Specified	Typical
25 mm (1 in)		100		
19mm (3/4 in)	100		100	100
4.75mm (No. 4)	35-70	25-80	35-70	50
4.25um (No. 40)	15-30		15-30	17
75um (No. 200)	8-15	8-20	8-17	12

To determine the stiffness of the compacted 'A base' a 317.5 mm (12.5 in) square plate was placed on the top surface of the base and was loaded using an MTS actuator. Each base test was loaded up to 40 kN (9 kips) to determine the modulus of the subgrade. The base test locations are shown in Figure 3-4. The first base test was conducted at the middle location. The base was preloaded a few times which accounts for the high modulus. The second base test was conducted at the south end of the test bed. For the third base test, the north end of the test bed was used. During setup of the test, the base was again preloaded. In order to establish the possible increasing stiffness during consecutive tests, the base was tested again at the north end, immediately following the previous test. Since loading of the test specimen takes place at the middle, the second loading of the north end had no effect on the results due to the expected slab uplift in this

area. Base tests were conducted following each slab test to monitor any changes the base material. The results from all the base tests are presented in Table 3-6. The load versus deflection plots of the base material can be found in appendix A.

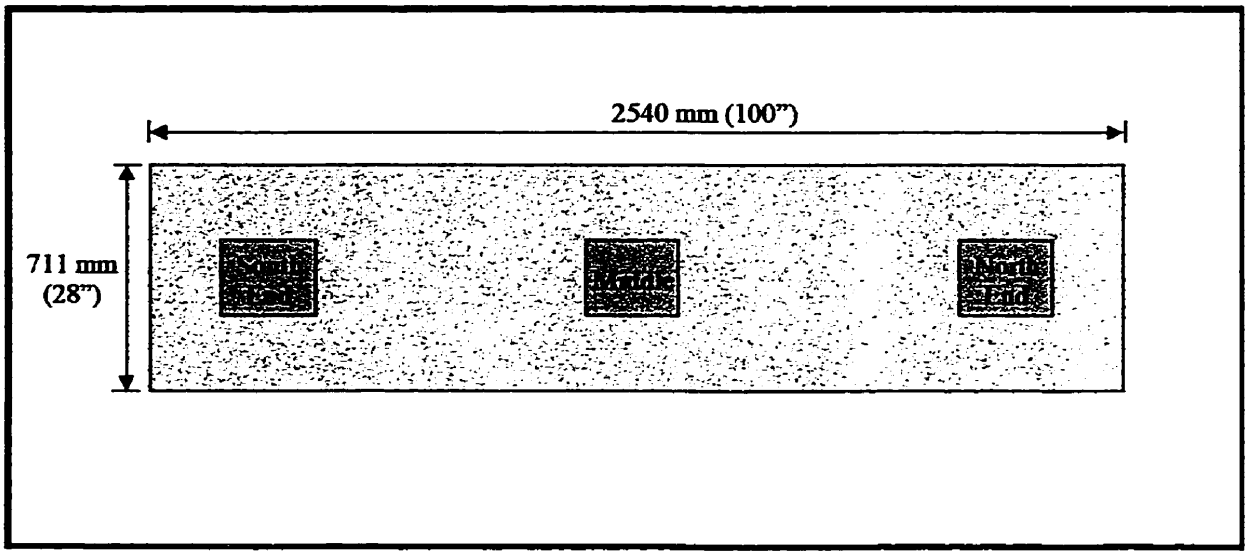

Figure 3-4: Location of base tests on 'A base' bed

Table 3-6: Subgrade Modulus for the First Phase II Slab Subbase based on a 317.5 mm (12.5 in.) bearing plate

Base Test ($x10^3$ kN/m^3)						
Load	Before Slab Testing					
	Middle Test	South End Test	North End Test	Following Steel Test	Following FiberDowel Test	Following Glasform Test
Initial	385.4	112.6	317.9	137.9	139.3	122.7
Reloading			525.2			

From the results obtained from the base tests, the subgrade modulus can be taken to be approximately 133.3 $x10^3$ kN/m^3 (394 lbs/in^3) based on the tests between the slab tests. This value can be compared to the value that was anticipated to provide an adequate densely packed subgrade to simulate the field conditions.

Base tests were also conducted before and between the second test of the phase 2 slabs. All tests were conducted at the middle location of the gravel bed. The subgrade moduli are summarized in Table 3-7. The measured values suggest the base material lost significant strength due to repeated loading conditions. This could have occurred due to the repeated loading the base material experienced where the aggregates significantly degraded.

Table 3-7: Subgrade Modulus for Second Phase II Slab Subbase based on a 317.5 mm (12.5 in.) bearing plate

	Base Test ($x10^3$ kN/m^3)					
Load	1st Middle Test	2nd Middle Test	3rd Middle Test	Following Glasform Test	Following Steel Test	Following FiberDowel Test
Initial	177.3	175.5	530.5	126.3	232.5	92

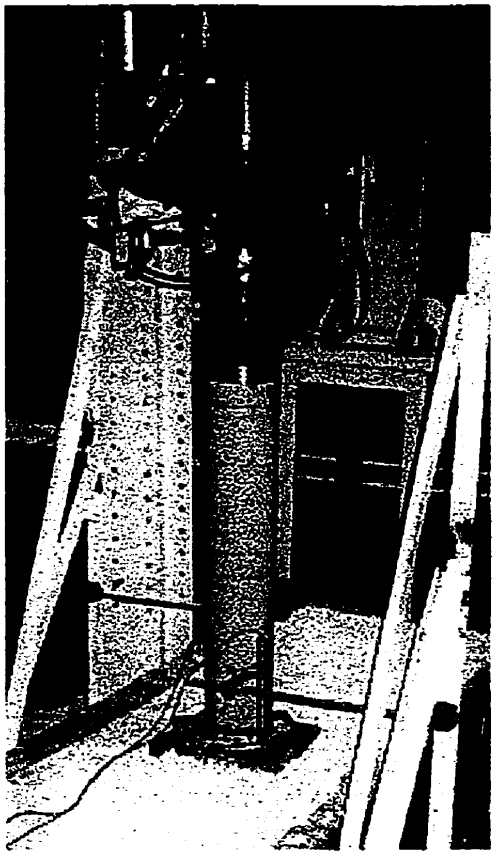

Figure 3-5: Test set-up for base tests

3.4 Fabrication of the Test Specimens

Plywood forms were used to cast the entire jointed slab specimen. The form was coated with a long-term form paint for easier removal of the concrete and for reuse for the following specimens. For phase I, the specimens represent a construction joint containing a contraction gap of 3 mm (1/8 in) at the joint. This was achieved by placing a piece of sheet metal at the joint.

After curing, the slab was moved using eight inserts placed in locations matching the location of holes in a steel channel strongback. The inserts were fixed in place using a narrow plywood member during casting.

Two more forms were constructed using 19 mm (¾ in) paper-lined plywood to facilitate multiple castings. These forms were built to the same internal dimensions but pieced slightly different to ease removing the concrete specimen.

For phase II and III the same formwork were used with some minor adjustments. The specimens in these phases represent a typical construction joint, therefore no contraction gap was provided. The specimens were cast over a two-day period with a temporary plywood divider placed at the location of the joint during casting of the first slab of each specimen. This provided the separation and a smooth surface to eliminate the aggregate interlock mechanism at the joint. Other preparations were similar with regards to the location of the inserts for lifting purposes. The second day of casting consisted of removing the plywood divider and casting against the concrete face.

3.5 Instrumentation

3.5.1 Phase I

3.5.1.1 Steel Dowels

The test was instrumented, as shown in Figure 3-6, to obtain complete data on the performance of the steel dowels under various load levels. Linear variable differential transducers (LVDTs) and dial gauges were located as shown in Figure 3-6. In some cases, dial gauges were used to duplicate the LVDTs as well as to measure deflections along the slab. Demec points were placed on both sides of the slab joint at the top and the bottom to measure possible contraction, separation or rotation along the joint. The construction joint provided for this specimen had a 3 mm gap to model a possible thermal contraction gap that a construction joint in the field would have in the winter. Demec points were used to measure relative movement of the two slabs at the joint. By increasing the applied load, it was observed that the gap closed rapidly causing the top edges of the slabs to be in contact. The compressive stresses caused by the excessive deflection and the contact of the two slabs led to the crushing of the concrete and edge spalling. Measurements, in the compression zone, were recorded up to a load level of 45 kN (10 kips).

3.5.1.2 GlasForm and FiberDowel Dowels

The first FiberDowel specimen was instrumented in a similar fashion as the first steel specimen, as shown in Figure 3-7. To obtain complete data on the performance of the glass dowels, linear variable differential transducers (LVDTs) and dial gauges were placed to measure deflections along the slab. Demec points were placed on one side of

the slab joint at the top and the bottom to measure possible contraction, separation or rotation under different load levels. In order to measure the direction and absolute value of movement of each side of the slab, dial gauges were added and fixed to the testing floor to measure the deflection at the joint. These two specimens also had a 3 mm (1/8 in) gap at the joint.

3.5.2 Phase II

There were six concrete slab tests within phase II divided into two sets. Both sets of specimens included epoxy-coated steel dowels, FiberDowels, and Glasform dowels. The first three specimens were instrumented as illustrated in Figure 3-8 and additional instrumentation was added to the same specimens when they were reloaded as shown in Figure 3-9. After analysis of the data, a revised instrumentation scheme was used for the second set of specimens as illustrated in Figure 3-10. The measured load-deflection relationship for each specimen was used to evaluate the behaviour under different load levels. The deflections were measured on each side of the joint to determine the differential deflection occurring at the joint to assess the joint effectiveness.

Following the first set of the phase II slabs, the location of the LVDTs across the joint was lowered to prevent the disturbance of readings caused by corner cracking. This in turn created a problem in reading demec points across the joint. For the second testing of first three slabs, the demec points were not used. Demec points were used on the following three specimens, Figure 3-10, by raising them off the surface of the concrete, which allowed the demec gauge to span the LVDT's and complete a reading.

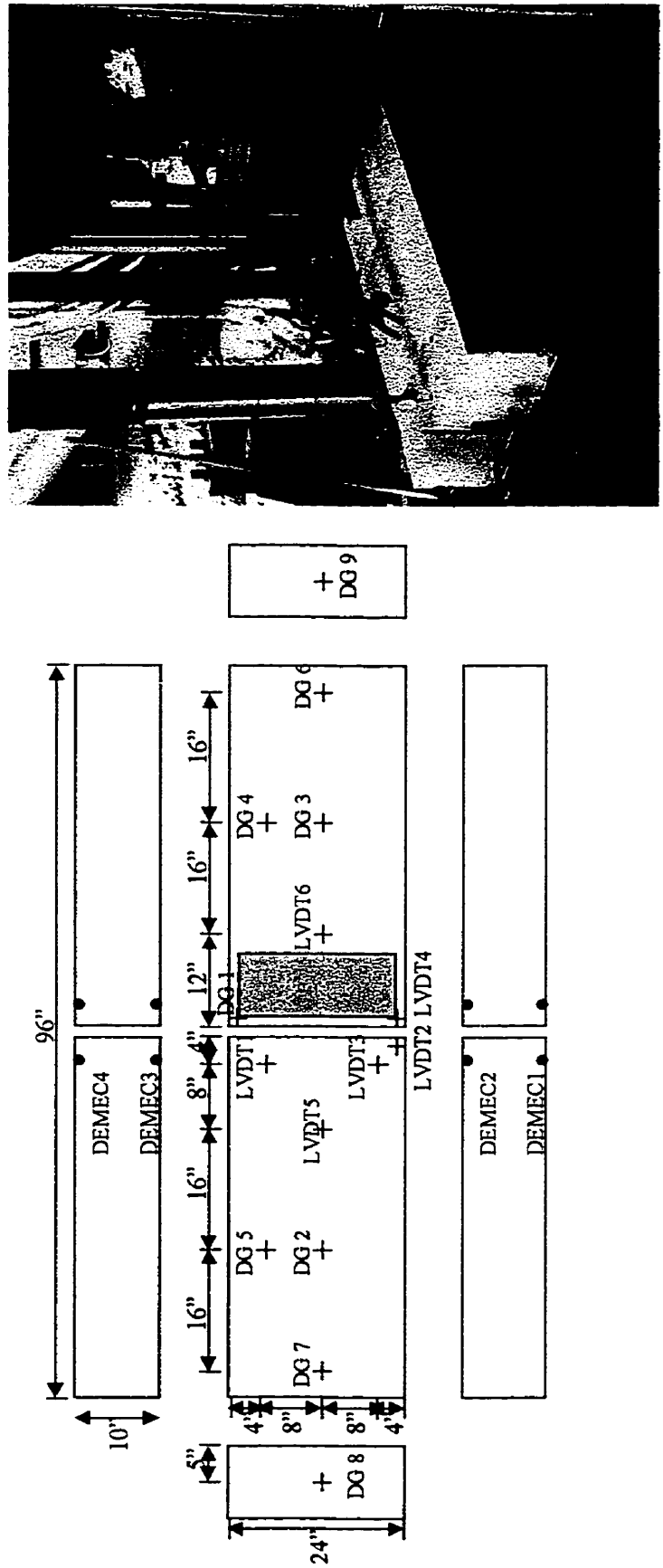

Figure 3-6: Instrumentation layout for pilot test

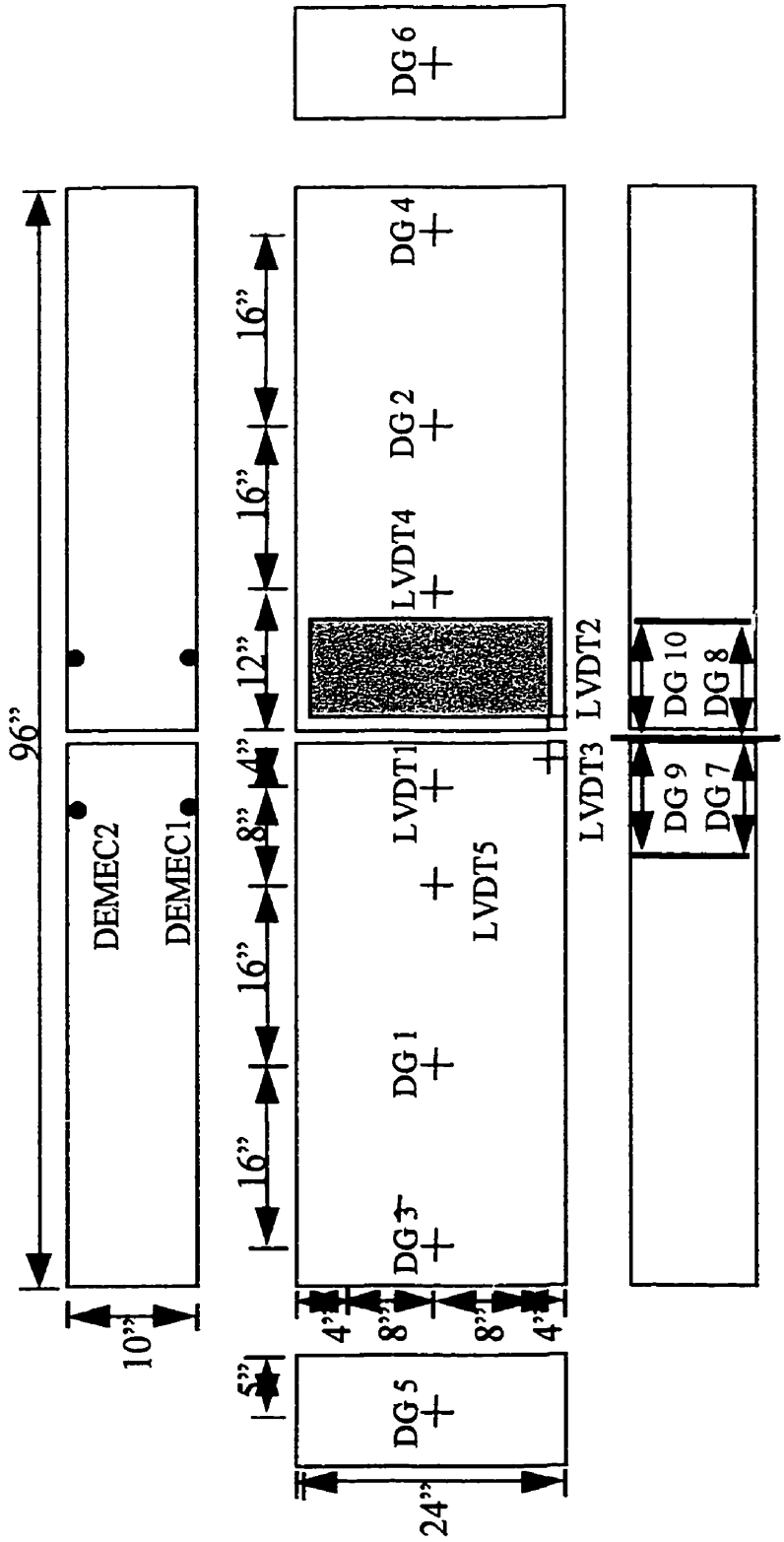

Figure 3-7: Instrumentation layout for FiberDowel and Glasform Tests

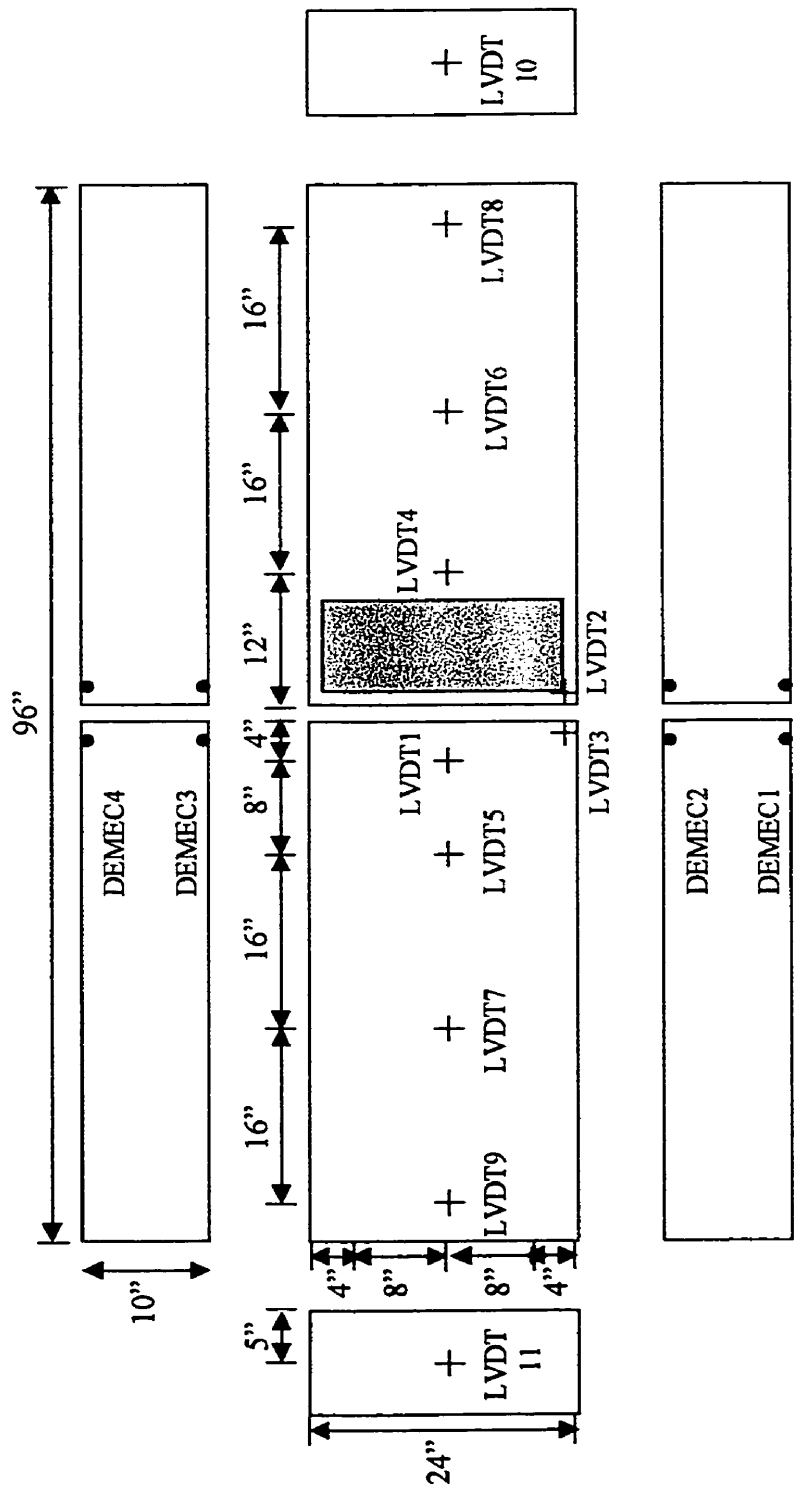

Figure 3-8: Instrumentation layout for the first set in Phase II

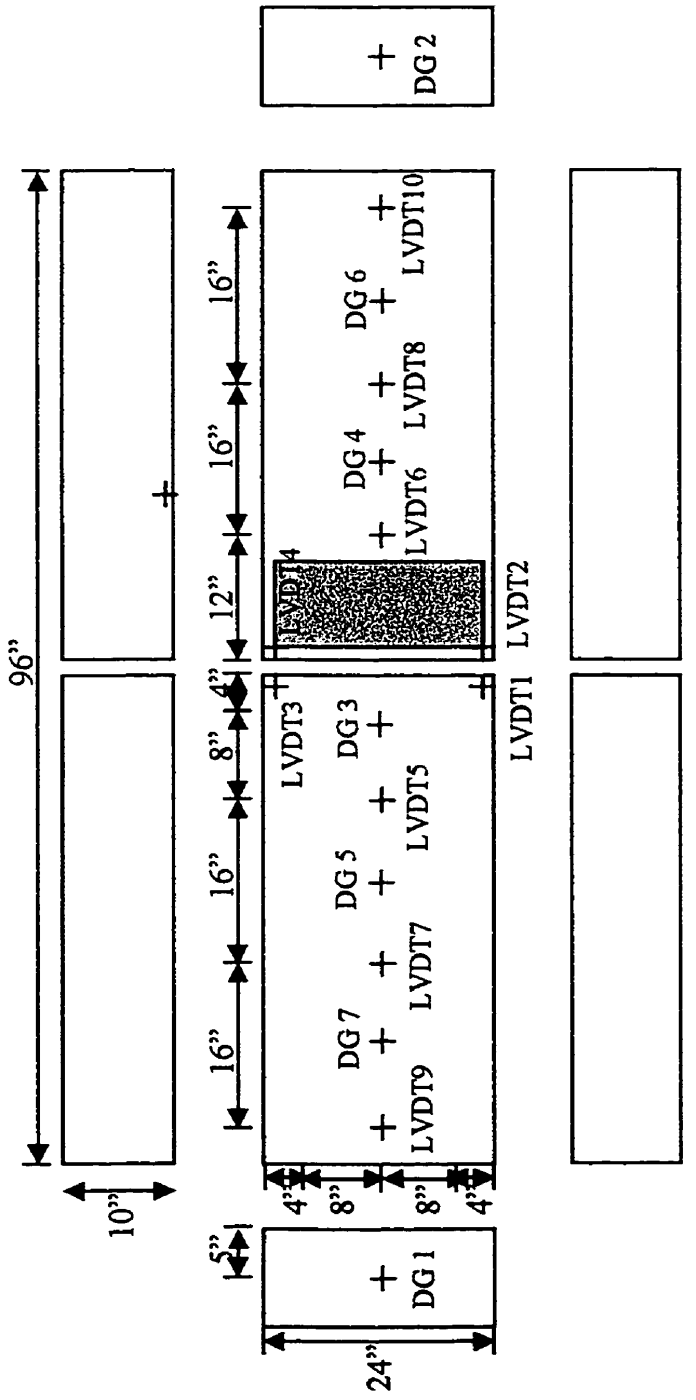

Figure 3-9: Instrumentation layout for reloading the specimens in Phase II

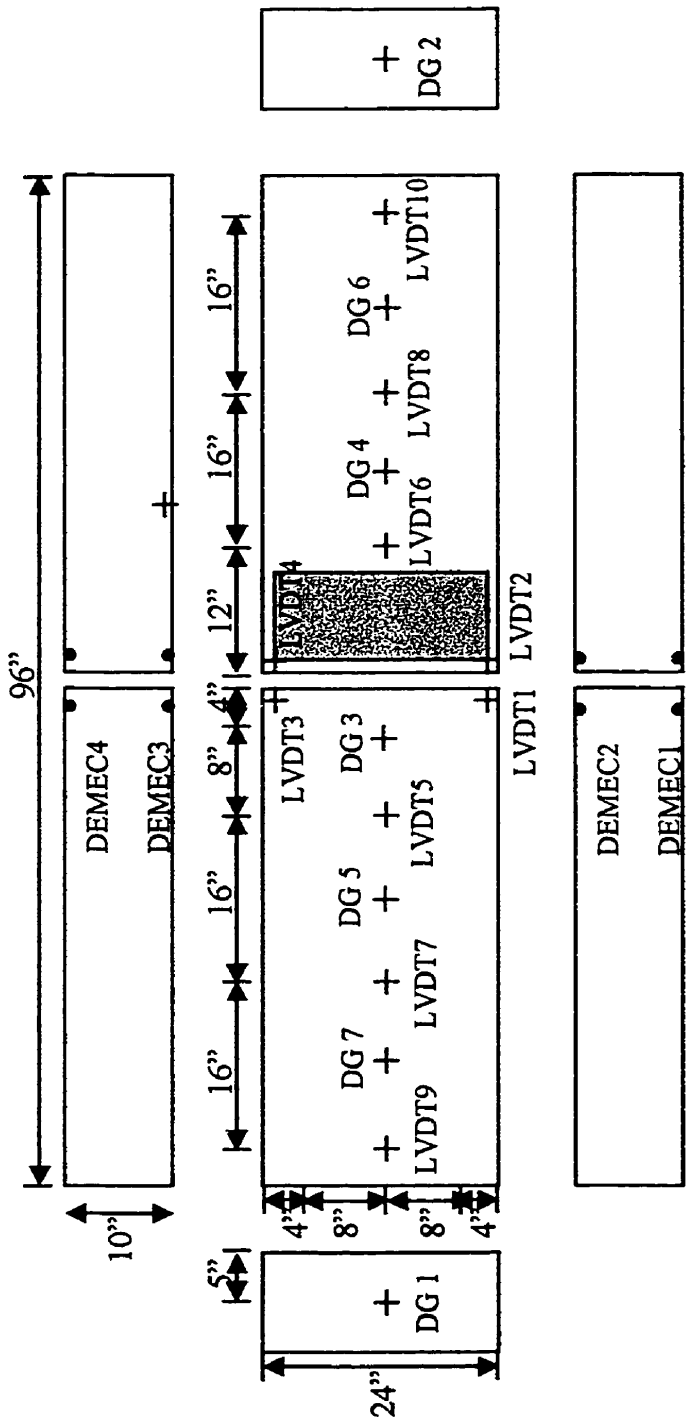

Figure 3-10: Instrumentation layout for the second set of specimens in Phase II

3.5.3 Phase III

The instrumentation for phase III is shown in Figure 3-11. Minor alterations have been made on the instrumentation for this phase. The Demec points have been removed from both sides of the slab. The instrumentation is used only during the static-testing conducted between the cyclic loading portion of this phase.

3.6 Testing Procedure

3.6.1 Phase I

The test setup for phase I consisted of steel springs to simulate the subbase. An array of springs was used to provide equal support to the two slabs of the specimen. The number of springs required was based on the effective tributary area for each spring. Thirty-six springs were used to support the slab, therefore each spring supported a 200 x 200 mm (8 in x 8 in) area.

The preparation of the springs included welding of square steel plates to each end of the springs and testing of a sample number of springs to determine their average stiffness. The welding was performed to ease the multiple setups expected, to provide a flat base on which the slab was supported, and to define each spring's tributary area. One end of the spring had a 175 x 175 mm (7 in x 7 in) plate welded onto it while the other end had a 100 x 100 mm (4 in x 4 in) plate. Each spring was then numbered so it could be placed in the same location for subsequent tests. These numbers were transferred to a plywood template created for the welded plate on one side of the springs. This numbering system also aided in tracking the springs that were tested.

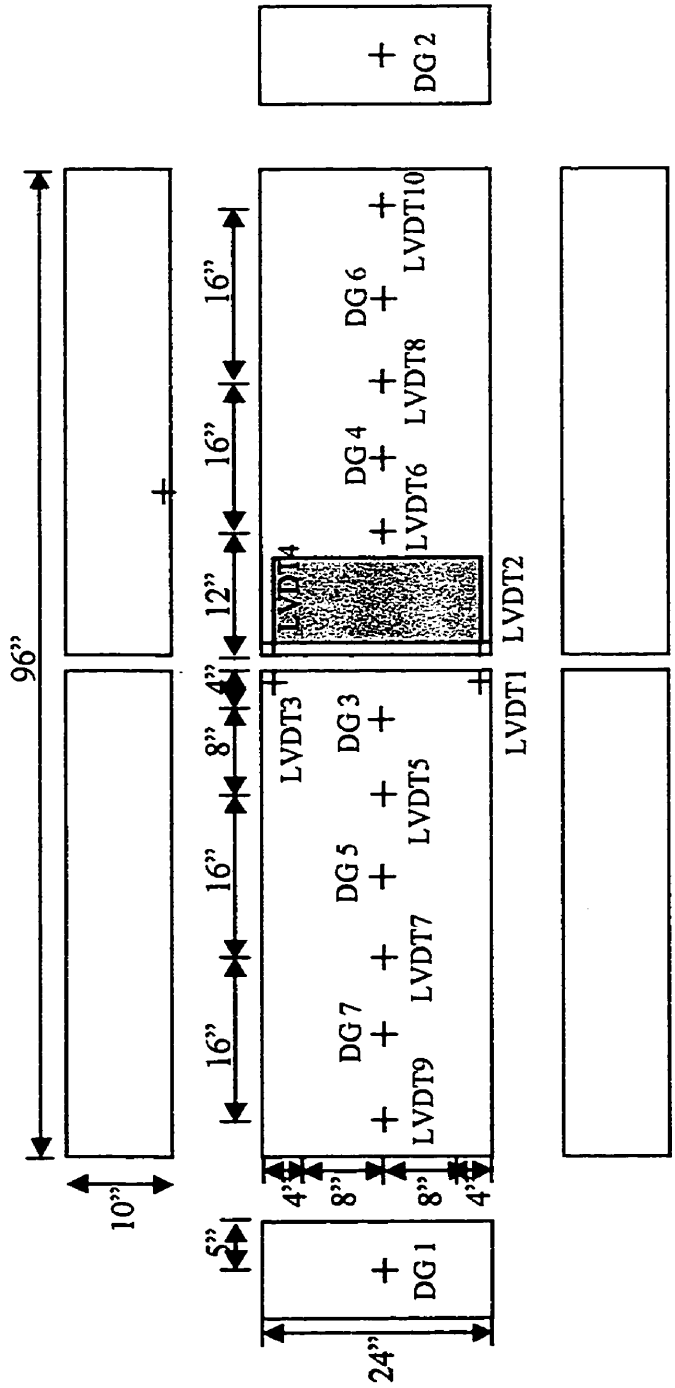

Figure 3-11: Instrumentation layout for Phase III tests

The setup started with placement of three strips of 50 mm (2 in) thick, 200 mm (8 in) wide, steel plates. These plates were used to provide stiff and level support for the plywood template and springs. Once these plates were positioned, the location for the template was determined and put into place. The springs were then put into their assigned locations until the 3 by 12 array was completed.

Using a steel channel section as a strong back, the plain concrete specimen was lifted, aligned, and set on top of the support springs. The specimen was painted with whitewash to facilitate crack observation during testing.

A loading plate, representing the area of a half axle truck tire is placed on top of the slab at one side of the joint. First a 12 mm (1/2 in) thick, 200 mm (10 in) wide, 600 mm (2 feet) long, sheet of neoprene is placed on the load location between the loading plate and the concrete surface to avoid local crushing and to distribute the load evenly. The main loading plate is placed and aligned with the previous blocks and the actuator.

3.6.2 Phase II

The subbase of the phase II used a limestone base material to support the concrete slab model. A box was constructed using steel channel sections to contain the base material. The steel channels were connected together using angles and bolts at each corner of the box.

A nylon sheet was placed into the box to contain the base material. A leveling course of base material is placed in the bottom of the box until a thickness of 25 mm (1 in) to 38 mm (1.5 in) is obtained. This course is then covered by 19 mm (¾ in) plywood to provide a level surface for the remaining base material.

The base material is added in three layers of 100 mm (4 in) each with compaction following each lift. The compaction was achieved using a 508 mm by 457 mm (20 in by 18 in); 1.16 kN (260 lbs) vibrating plate compactor. Two complete passes were made per lift to ensure adequate packing of the material. Once the final 100 mm (4 in) lift was added and compacted, a final layer of base material 12 mm to 25 mm (1/2 in to 1 in) was added and compacted to bring the base up to grade.

The load was applied using an MTS actuator supported by a steel frame fixed to the strong floor of the structural testing lab as shown in Figure 3-12.

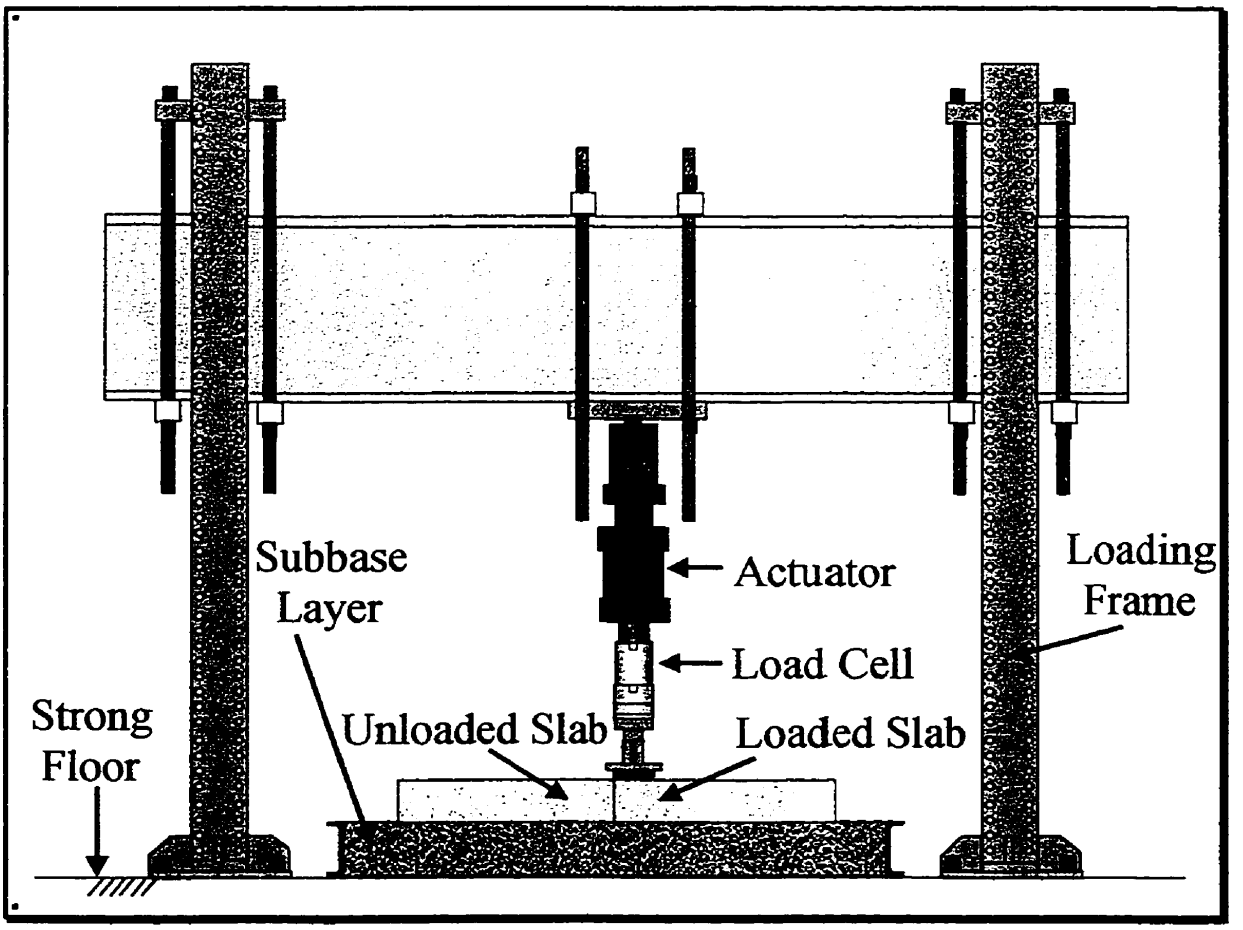

Figure 3-12: Complete test setup including testing frame, actuator, and base layer

Before testing, the modulus of subgrade reaction of the compacted limestone base was determined using a 318 x 318 mm (12.5 x 12.5 in) plate placed upon the base material and the load was applied by the actuator, Figure 3-5. The load cell attached to the actuator was connected to a data acquisition system allowing for readings of the load and the stroke of the actuator. Three tests were made to ensure that the compacted base material had a relatively consistent modulus.

Placing each specimen involved lifting the plain concrete pavement sections using a steel channel strong back and maneuvering them into location on top of the base material. Following the placement of the slab, the loading platen is placed in the loading area. A swivel plate was used to adjust the alignment.

3.6.3 Phase III

The subbase for the phase III of testing is the same as in phase II where the placement, packing, and testing of the subgrade modulus are repeated. Cyclic testing was applied using a 5000 kN (1.2 million lbs) capacity MTS closed loop servo-controlled testing machine. The specimens were tested to a total of 1 million cycles with a load range from 20 kN (4.5 kips) to 130 kN (29.2 kips). An initial monotonic test on each specimen was conducted to a load level of 130 kN (29.2 kips) and subsequent monotonic tests were performed to the same load level after certain number of cycles as shown in Table 3-8. The time required for each set of cycles is also shown for the two different cycle speeds, 1 Hz and 6 Hz. The 1 Hz cycling speed allowed for fine tuning of the controller during the first 100 cycles as the 16.7 seconds for the 6 Hz would not have allowed sufficient time to acquire the load range required. Since the test is load controlled, the deflections increase with the cycles. In order for the actuator to

continuously apply the required load it must travel at a higher speed. Periodically the MTS machine would be checked to ensure the load level was within the specified range.

Table 3-8: Cycle levels at which Static Tests are Conducted

Monotonic Test	Cycles Before Test	Cycles between Readings	Time for Cycles to Complete	
			1 Hz	6 Hz
1	0			
2	100	100	100 sec	16.7 sec
3	1000	900		2.5 min
4	10000	9000		25 min
5	100000	90000		4.2 hours
6	300000	200000		9.3 hours
7	600000	300000		13.9 hours
8	1000000	400000		18.6 hours

Chapter 4 Test Results

4.1 Test Results of Phase I: Static Tests

The slabs in phase I were placed on a weak subgrade made of steel springs. The weak subgrade stiffness allowed the assembly to deflect excessively under the applied load. The three slabs tested contained epoxy-coated steel dowels, FiberDowel dowels and Glasform dowels. This section of the thesis presents the measured data and the failure modes.

4.1.1 Steel Dowels

The test set up and the data acquisition system is shown are Figure 4-1. The measured deflections at different load levels are shown in Figure 4-2. The deflections immediately under the load are estimated from corner readings, since the loading plate and cracking of the slab prevent the precise measurement of deflections at the center of the joint. It should be noted that the large measured deflections under the applied load are not typical for concrete pavement highway conditions. It should also be mentioned that this phase is designed to simulate weak subgrade or voids in the base layer. It was observed that the deflection of the loaded side of the slab is larger than that of the unloaded side throughout the test.

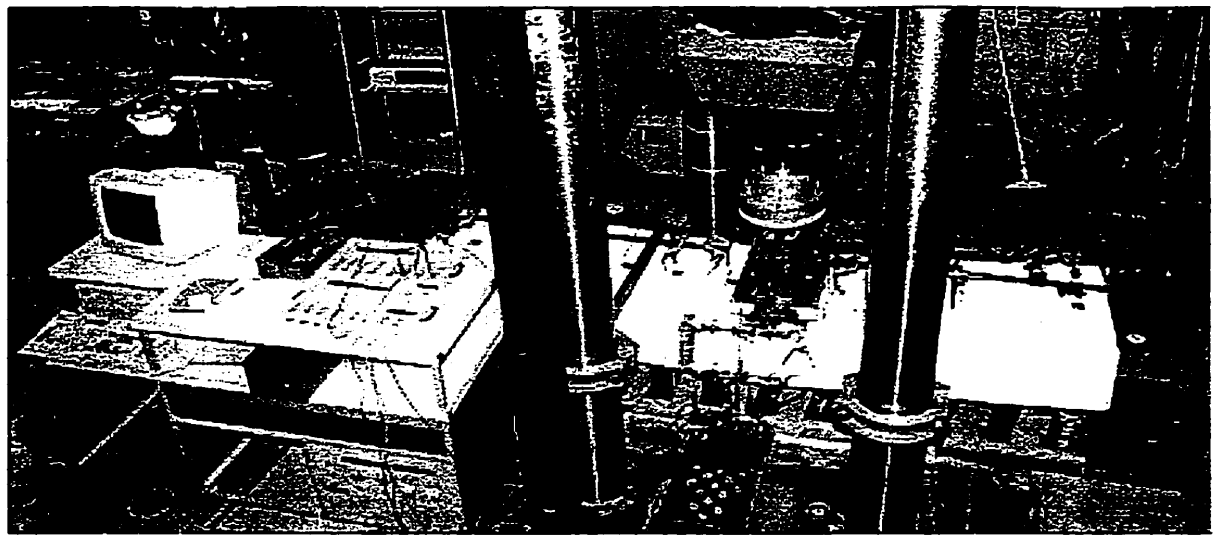

Figure 4-1: Test setup for Steel dowel specimen I on simulated spring subgrade

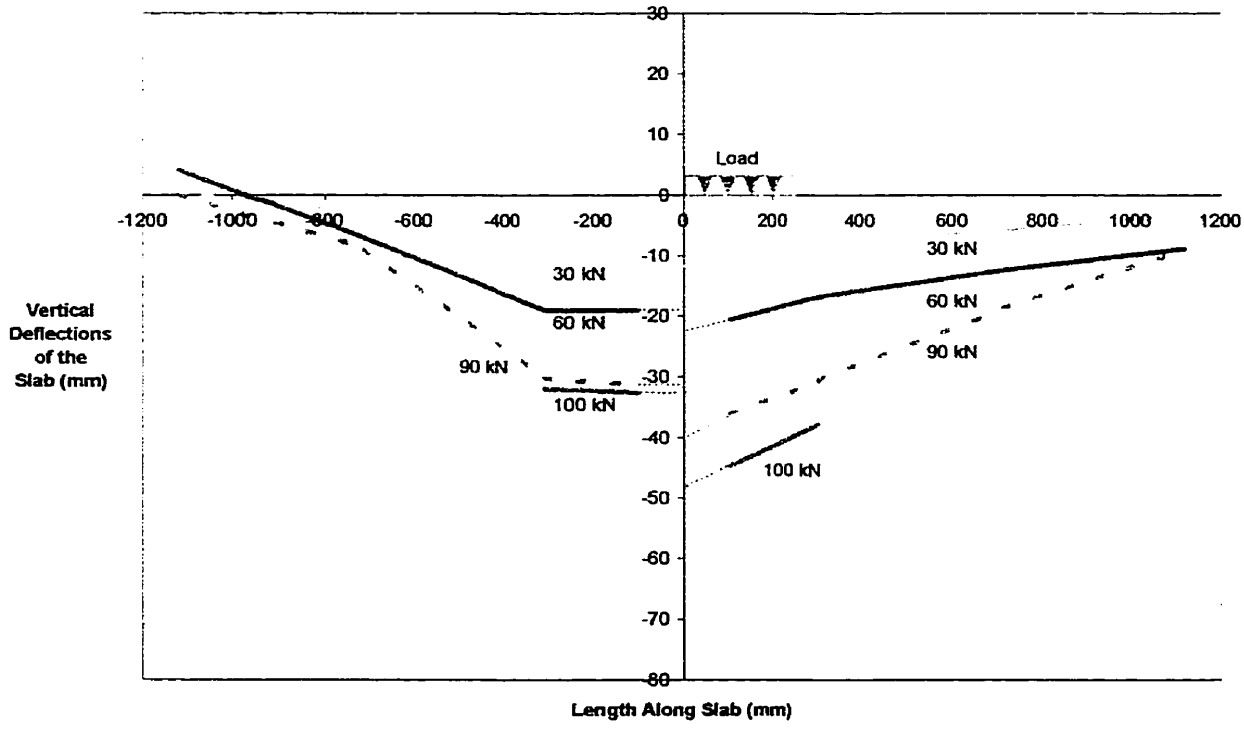

Figure 4-2: Deflection of Steel dowel slab in Phase I

The test was stopped where excessive deflections in the steel springs were observed at a load level of 114 kN (25.65 kips). At this stage, the springs were experiencing not only the vertical deflection, but also a side sway under the loaded side of the slab. This sway occurred due to rotation of the springs under excessive deflections. The bearing pressure immediately under the loading plate initiated small cracks. Larger cracks were observed at a load level of 75 kN (16.87 kips), as shown in Figure 4-3.

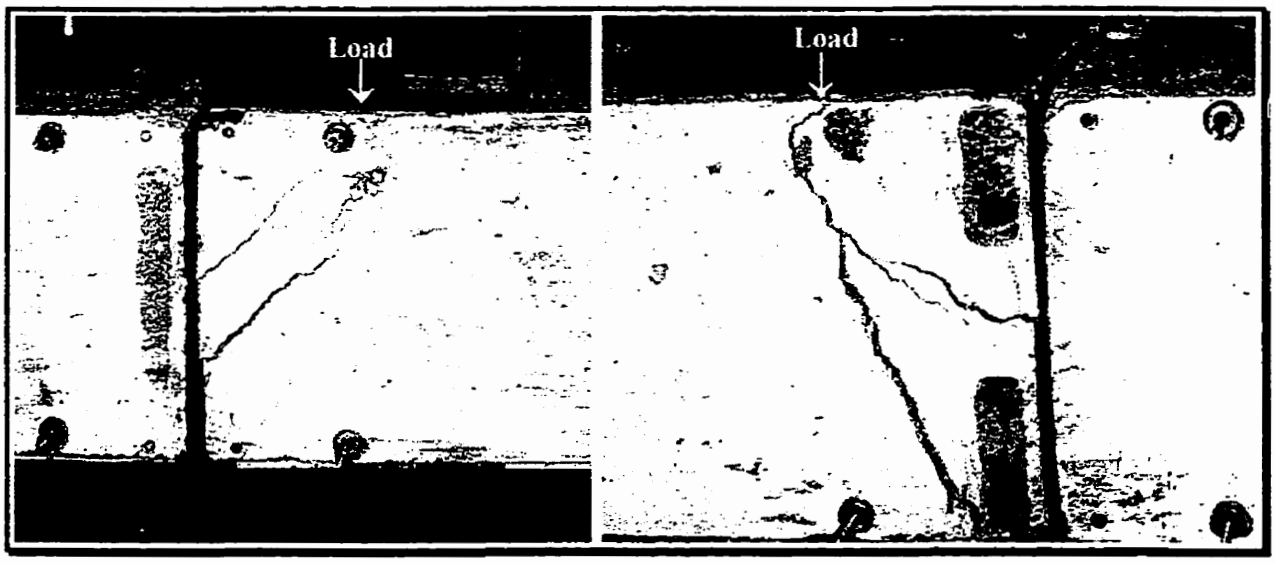

Figure 4-3: Cracks on both sides of the Steel doweled specimen in Phase I

The concrete slab maintained the applied load in spite of the excessive deflection experienced by the springs. The flexural stiffness of the dowel bars and the contact pressure under the load caused the concrete cracking pattern observed under the loading plate.

4.1.2 FiberDowels

The load-deflection diagram at different load levels is given in Figure 4-4. The deflections immediately under the load are estimated from corner readings, since the

loading plate and cracking of the slab prevent the precise measurement of deflections at the center of the joint .

During the test, the major cracking began at a load of 66 kN (14.85 kips). The loading continued to a level of 114 kN (25.65 kips), at which excessive deflections and side sway of the steel spring subbase were observed. In Figure 4-5, the side sway of the springs can be seen before termination of the test.

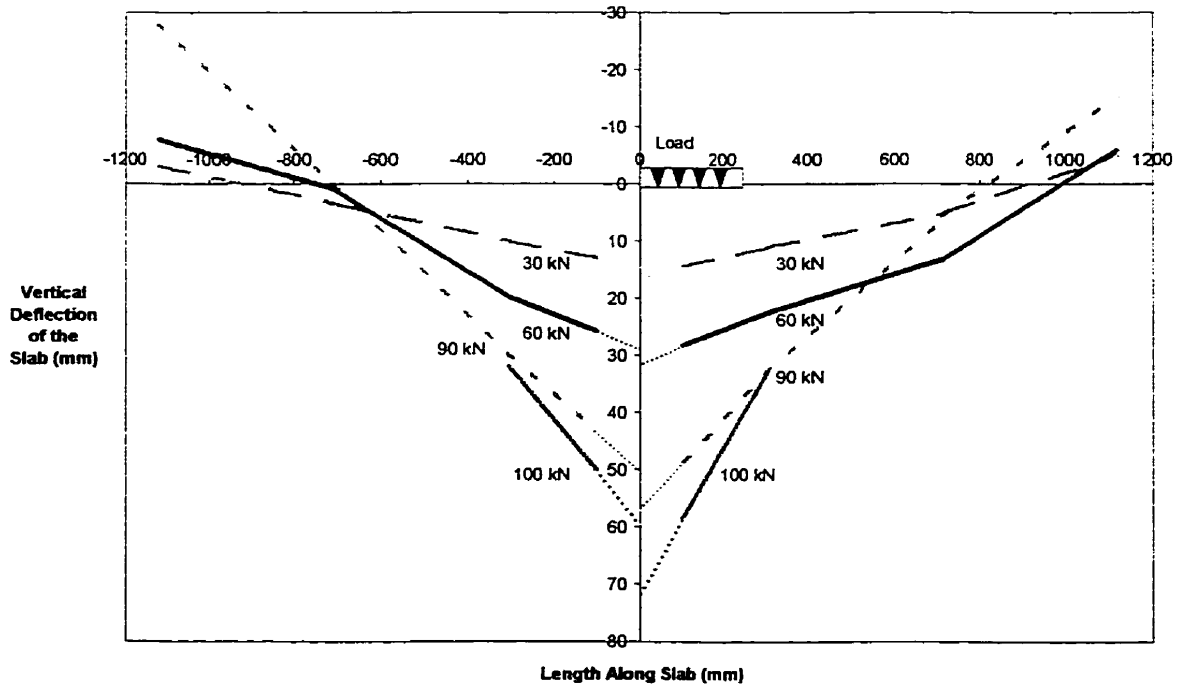

Figure 4-4: Load deflection curves: Phase I - FiberDowel

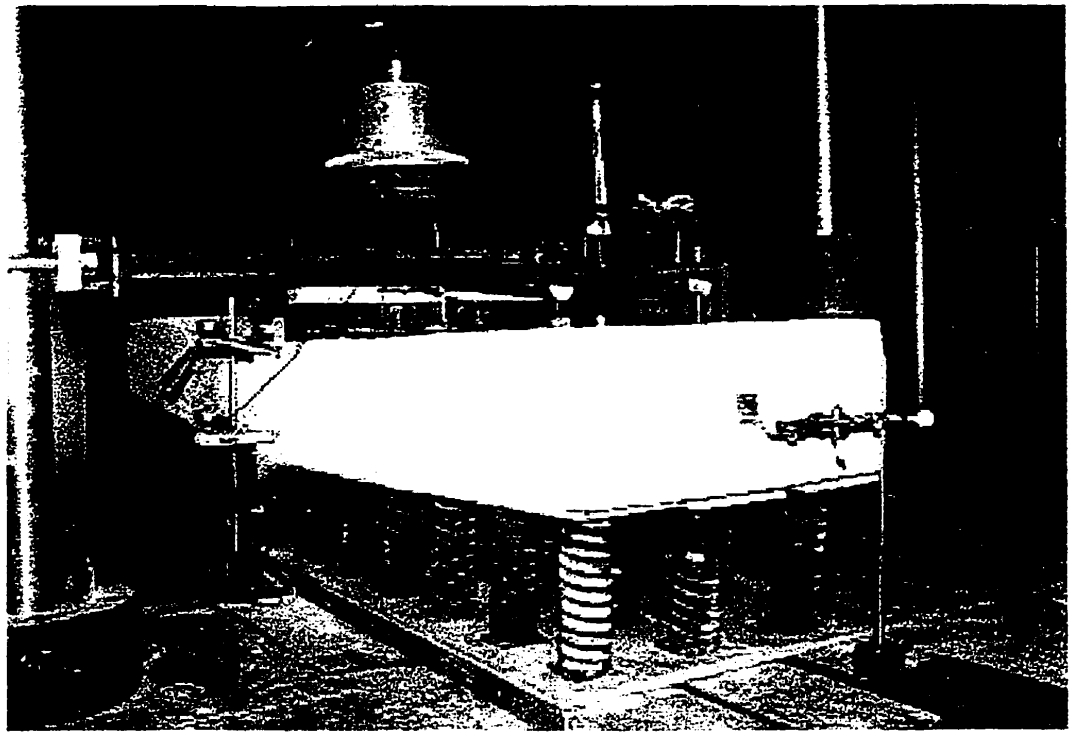

Figure 4-5: Side sway of the springs at load level 114 kN (25.65 kips)

4.1.3 Glasform Dowels

The measured deflection at different load levels for the specimen with Glasform dowels is shown in Figure 4-6. The joint deflection is extrapolated as illustrated by the dotted lines extending at each load level to the joint faces. This estimation can be made by assuming that no deformations take place in the slab during the test. This assumption is acceptable because of the linear deflection of the concrete slab throughout the test.

The first crack was observed at a load level of 54 kN. The load was continued to a load level of 135 kN which is slightly higher than the previous two tests. Again, the test was stopped due to excessive deflections and side sway of the steel springs supporting the slab.

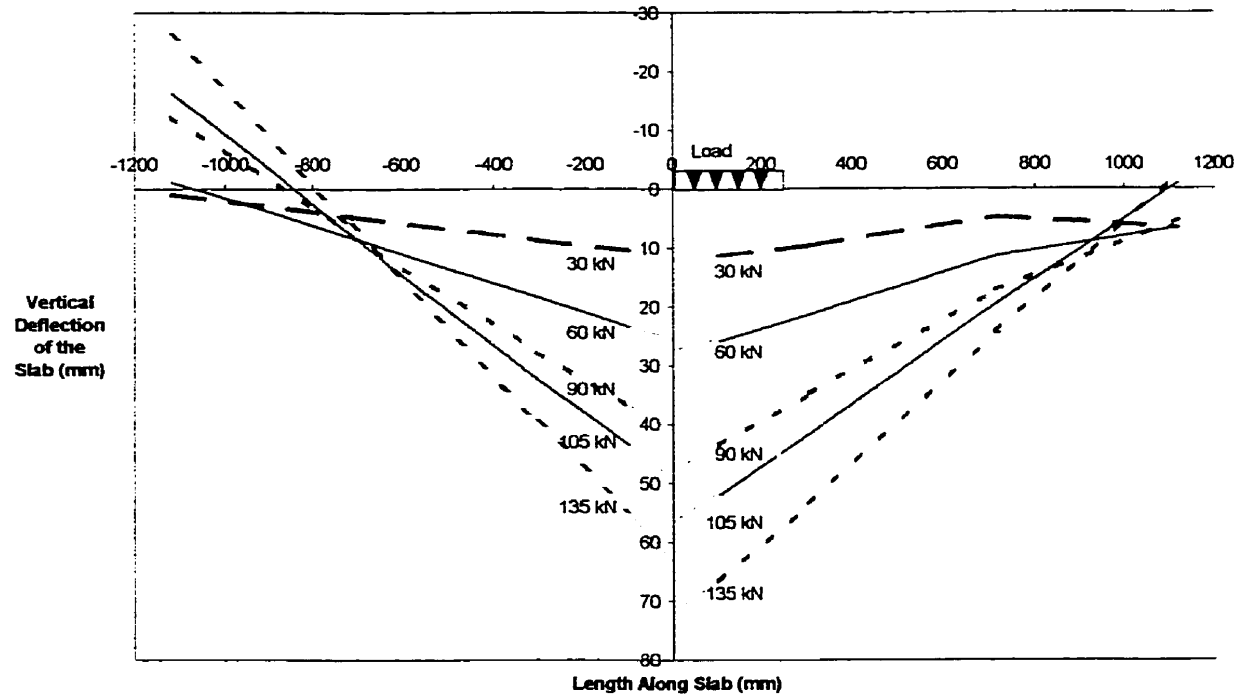

Figure 4-6: Load deflection curves: Phase I - Glasform dowels

4.2 Test Results of Phase II: Static Tests

This section of the report presents the data measured for the six specimens tested in phase II. Two specimens were cast for each of the epoxy-coated steel dowels, FiberDowels, and Glasform dowels. The load-deflection relationship along the length of the slab were measured for each specimen to determine the behaviour under different load levels. The deflection given on each side of the joint is used to assess the joint effectiveness. Comparisons of the behaviour of the two sets of slabs will be made in chapter 5.

4.2.1 Steel Dowels

Measurements of the deflection for the specimens with steel dowels are shown in Figure 4-7 and Figure 4-8. The behaviour of the two slabs remained linear during the test and caused lifting of the outer edges of the slab. The dotted lines have been extrapolated from the measured deflection at discrete points along the length of the slab.

The first crack under the loading plate occurred at a load level of 170 kN (38.25 kips) and continued to widen throughout the test. A second crack occurred on the opposite side of the slab from the first crack at a load level of 230 kN (51.75 kips). A new crack occurred on the loaded slab at a load level of 230 kN (51.75 kips).

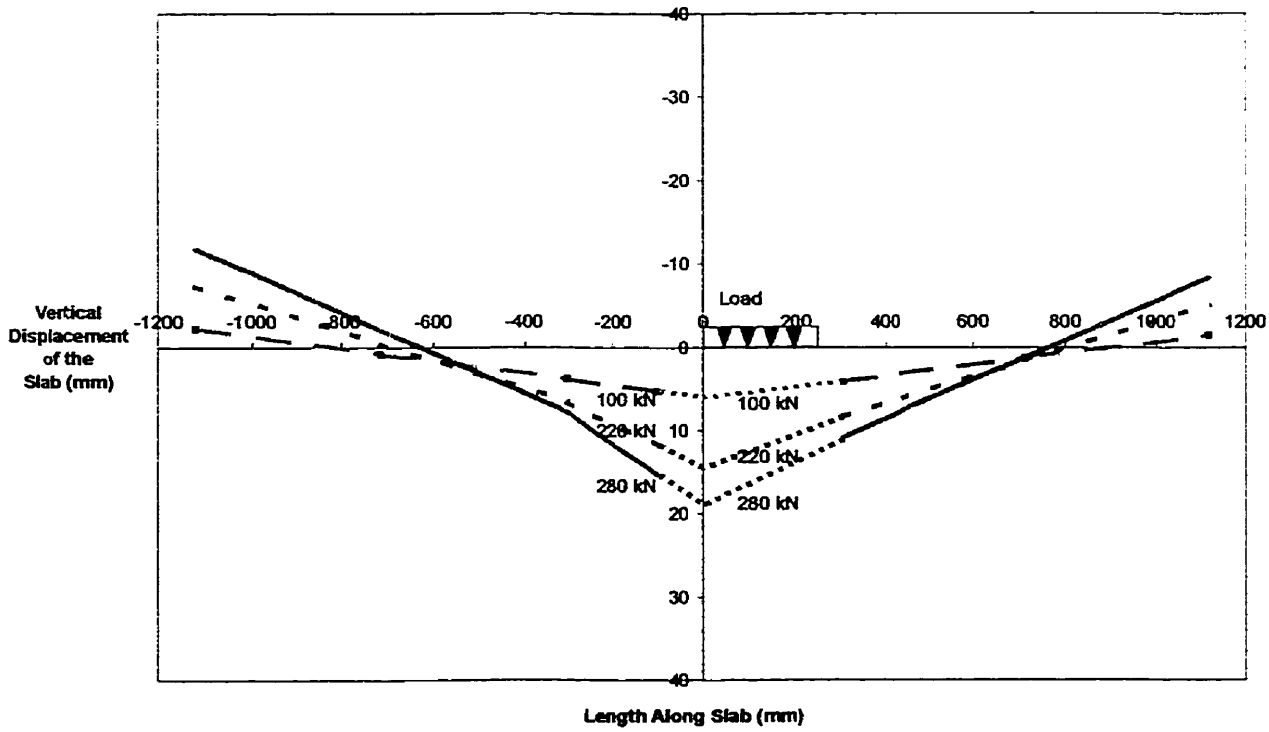

Figure 4-7: Deflection of Steel dowel slab from Phase II

The reloaded steel dowel slab was significantly cracked at a load level of 325 kN (73.1 kips), however, the loading continued up to a maximum load level of 650 kN (140.6 kips) at failure. Dial gauge readings and LVDT readings were found to correlate very well. Figure 4-8 illustrates the load-displacement when the specimen was reloaded up to failure. Steel dowels transferred the load to the unloaded slab causing the concrete to crack on the unloaded slab as seen in Figure 4-9.

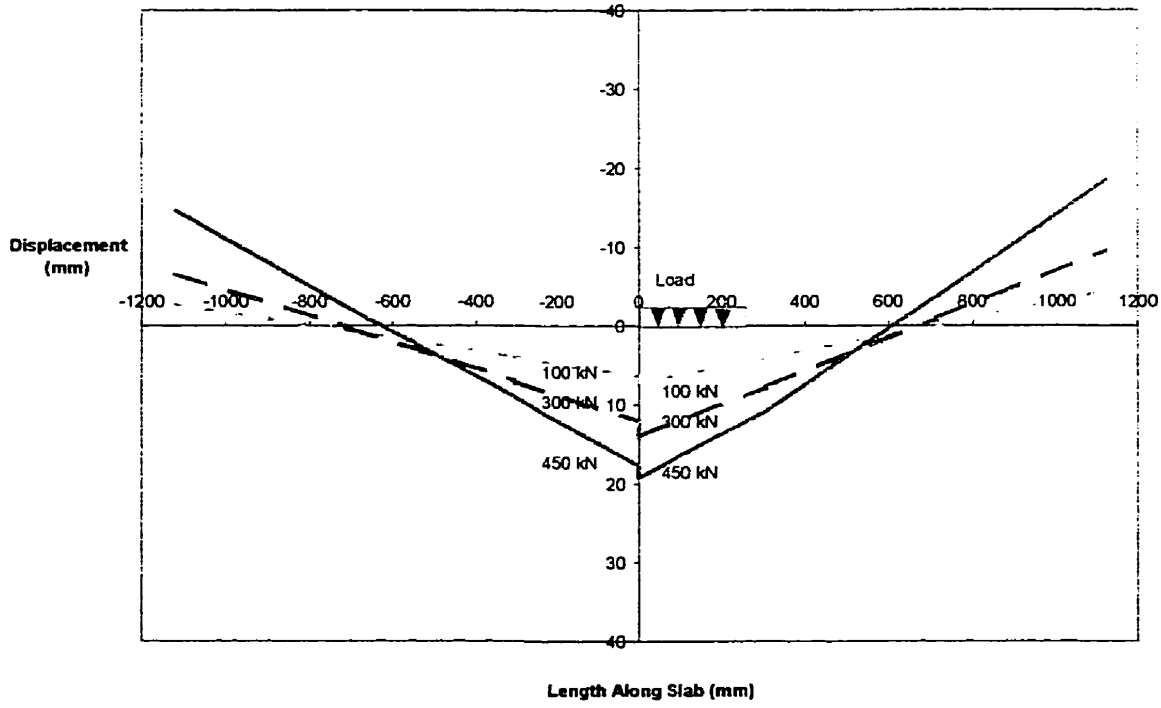

Figure 4-8: Behaviour during reloading the Steel doweled specimen to failure

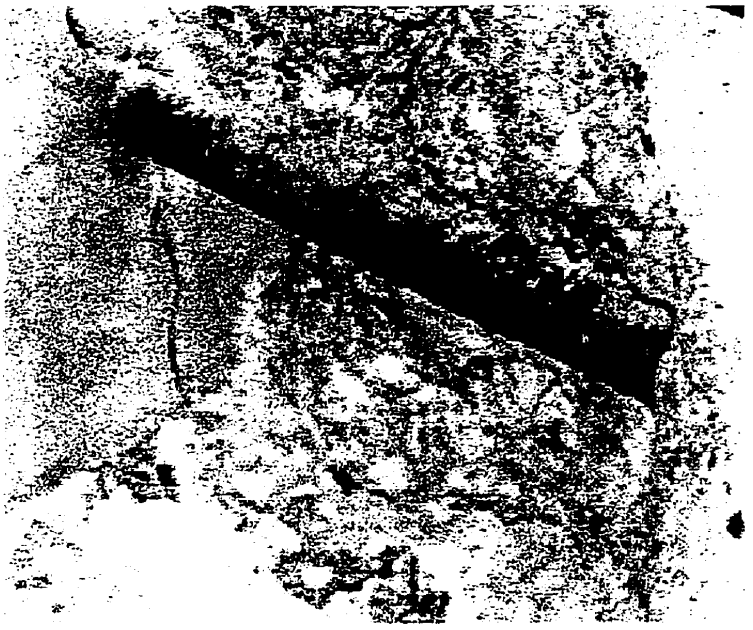

Figure 4-9: Exposed Steel dowel after slab failure: Phase II

A second steel-doweled specimen was tested in phase II. The displacement of this specimen under various load levels is shown in Figure 4-10. The linear displacement of the loaded side of the slab joint is disrupted by a severe crack that propagated through the specimen. Once this crack occurred, a large uplift at the end of the loaded side was observed.

First cracking of this specimen occurred at the loading plate at a load of 100 kN (22.5 kips). A second and third fine crack occurred on both sides of the specimen below the mid-line between a load of 180 kN (40.5 kips) and 220 kN (49.5 kips). At a load of 350 kN (78.7 kips) a very large crack was experienced at a distance of 400 mm (16 in) from the joint on the loaded side. This crack traveled the entire width and depth of the specimen and the slab experienced a large drop in the applied load. A crack also developed on the unloaded side once the slab reached the same load level. The unloaded side cracked again at a load of 500 kN (112.4 kips).

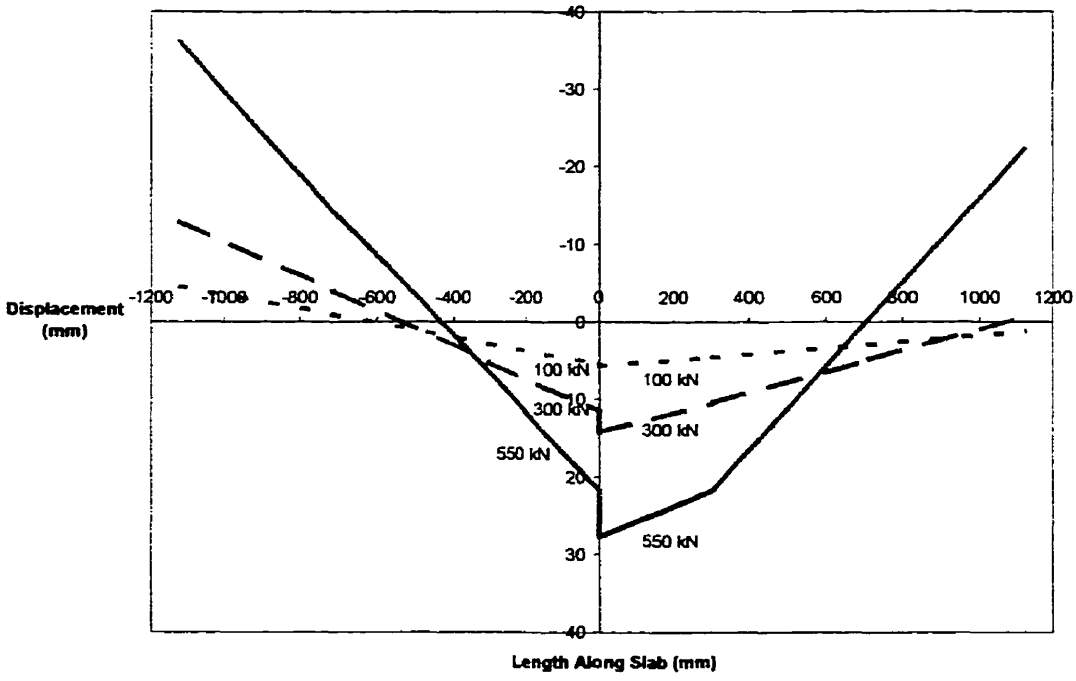

Figure 4-10: Deflection of second Steel dowel slab in Phase II

4.2.2 FiberDowels

The measured deflection of the slab with FiberDowels is shown in Figure 4-11. Throughout the test, hair cracks were observed due to bearing of the top edges of the slabs against each other starting at a load level of 310 kN (69.75 kips).

The specimen was reloaded to failure. Noticeable cracking occurred at loads ranging from 310 to 390 kN (69.75 to 87.75 kips). Extensive cracks occurred at a load of 540 kN (121.5 kips) as shown in Figure 4-12 at ultimate. It was observed that one dowel was completely sheared at this load level as shown in Figure 4-13. The other dowel had significant stress marks evident by whitened epoxy zones, and delamination of the fibers located at the maximum shear location as shown also in Figure 4-13.

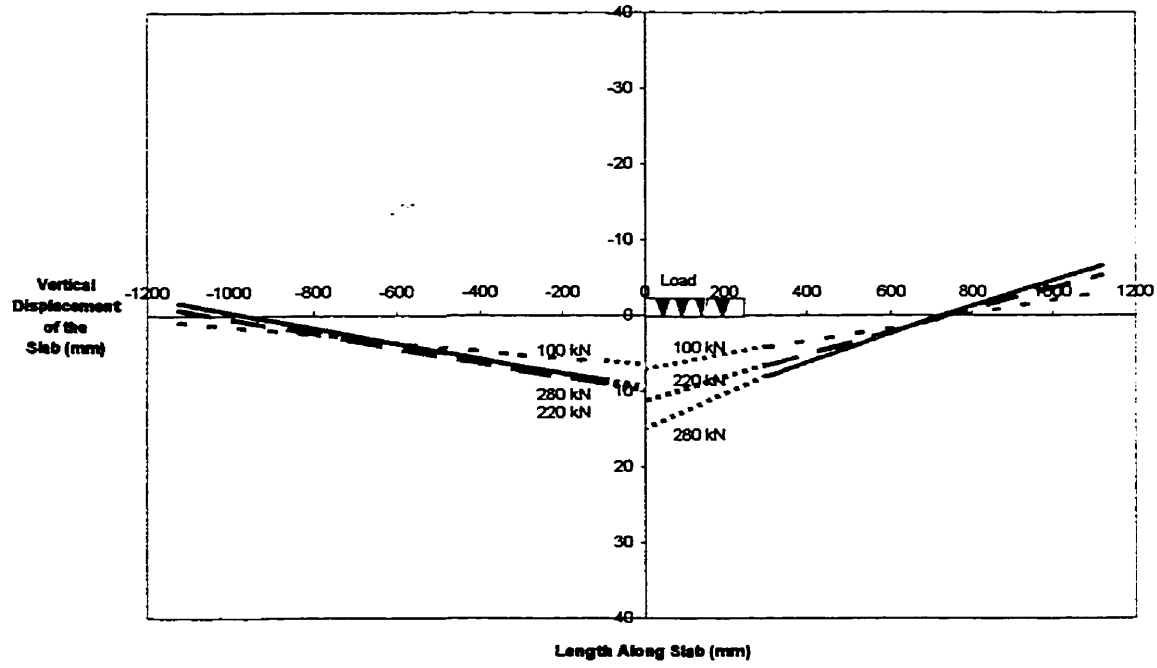

Figure 4-11: Deflection of specimen with FiberDowels from Phase II

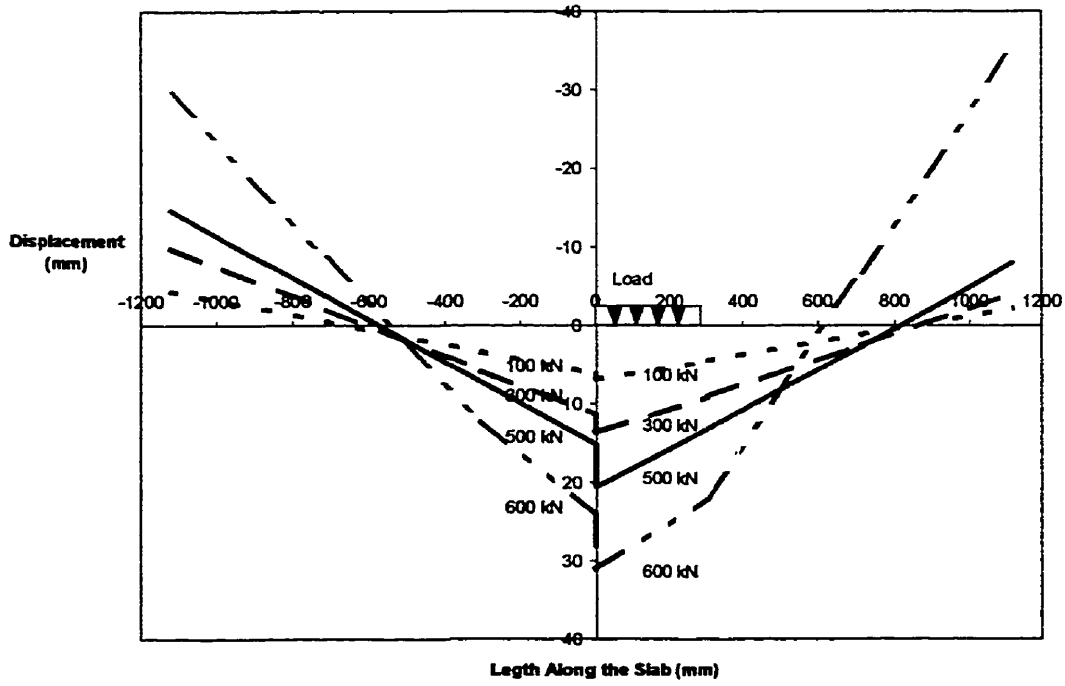

Figure 4-12: Deflection during reloading of the slab with FiberDowels in Phase II

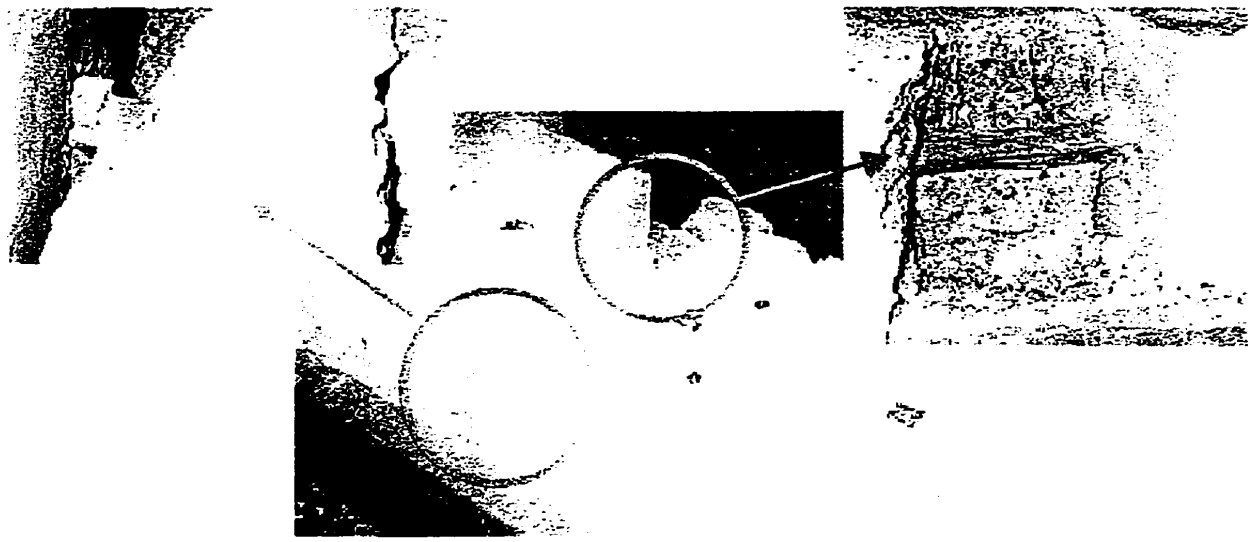

Figure 4-13: Failure of FiberDowel at load of 540 kN (121.5 kips) from Phase II

A second FiberDowel slab specimen was tested in phase II. This specimen was tested and the experienced deflections are shown in Figure 4-14. The test was stopped due to the extreme cracking that the specimen had experienced.

The first cracks occurred due to bearing of the tops of the joint at a load of 100 kN (22.5 kips). The next crack occurred below the mid-line of the slab at a load level of 260 kN (58.5 kips). A large crack on the loaded side occurred at 400 kN (90 kips) and passed through the entire slab. This crack created a similar non-linearity, or change in linearity, to the specimen as had occurred in the steel specimen. Other cracks developed near the mid-line at loads of approximately 550 kN (123.7 kips) including a crack on the unloaded side of the specimen.

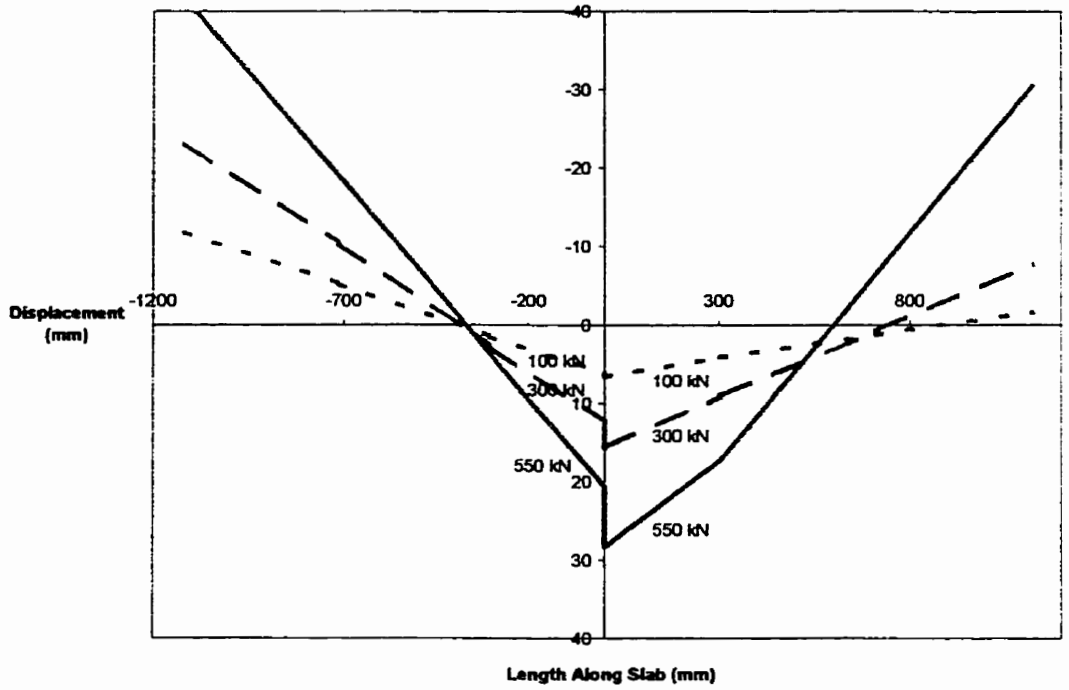

Figure 4-14: Deflection of second FiberDowel specimen in Phase II

4.2.3 Glasform Dowels

The measured deflections along the length of the slab are shown in Figure 4-15. This slab experienced its first crack at a load of 150 kN (34 kips) located at the top of the slab. The opposite side of the slab experienced a similar crack at a load of 250 kN (56 kips).

The specimen was reloaded to failure. The deflections that occurred during testing to ultimate can be found in Figure 4-15. The next cracking occurred at a load of 320 kN (72 kips), and a larger crack occurred at 500 kN (112.5 kips). The concrete that had failed was removed after the test to investigate the dowels. Both dowels appeared in good condition but the concrete was significantly crushed.

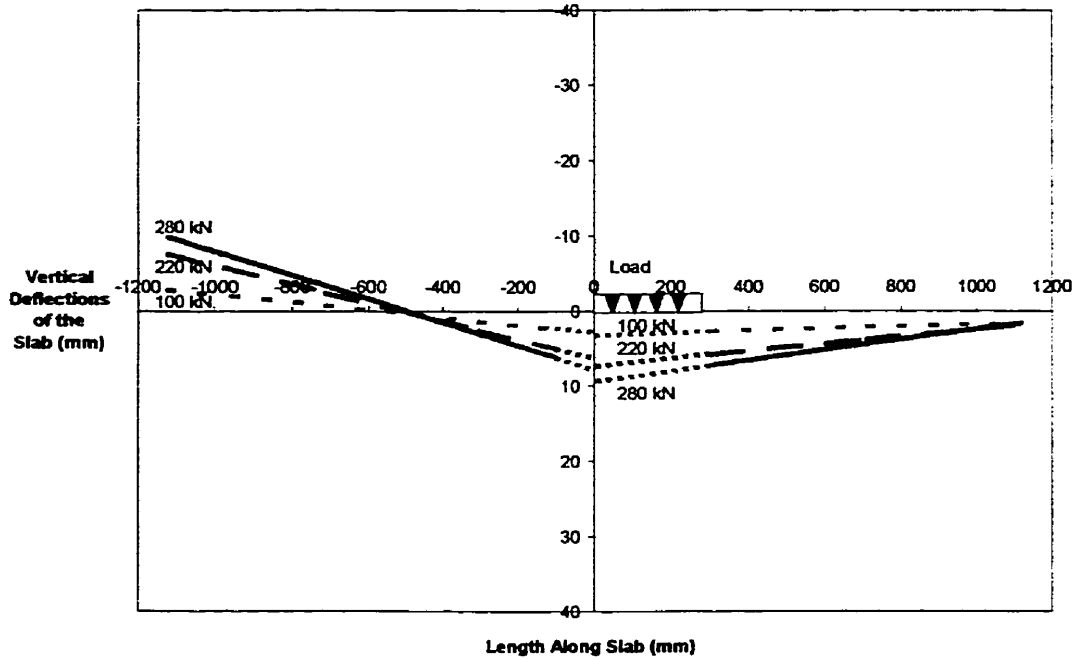

Figure 4-15: Deflection of the first Glasform specimen in Phase II

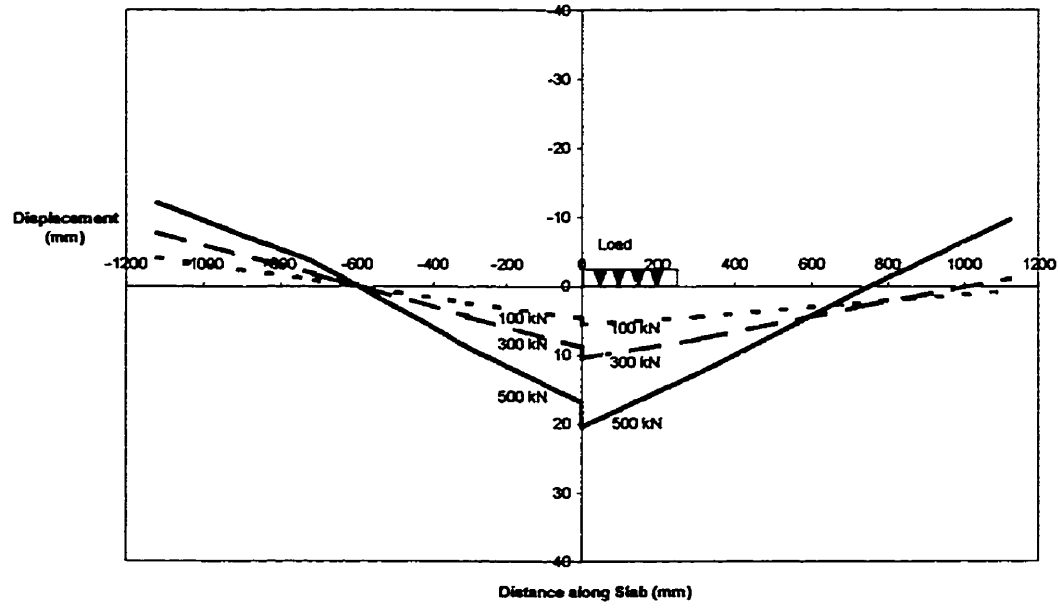

Figure 4-16: Behaviour during reloading first Glasform specimen in Phase II to failure

A second Glasform dowel slab was tested in phase II. The deflection of the GFRP Glasform specimen is shown in Figure 4-17. A large crack developed again on the loaded side of the specimen. This crack occurred at a load of 260 kN (58.5 kips), slightly less than the previous two specimen.

The first cracks observed were bearing cracks at a load of 80 kN (18 kips) followed by a crack just down from the top of the slab at a load of 140 kN (31.5 kips). A third crack occurred on the opposite side of the slab in the same manner at a load of 180 kN (40.5 kips). The next crack was a large crack through the specimen followed by some cracking of the unloaded side of the specimen between loads of 350 kN (78.7 kips) to 450 kN (101.2 kips). This test was stopped due to the crushing of the concrete in the compression zone as shown in Figure 4-18.

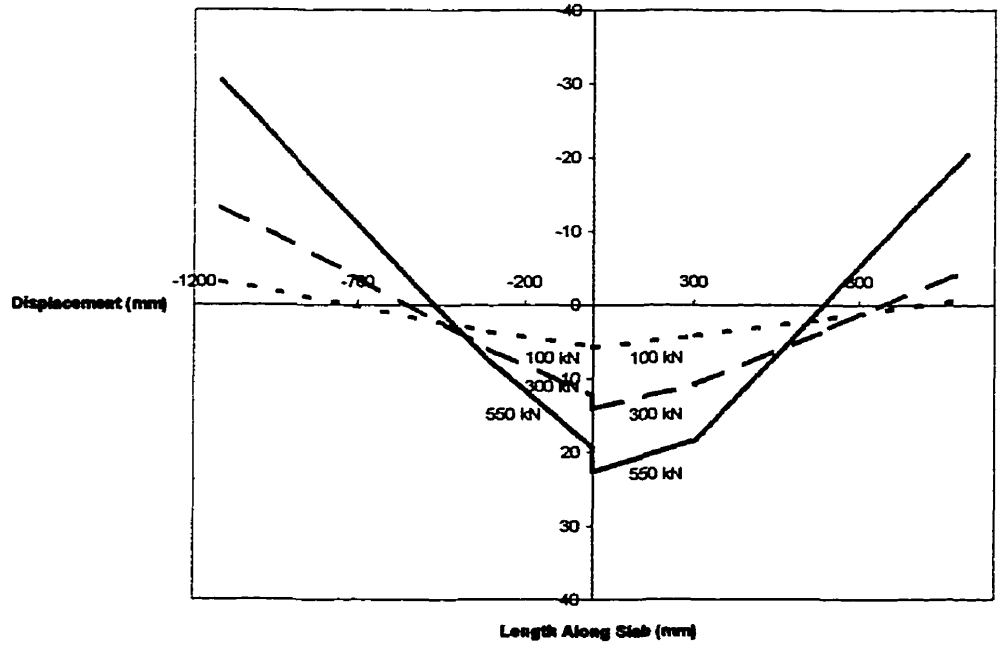

Figure 4-17: Deflection of second Glasform specimen in Phase II

Figure 4-18: Crushing of concrete on the second Glasform specimen in Phase II

4.3 Test Results of Phase III: Cyclic Tests

Slabs with the three types of dowels were subjected to cyclical loading. All slabs were supported by a compacted 'A-Base' limestone. Instrumentation used were similar to the one for phase II and typically shown in Figure 3-10. After completion of a certain specified number of cycles, static tests were performed to examine the efficiency of the joint between sets of cyclic testing. Each slab was tested to a total of two million cycles of applied static load. The limestone subbase was tested before placement of each slab and again following the completion of the cycles. A summary of each dowel type follows.

4.3.1 Steel Dowels

The results gathered from the testing of the steel doweled slab under cyclic loading showed no signs of concrete failure under the load range of 20 kN (4.5 kips) to 130 kN (29.25 kips). The slab was statically tested to the maximum cyclically applied

load of 130 kN (29.25 kips) following a set number of cycles, as shown in Table 3-8. The displacement along the length of the slab at a load level of 130 kN is shown for all the cycles in Figure 4-19. The largest change in displacement can be seen to follow the first static test when the base material is initially compressed under the applied load.

4.3.2 FiberDowels

The FiberDowel slab results were consistent with the steel dowel results with respect to the base behaviour. As can be shown in Figure 4-20, the initial static test experienced a larger displacement as the base material compacted. The magnitude of the remaining displacements compare to those experienced with the steel specimen. Following the 100000 cycle, a crack at the joint location was noticed. It was a very fine crack and did not appear to increase in size with the additional cycles.

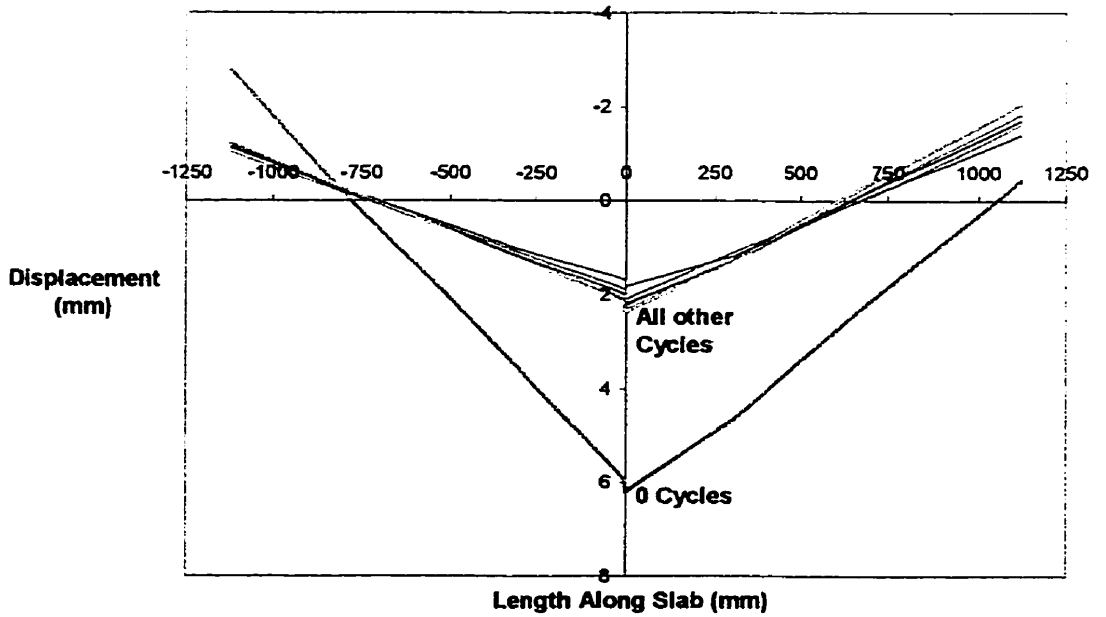

Figure 4-19: Displacement along Steel dowel specimen in Phase III at 130 kN (29.25 kips)

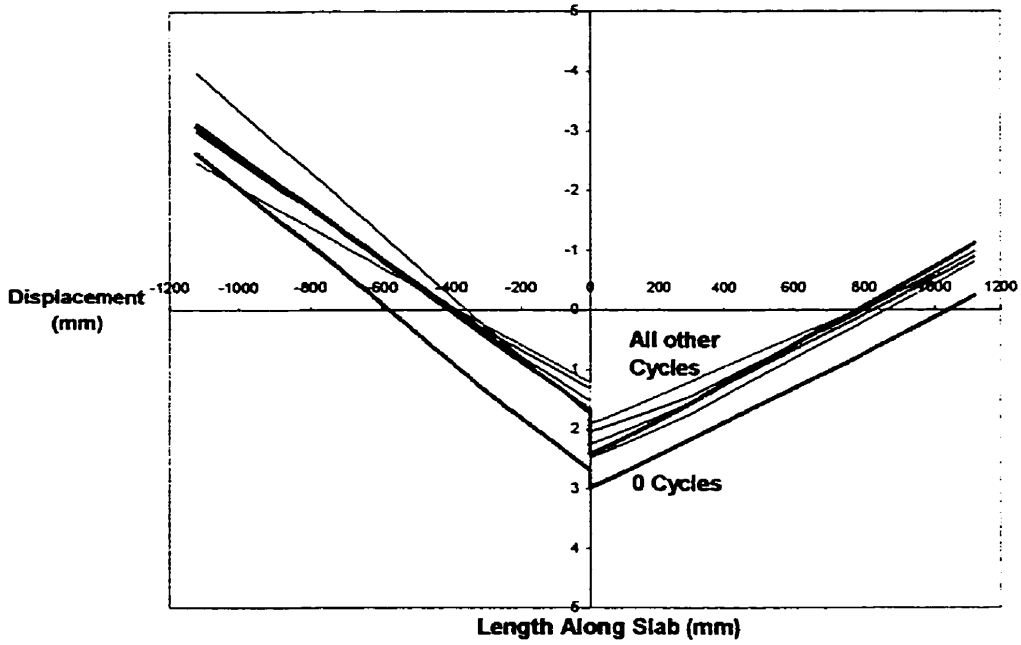

Figure 4-20: Displacement along FiberDowel specimen in Phase III at 130 kN (29.25 kips)

4.3.3 Glasform Dowels

The results from the eight static tests conducted on the Glasform specimen are provided in Figure 4-21. Displacement of the slab under the initial static loading was larger due to the increase in compaction of the base material. Subsequent static tests experienced little variation in the magnitude of the displacement.

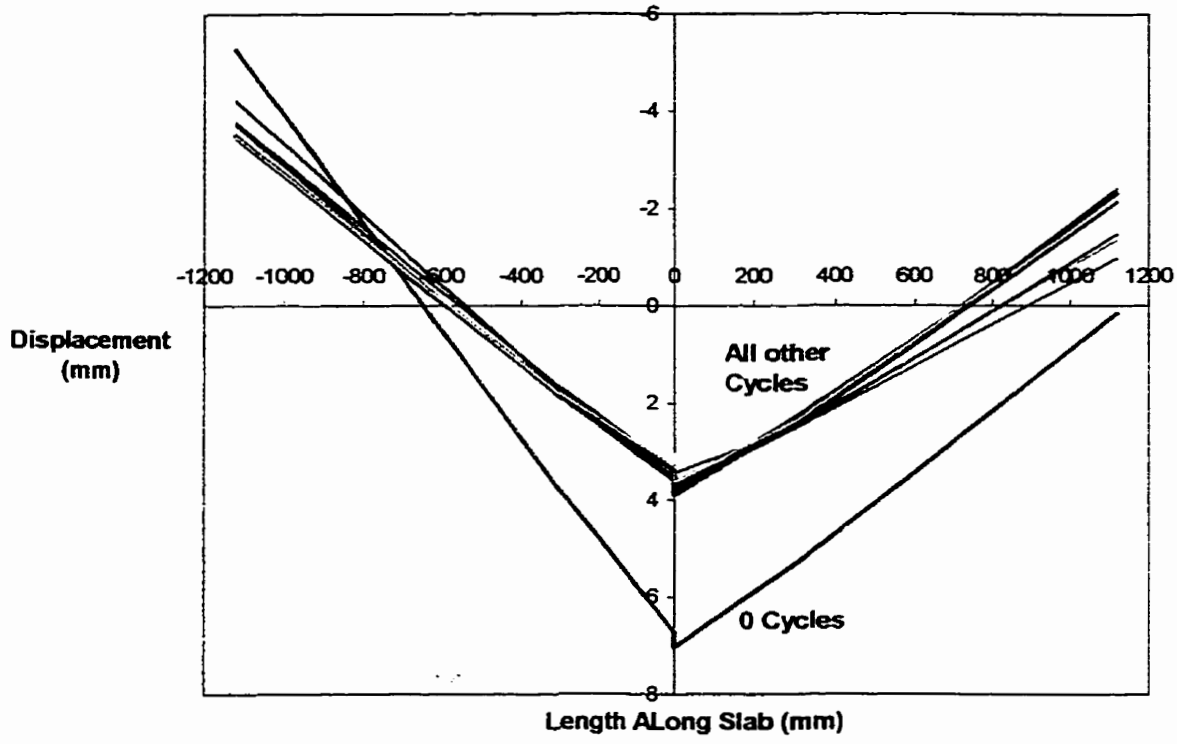

Figure 4-21: Displacement along Glasform specimen in Phase III at 130 kN (29.25 kips)

Chapter 5 Analysis of Test Results

5.1 Analysis of Phase I: Static Tests

The first phase of this program included three specimen using steel, Glasform, and FiberDowel dowels. A series of springs were used to simulate weak subgrade soil conditions and possible settlement of soil at the joint location. Performances of the three types of dowels were almost identical and controlled by failure of the concrete pavement. The joint effectiveness of transferring the load ranged from 86 to 100 percent. The load versus the deflection of the joint differential displacement, loaded deflection minus the unloaded deflection, is shown for all the types of dowels in Figure 5-1. The initial results suggest that the use of GFRP dowels could provide similar load transfer mechanisms as epoxy coated steel dowels even for the severe weak soil conditions.

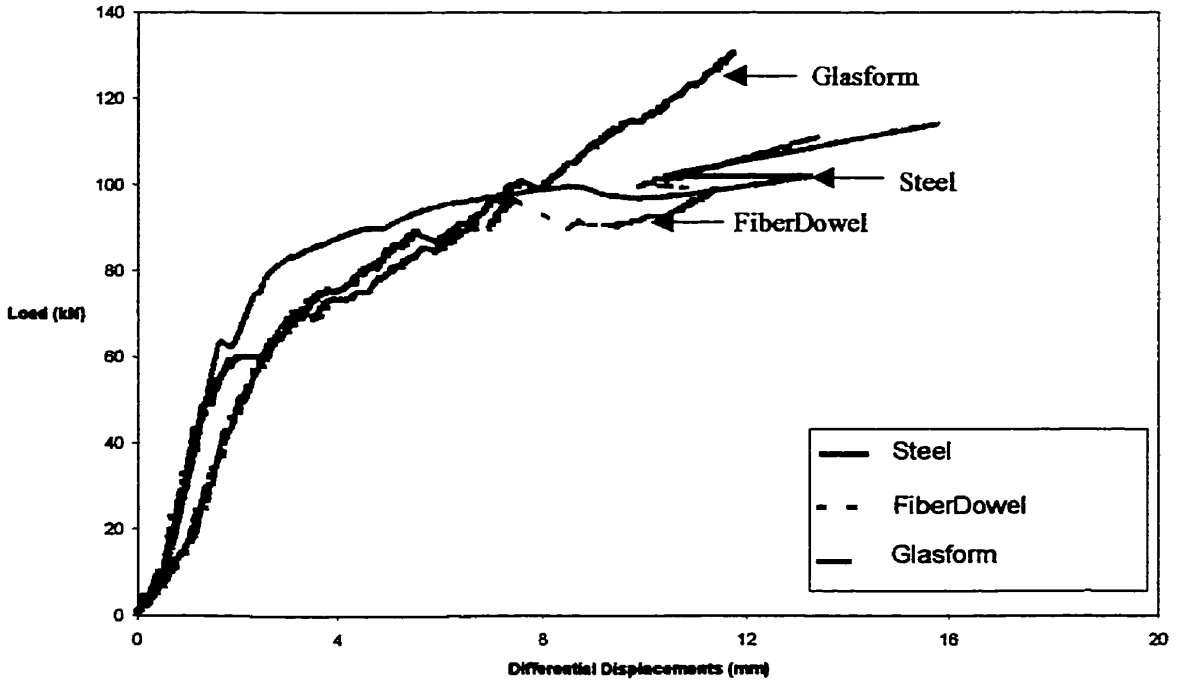

Figure 5-1: Differential displacement at the location of the applied load for Phase I

To determine the effectiveness of the dowels, the deflection of each of the loaded and unloaded slabs is required to determine the effectiveness based on Equation 2-2. Figure 5-2 illustrates the dowel bars effectiveness over the load range. It can be seen that the dowels continue transferring the load up to a maximum value in the range of 60 kN (13.5 kips) before a loss of effectiveness. Significant reduction of the effectiveness was observed, as shown in Figure 5-2, for all types of dowels due to the weakness of the supporting soil. In phase I, the joint effectiveness of all types of dowels tested was relatively high and in the range of 90 percent when compared to an acceptable effectiveness value of 75 percent.

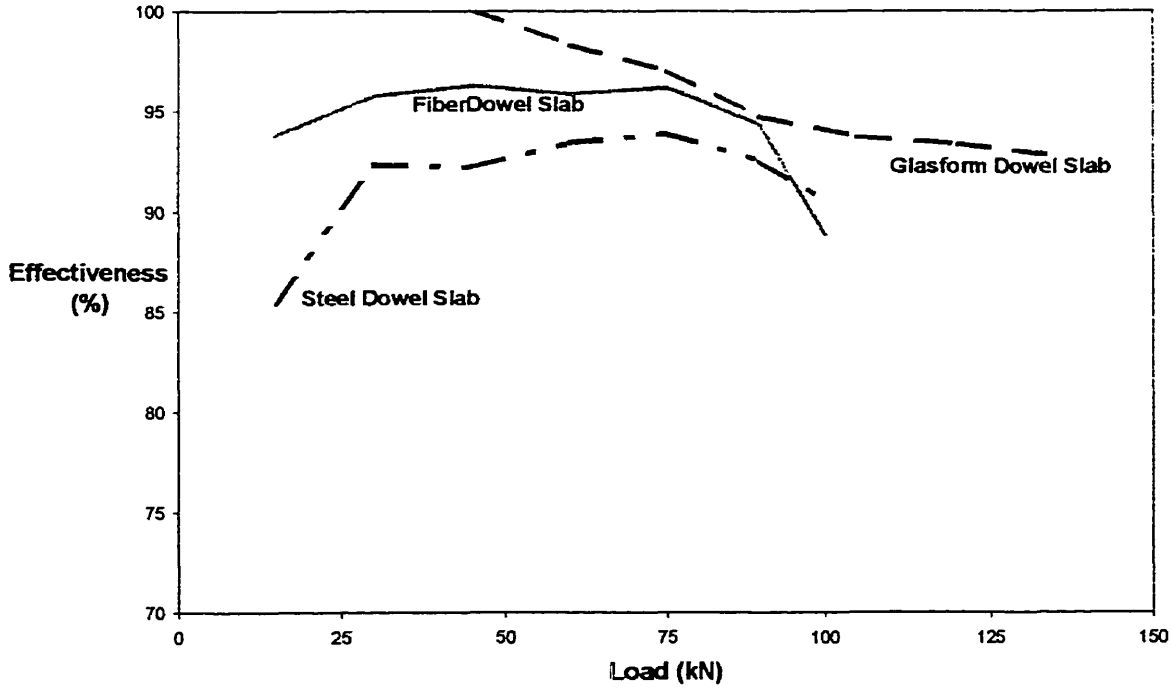

Figure 5-2: Joint effectiveness of slabs from Phase I

5.2 *Analysis of Phase II: Static Tests*

The second phase of this program included six specimens using the same three types of dowel materials used in the first phase. The slabs were supported by a compacted, graded 'A base' gravel material which provided a dense subgrade with a subgrade modulus in the range of 133.3×10^3 kN/m^3 (394 tons/ft^3). The effectiveness of the joints ranged from 96 to 99 percent at a load of 280 kN. Table 5-1 and Table 5-2 summarize all the dowel materials and their corresponding load transfer effectivenesses and displacements at three distinct load levels for the first slab in phase II. The base materials modulus was measured between tests and no large difference was found. In observing the dropping magnitude of the ultimate displacements of the first test, some compaction of the base material must be assumed. The retested slab does not experience this difference in ultimate displacement. Each slab experienced a displacement within a few of millimeters of each other. One of the main differences comes when comparing the initial joint effectiveness. The retested slab's joint effectiveness is reduced by up to 8 percent. This could be due to the compaction of the subbase or the crushing of the concrete surrounding the dowels allowing for greater kinking in the dowel.

The loads versus the differential deflections of the three joints are shown in Figure 5-3 and Figure 5-5. From these figures, correlation can be made between the behaviour of the slab and the slope of the curve. When one of the curves experiences a sharp change in slope, or a drop in load, a crack has occurred somewhere within the joint region.

The load transfer effectiveness was determined for each type of dowel using the measured displacement of the unloaded and loaded slab at the joint as determined from

Equation 2-2. These effectivenesses are shown in Figure 5-4 for the first slab tests, where the specimens were tested up to a load level of 280 kN (63 kips), and in Figure 5-6 for the retested slabs, for the same specimens tested to failure. The results suggest that GFRP could even provide better effectiveness under static loading conditions in comparison to steel dowels.

Table 5-1: Dowel Effectiveness and Relative Displacements for First Slabs in Phase II

Dowel Material	Effectiveness (%)			Relative Displacement (mm)		
	100 kN	200 kN	280 kN	100 kN	200 kN	280 kN
Epoxy-Coated Steel	97.9	96.1	96.5	6.4	11.7	16.4
FiberDowel	99.5	97.1	96.7	4.6	6.4	8.3
Glasform	100	98.9	99.4	2. 5	5.3	6.9

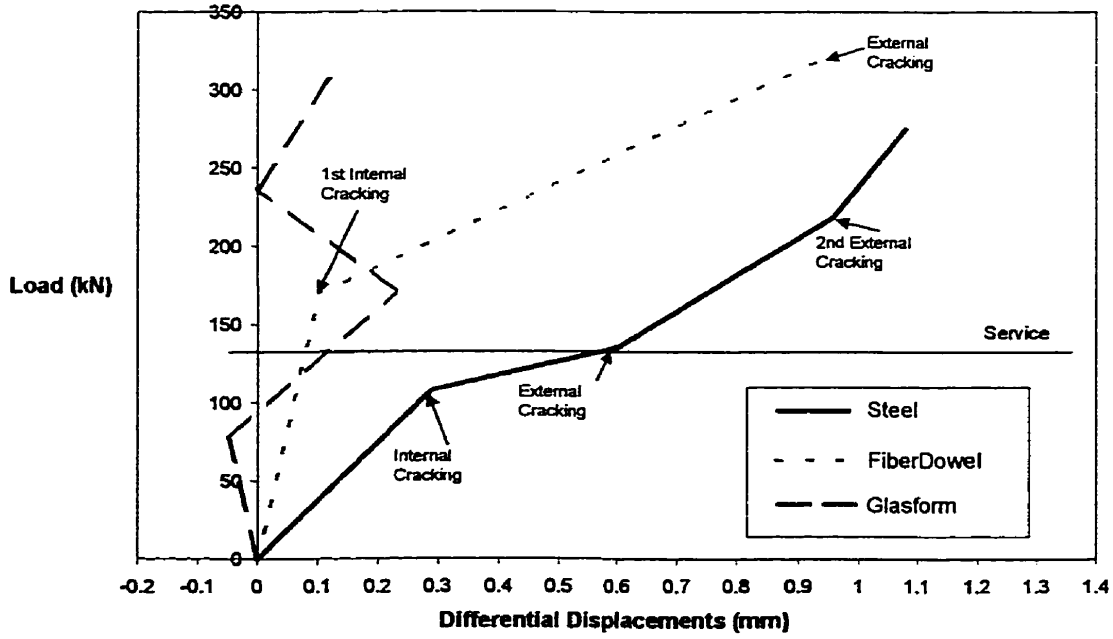

Figure 5-3: Differential displacements of first slabs from Phase II

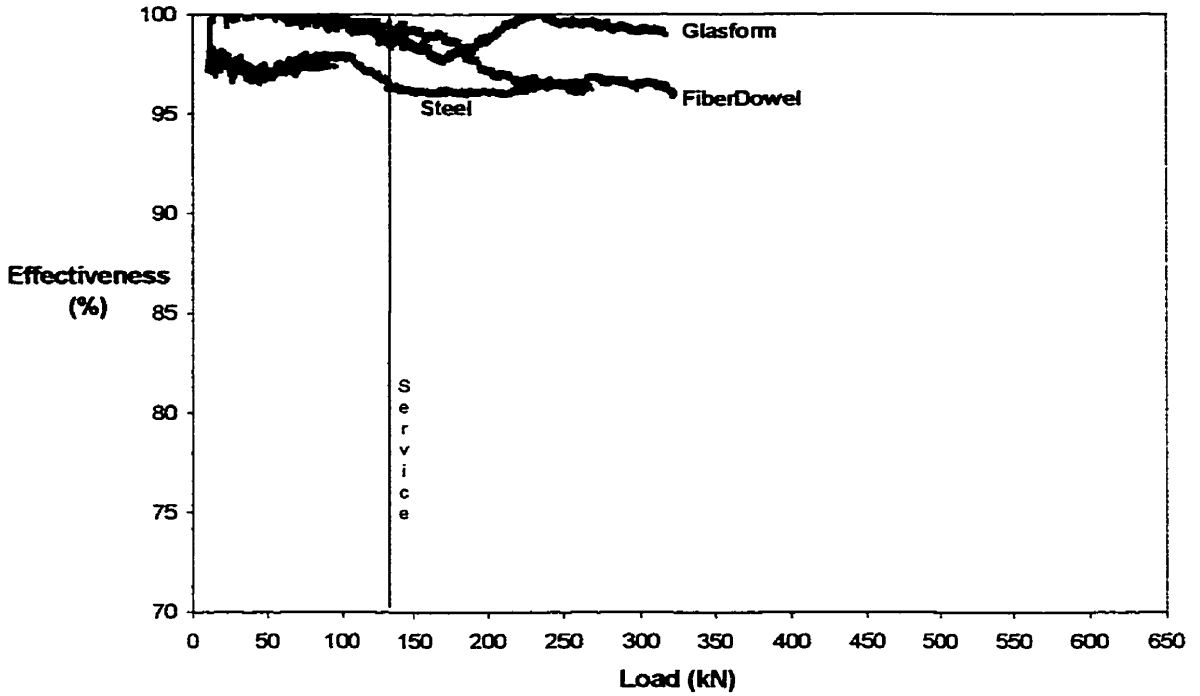

Figure 5-4: Joint effectiveness for first set of slabs tested in Phase II

Table 5-2: Dowel Effectiveness and Relative Displacement for Retested Specimen tested in Phase II

Dowel Material	Effectiveness (%)			Relative Displacement (mm)		
	100 kN	200 kN	400 kN	100 kN	200 kN	400 kN
Epoxy-Coated Steel	94.3	93.8	95.9	7.2	10.8	17.2
FiberDowel	94.4	92.9	87.3	6.9	10.8	20.4
Glasform	91.9	92.7	91.8	5.5	8.1	17.1

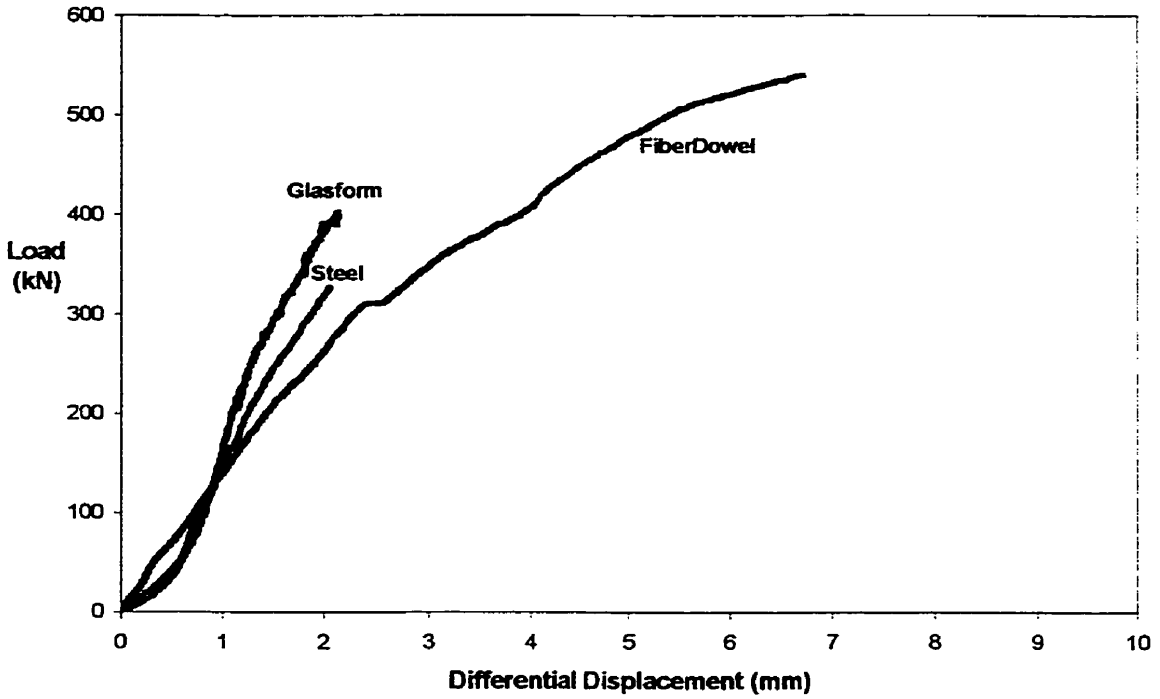

Figure 5-5: Differential displacements of retested first set of slabs from Phase II

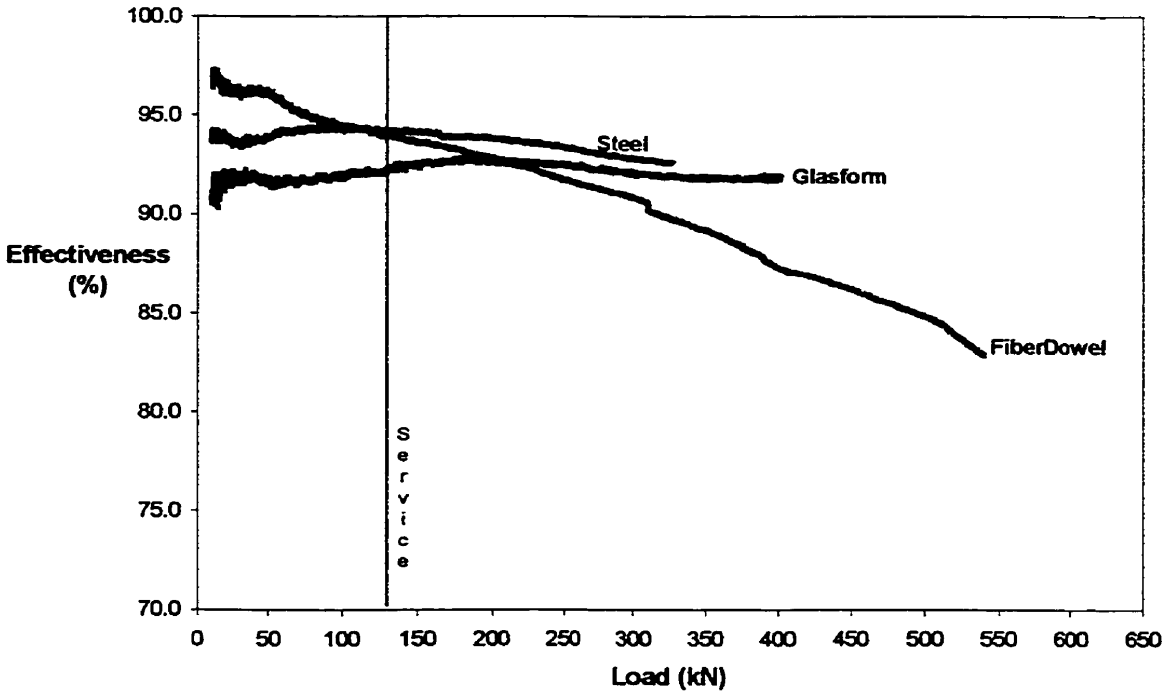

Figure 5-6: Joint effectiveness for Retested first set of slabs from Phase II

In comparing the joint effectiveness figures from the two tests conducted upon the first slabs in phase II, it is readily noticeable that the effectiveness has been reduced. When the slabs were retested, the steel and the Glasform dowels appear to have a stable joint transfer effectiveness whereas the FiberDowel has a steadily declining effectiveness which starts at the same level as where it left off from the first test. The other two materials did not have this similar continuation of effectiveness between tests.

To illustrate any trends that may occur with the materials tested, a second set of slabs was tested. Table 5-3 contains the joint effectiveness and relative displacements at the same three distinct load levels as the first slab. These slabs were tested continuously to failure without interruption. The joint effectiveness at a load level slightly below service ranges from 97 to 99 percent with relative displacements in the range of 6 to 7 millimeters. The base material used for these tests was stable and the differential displacements between the tests were within a few millimeters. The magnitude of the displacements compared also to those experienced when the first slab was retested.

Since this test was continued to failure, the joint effectivenesses must be compared to those from the first test. At the 100 kN load level, the steel and the Glasform specimen match within less than a percentage but the FiberDowel varies by almost 5 percent. At the next load level of 200 kN, all specimen vary by approximately 6 percent. Since the load level of 400 kN is only provided for the retested slabs, the effectiveness at this level will be used for comparison. The steel and Glasform slabs vary by approximately 3 percent but the FiberDowel is at the same joint effectiveness. This would follow the finding from the two tests conducted on the first slab where the FiberDowel slab experienced a continually declining joint effectiveness.

Table 5-3: Dowel Effectiveness and Relative Displacements for the Second Slab in phase II

Dowel Material	Effectiveness (%)			Relative Displacement (mm)		
	100 kN	200 kN	400 kN	100 kN	200 kN	400 kN
Epoxy-Coated Steel	97.3	90.6	92.8	5.7	10.6	19.7
FiberDowel	95.2	90.1	87.5	7.3	11.8	22.0
Glasform	99.2	93.5	94.2	5.8	10.0	17.6

The data gathered from the tests conducted on the second set of slabs in phase II have been organized into similar figures as the first set. Figure 5-7 illustrates the differential displacements of the loaded to unloaded side of the slabs. As mentioned before, any large change in slope means that the slab has experienced a crack and subsequent loss in load.

The joint effectiveness for each slab, as shown in Figure 5-8, initially have stable values up until the service load. The FiberDowel slab begins to loose stability at approximately 100 kN as opposed to after the 130 kN service mark. After the load is beyond the service mark, all the dowels' joint effectiveness decline. When cracking occurs following the service load, the joint effectiveness is effected. The slab, following cracking, must settle or displace and may do so in a manner that may make the joint effectiveness value increase. This would mean that either more load was transferred due to some local concrete failure, creating more deflection on the unloaded side, or the loaded side experienced a crack which caused some of the concrete to rise. The second scenario, of the concrete cracking around the dowel and rebounding slightly, a fraction of a millimeter, seems to be the most plausible.

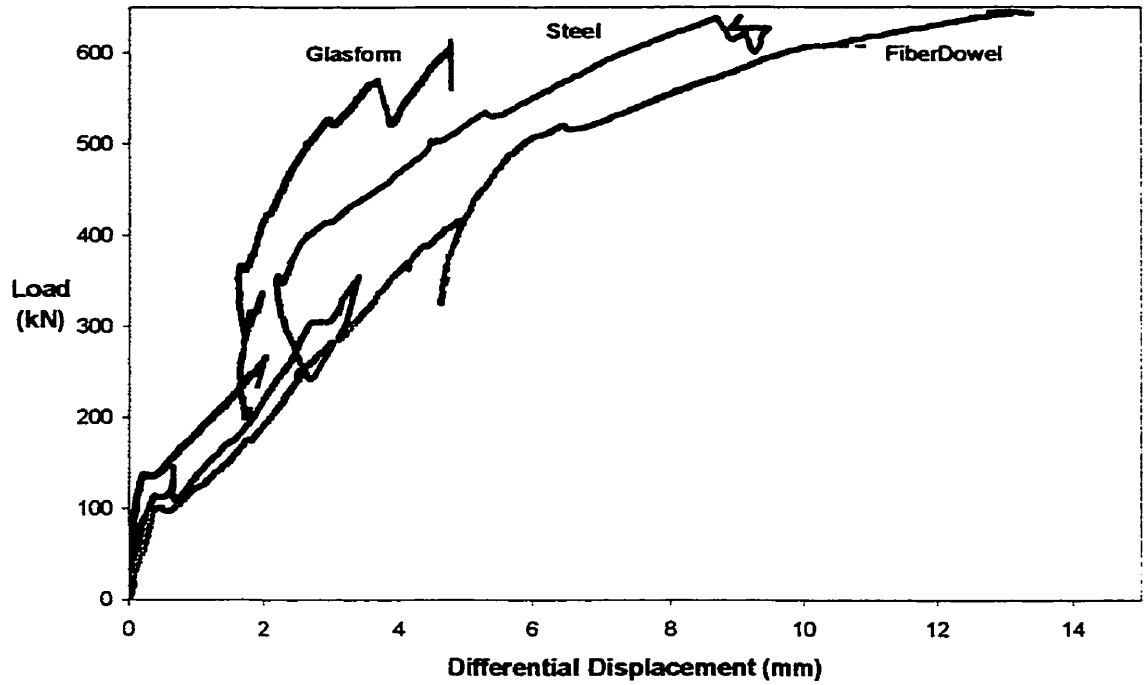

Figure 5-7: Differential displacements of second set of slabs tested in Phase II

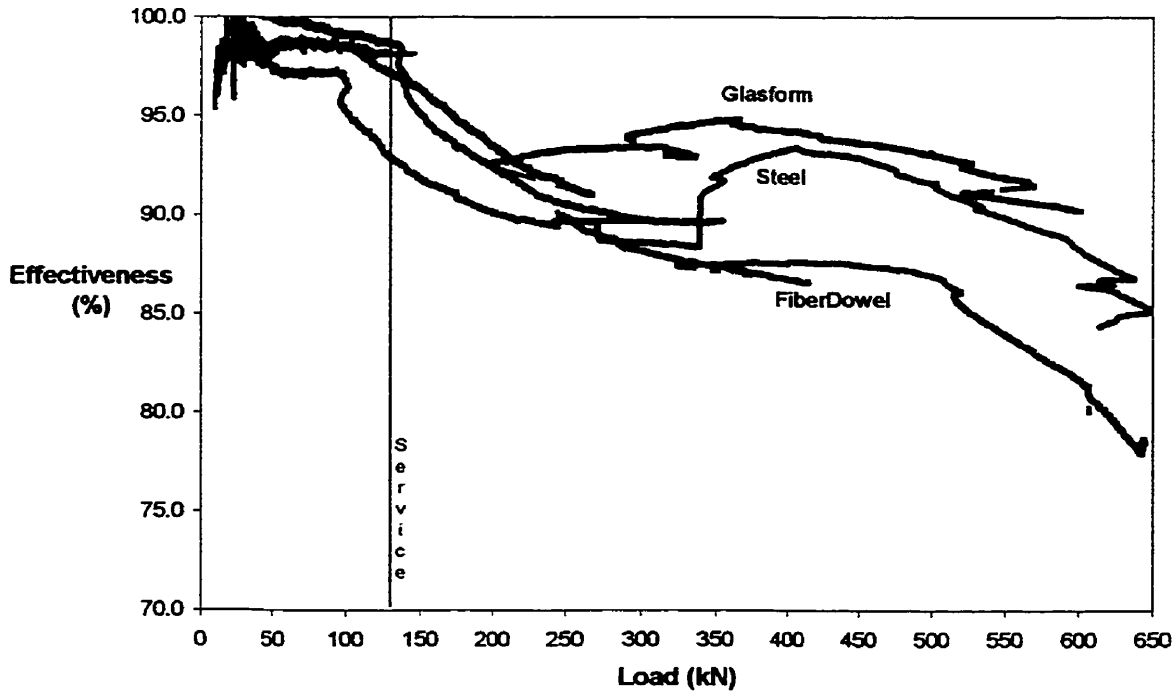

Figure 5-8: Joint effectiveness for second set of slabs from Phase II

5.3 Analysis of Phase III: Cyclic Tests

Three slabs were tested in phase III, each to one million cycles of a load range from 20 kN to 130 kN. Static tests were conducted to the maximum cyclic load level at certain intervals to monitor the joint effectiveness throughout. Each specimen received a freshly compacted subbase in which to start off the testing. An initial static test was conducted to determine the joint effectiveness before the cycles began and can be used to compare to the data gathered in phase II within the same load range.

The joint effectiveness of the steel doweled slab over the one million cycles is shown in Figure 5-9. The initial static test has an effectiveness in the range of 99 percent and the next test after one hundred cycles has an effectiveness of 96 percent. Each test after the second experiences a drop in effectiveness of less than one percent except the final test, at one million cycles, where it experiences a increase of approximately one percent compared to the test conducted at six hundred thousand cycles. This placed the joint effectiveness at one million cycles at the mid point of all the curves, giving a joint effectiveness of 95 percent. The total range of joint effectiveness for the steel dowel slab was from 93 to 96 percent.

In order to examine the loss of joint effectiveness trend, Figure 5-10 illustrates the gentle reduction of the joint effectiveness up to the one hundred thousand cycles. The next cycle step experiences a reduction followed by a rebound in joint effectiveness. Three load levels are plotted to monitor the dowel load effectiveness during the test.

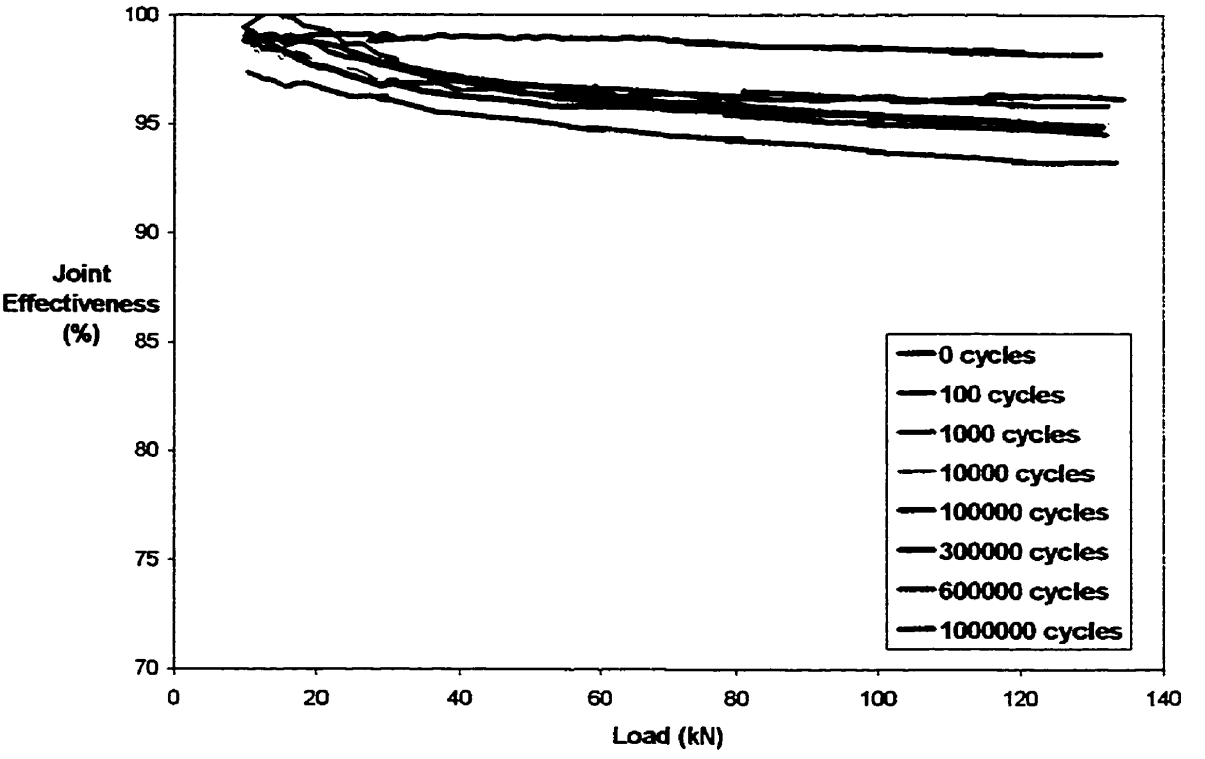

Figure 5-9: Joint effectiveness of Steel dowel slab under cyclic loading: Phase III

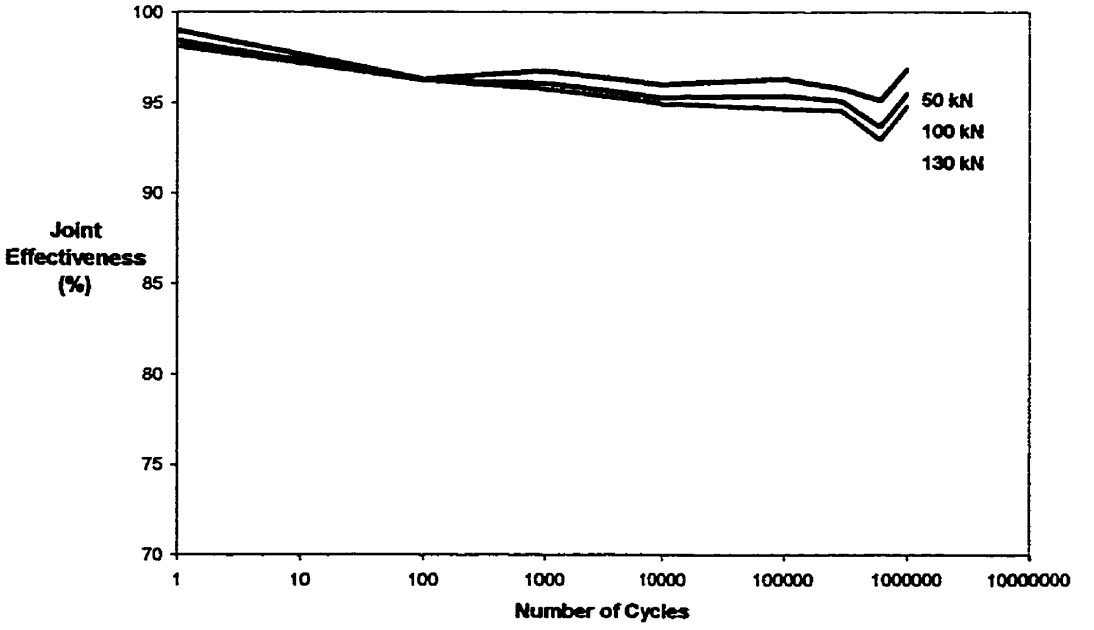

Figure 5-10: Steel dowel slab joint effectiveness vs. log number of cycles

The joint effectiveness of the FiberDowel slab tested in phase III is illustrated in Figure 5-11. An initial test before cycles were started was conducted but did not correlate to the rest of the measured data. A large reduction in the range of 10 percent was experienced from the first test to the second test. Subsequent tests behaved similar to those of the steel doweled slab, experiencing only minor reductions of effectiveness at each cycle step. Again, the slab experienced an increase of joint effectiveness with the final one million cycles. The range of joint effectiveness experienced for the FiberDowel slab was 77 to 83 percent. Although the magnitude of the effectiveness is still above the 75 percent acceptability level, the steel effectiveness is much greater.

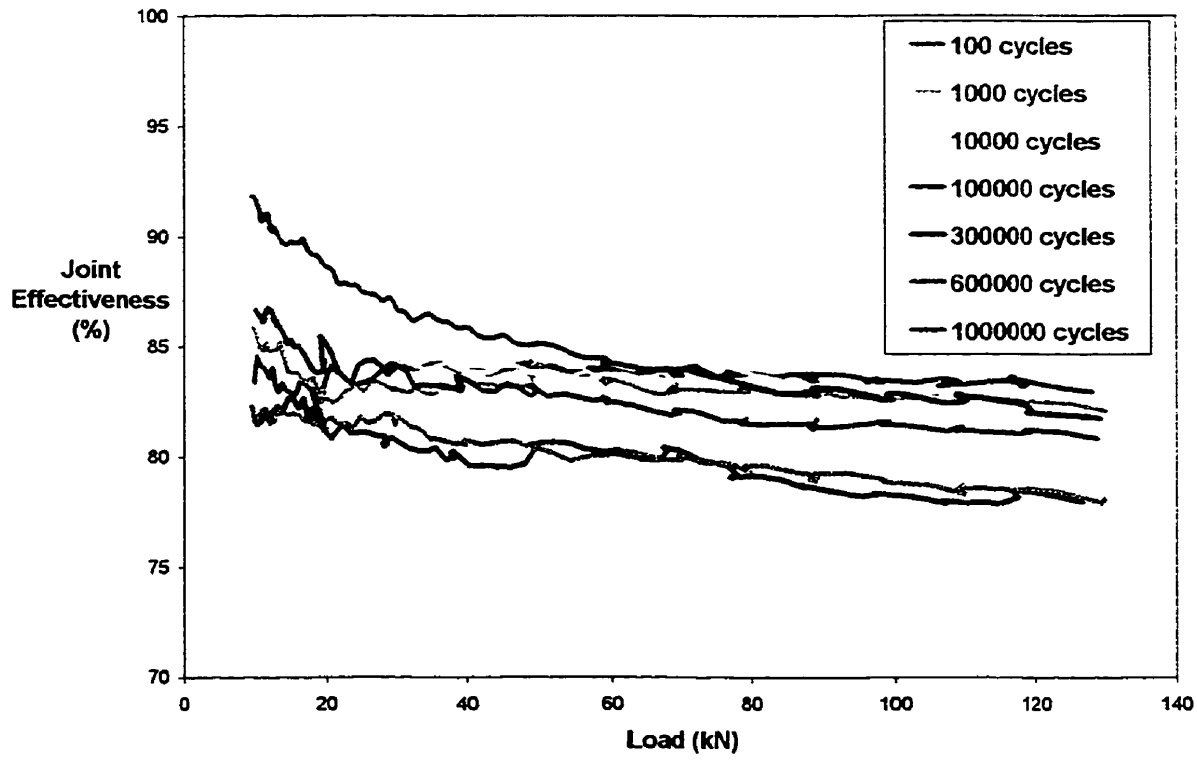

Figure 5-11: Joint effectiveness of FiberDowel slab under cyclic loading: Phase III

The joint effectiveness values for the FiberDowel slab are plotted against the number of cycles experienced in Figure 5-12. The initial test data is included to illustrate the dramatic decline in the joint effectiveness. After the initial reduction, the joint effectiveness remains steady up until three hundred thousand cycle mark where it again experiences a drop. At one million cycles the joint effectiveness rises, as it did the steel slab. All three load levels plotted along Figure 5-12 follow each other closely and provide a gauge in which the effectiveness can be compared.

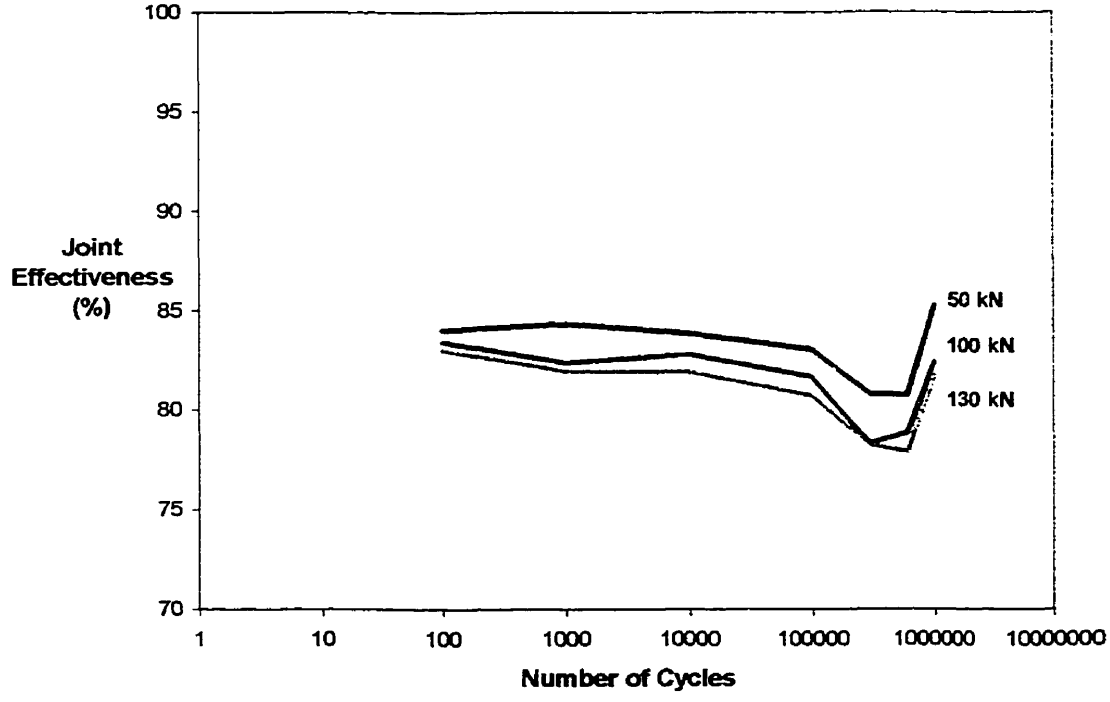

Figure 5-12: FiberDowel slab joint effectiveness vs. log number of cycles

The joint effectiveness of the Glasform doweled slab over the one million cycles of loading is shown in Figure 5-13. One set of data was omitted from the analysis of the Glasform slab analysis because its behaviour was erratic. The remaining data provided good correlation and allows for accurate comparisons. All joint effectiveness were found

to be above the 95 percent level. All the plotted curves show that the Glasform dowels provide a stable joint effectiveness.

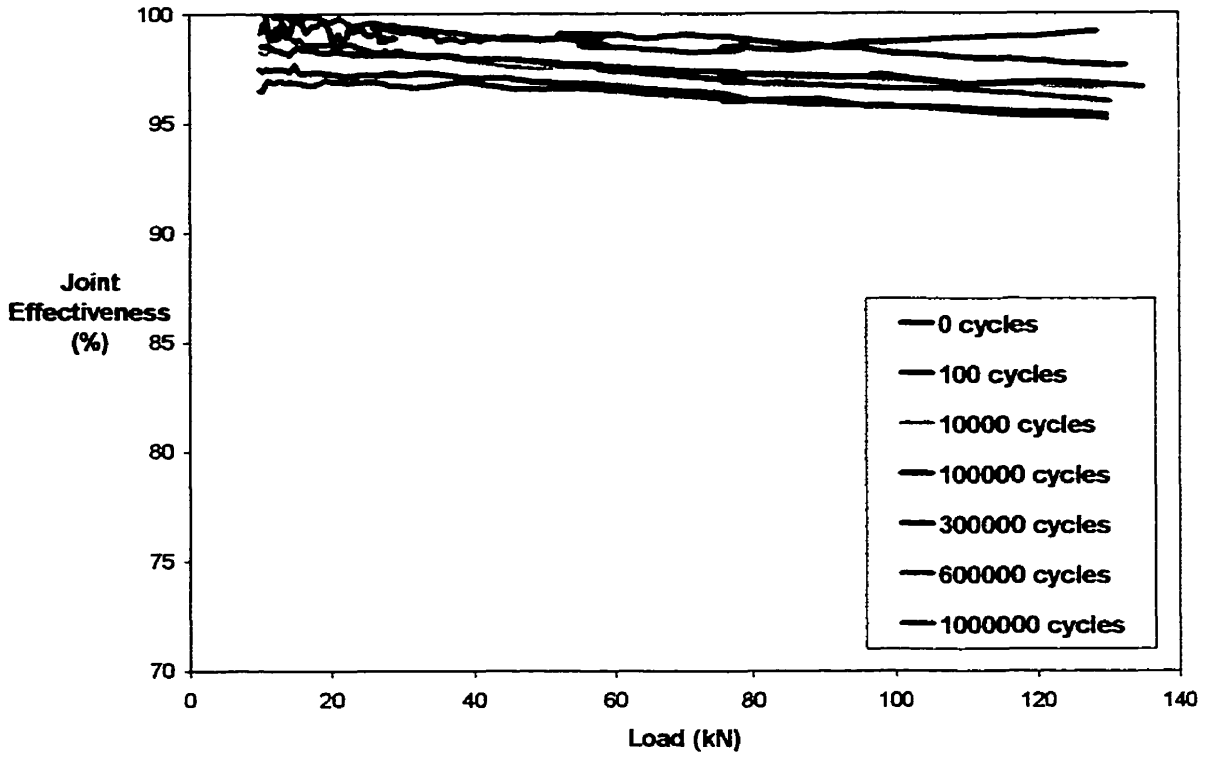

Figure 5-13: Joint effectiveness of Glasform dowel slab under cyclic loading : Phase III

The behaviour of the Glasform slab over the one million cycles is illustrated in Figure 5-14. Again, the behaviour of the slab is stable. The relation between the load levels is very interesting compared to the previous slabs. The difference between the load levels is very small, in the order of one percent where the other slabs were closer to two to three percent. No large increase in joint effectiveness was experienced at one million cycles for this slab as was for the other two dowel types.

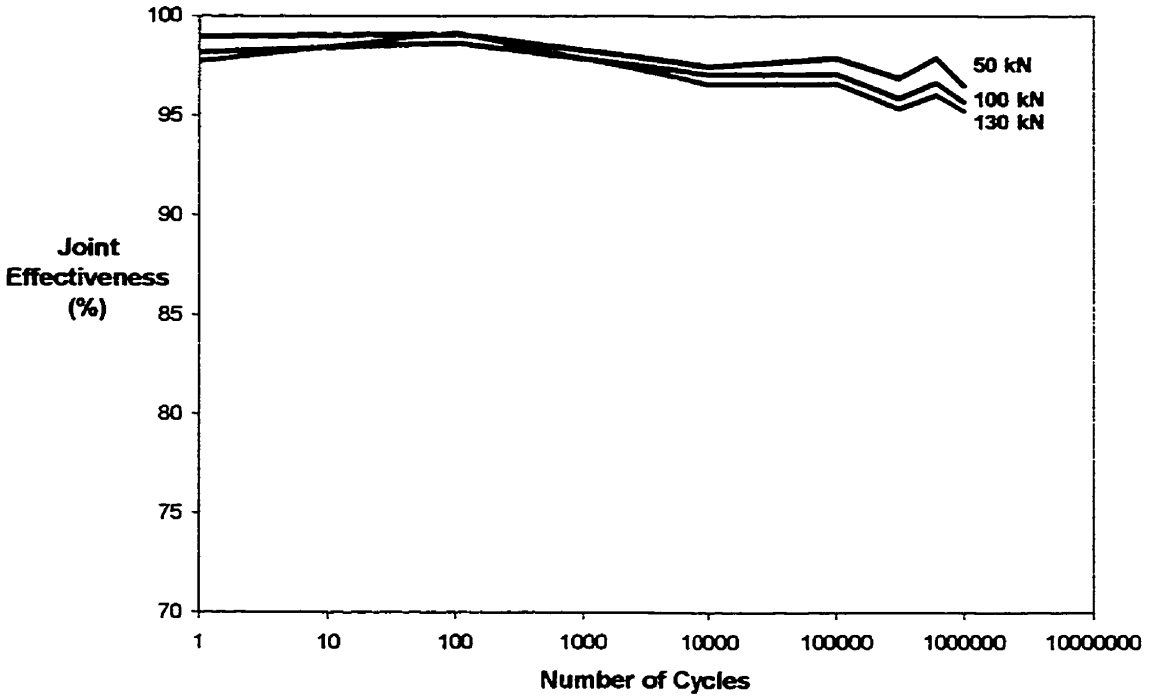

Figure 5-14: Glasform slab joint effectiveness vs. log number of cycles

In order to compare the slabs to one another, the test data must be joined together in representative graphs. The combination of the ranges of joint effectiveness of all the materials is shown in Figure 5-15. This illustration clearly shows the difference in the behaviour between the materials. Glasform comes out on top, followed by steel and finishing with the FiberDowel. A slightly different comparison with the same result is made when plotting the joint effectiveness versus the log scale of the number of cycles as shown in Figure 5-16.

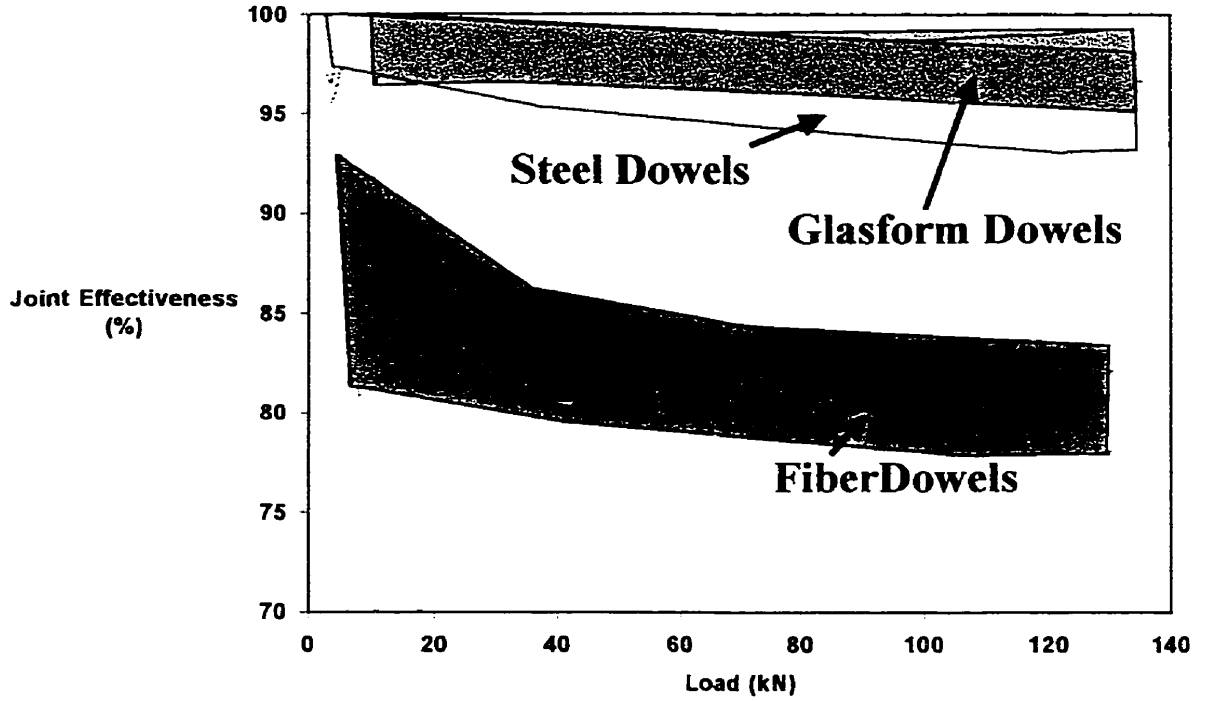

Figure 5-15: Joint effectiveness range vs. load for all materials in Phase III

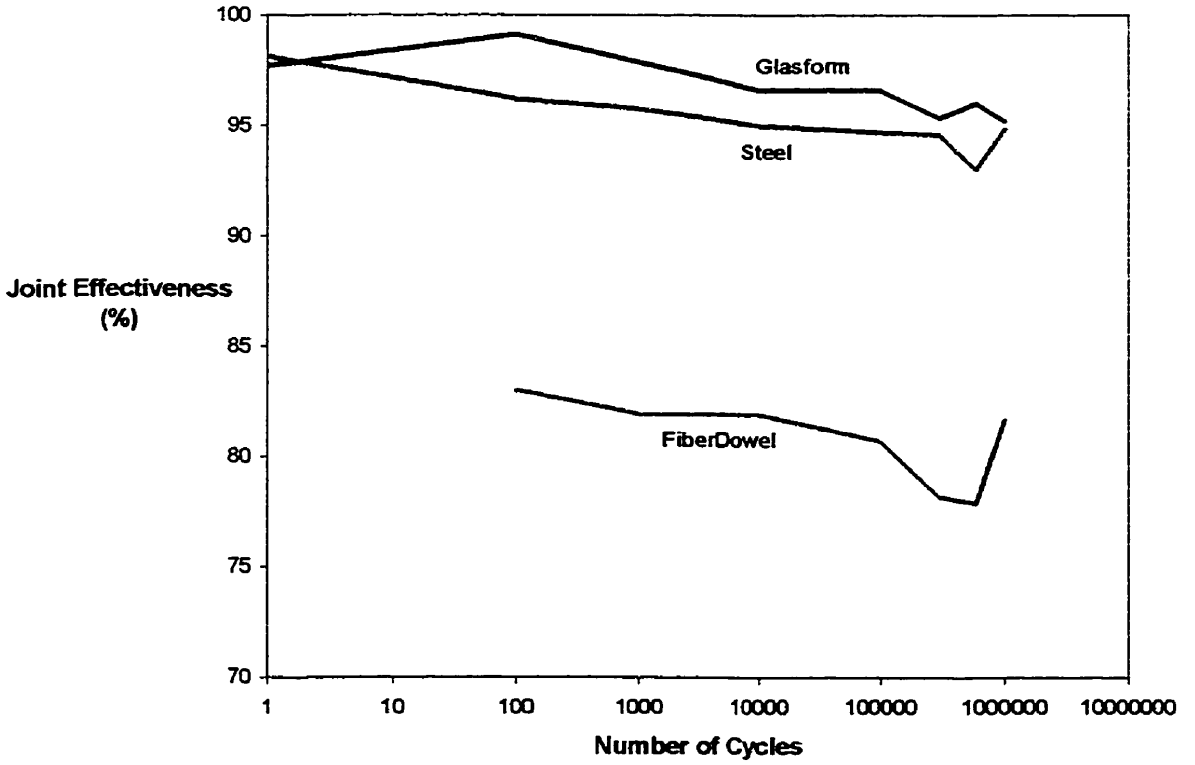

Figure 5-16: Joint effectiveness at service load vs. log number of cycles for all three dowel types in Phase III

5.4 Observed Failure Modes

There were four distinct failure modes observed during the testing program consisting of: excessive displacement, concrete crushing, extensive concrete cracking, and dowel failure. Each failure mode did not occur alone but in combination with the others.

During Phase I, the initial failure was due to the crushing of the concrete at the joint following the closing of the 3 mm gap. Subsequent failure of the concrete under the loading area defined further failure of the specimen. Since the subgrade supporting the slabs in Phase I is considered very weak, the excessive vertical displacements are the ultimate failure criterion for Phase I.

Phase II testing experienced three of the four failure modes. All six slabs experienced the initial concrete crushing following the closing of the joint. With the joint closed and each side of the joint bearing against each other, the dowel became the fulcrum point. This induced tensile stresses under the loaded area causing extensive cracking under this region. Two slabs experienced cracking on the unloaded side of the slab as well as the loaded but they occurred at higher load levels than those causing cracks on the loaded side. Also during this phase, two dowels experienced shearing failure. Both slabs containing the FiberDowels experienced shear failure of one of the dowels and extreme stress of the other. The load level at which failure took place was at five times the expected service load and compares to the tested shearing values.

The set of slabs in Phase III were tested under service load only and were not expected to encounter any of the failure modes. Only hair line cracks were observed and all slabs remained intact after testing up to one million cycles.

Chapter 6 Field Application

6.1 General

The pilot application of GFRP dowels in Canada is located in a test section along the newly constructed extension of Bishop Grandin Boulevard west of Waverley Street, Winnipeg, Manitoba. Three types of Glass FRP dowels were used. The first is manufactured by Glasform Inc. in San Jose, California; the second is FiberDowels produced by RJD Industries in Laguna Hills, California; and the third is produced by Creative Pultrusions, Inc., in Alum Bank, Pennsylvania.

Standard epoxy-coated steel dowel assemblies were used in the joints along the Bishop Grandin Boulevard. A straight test section on the eastbound lane contains the GFRP dowels. The location of the dowels is shown in Figure 6-1. Each set of GFRP dowels was separated by a set of 10 steel doweled joints. A total of 780 - 38 mm (1.5 in) GFRP dowels were used, 260 from each manufacturer, along the boulevard. Each dowel was 457 mm (18 in) long and was spaced at the typical 305 mm (12 in) center to center. The joints are skewed with is 0.3 m (1 ft) in 1.83 m (6 ft) or 16°. Two sets of baskets, one 4.27 m (14 ft) long and one 3.66 m (12 ft) long make up the total width of the pavement, provided a total of 26 dowels per joint.

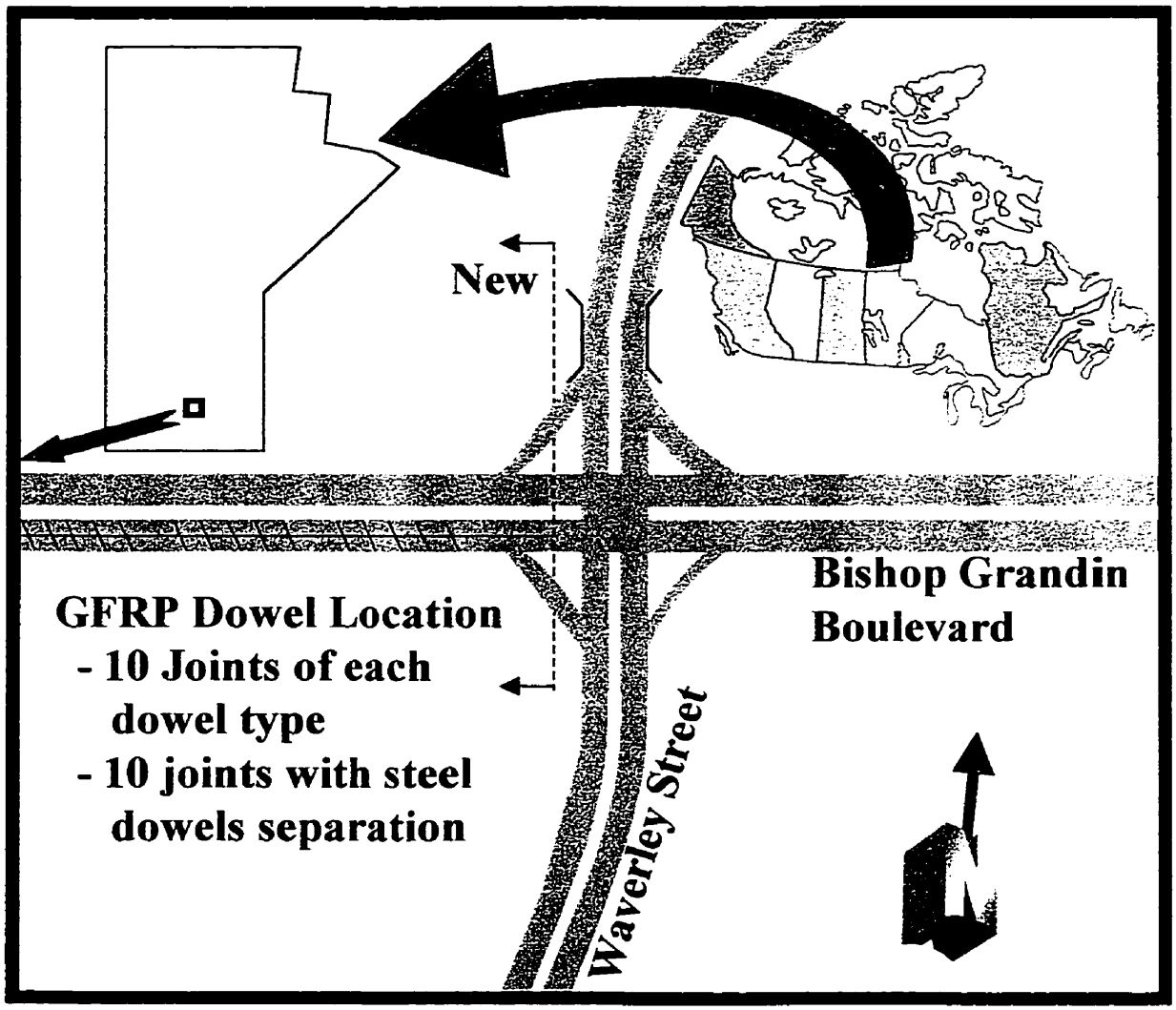

Figure 6-1: Field application location

6.2 Site Handling

Since this was the first use of these new dowels in the field, there were bound to be some adjustments to be made by the workers for proper handling. Due to the time constraints, the special baskets normally used for these materials were not used, the dowels were supported instead by the conventional basket approach. A local steel manufacturer supplied baskets for the GFRP dowels used in this project. Before the baskets were placed, the dowel ends were coated with asphalt to protect the glass fibers

from direct contact with the concrete. For assembling the dowels in the baskets, the dowels were slid in the open side and rested against finger pins as shown in Figure 6-2.

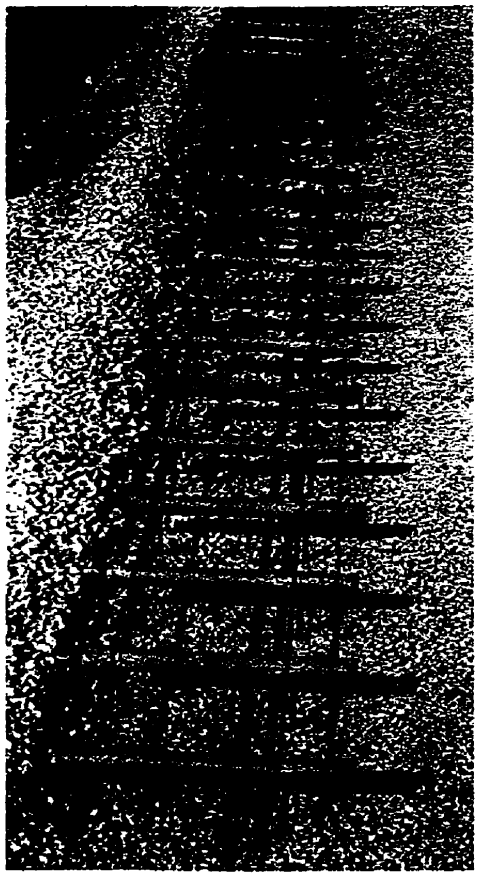

Figure 6-2: GFRP dowels in steel basket assemblies before placement of concrete

The baskets supported the dowels at midheight of the 225 mm (9 in) slab and were held in place by standard pins driven into the base material as shown in Figure 6-3. Because the dowels were not welded to the baskets, as the case for the steel dowels, the dowels tended to move during casting of the concrete. The finger pins were placed against the direction of casting to maintain the proper positioning of the dowels during casting, as shown Figure 6-4.

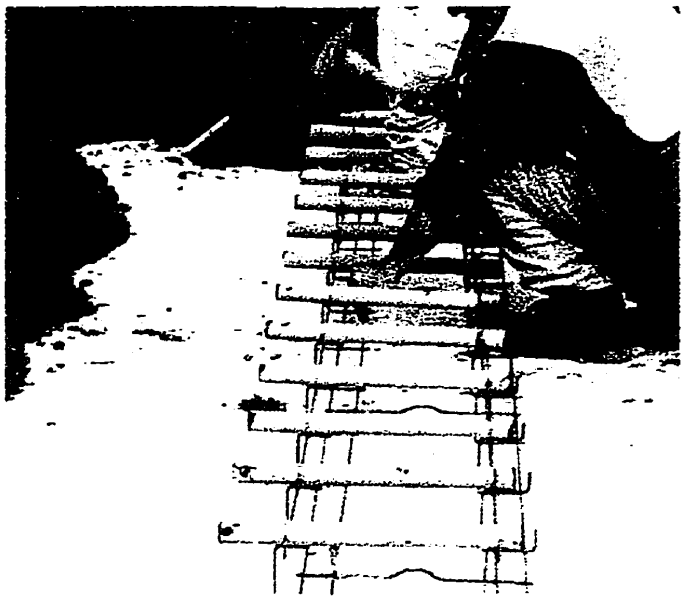

Figure 6-3: GFRP dowel assembly being nailed into place

Figure 6-4: Casting a Concrete pavement with GFRP dowels in steel baskets

6.3 Monitoring Performance

This field application provides excellent opportunity to monitor the long-term behaviour of GFRP dowels subjected to environmental and loading conditions. Monitoring of these GFRP dowels in comparison to steel dowels will provide unique information on the future use of these corrosion free dowels.

Initial monitoring will consist of visual inspections along the joints of the test section. Following casting, the test section joints were cut and it was observed that from the cut joints the concrete experienced local cracking to the base material as shown in

Figure 2-1. This cracking is expected and is a result of thermal expansion and contraction. Continuing visual inspections will be conducted approximately every six months.

More intensive monitoring involving actual testing on the joints will provide useful information. The Manitoba department of Highways and Transportation and the City of Winnipeg Transportation Department have access to Falling Weight Deflectometers that will be used along Bishop Grandin Boulevard to measure joint effectiveness and the long term service performance of the GFRP dowels.

Chapter 7 Summary and Conclusions

7.1 Summary

The objective of this research was to investigate the behaviour of FRP dowels for transverse construction joints under the effect of typical traffic loading. This was achieved through testing in three distinct phases. Phase I consisted of model slabs being monotonically tested upon a weak subgrade constructed of an array of springs. The three slabs tested in Phase I each contained two dowels of either epoxy-coated steel, FiberDowels, or Glasform dowels. Phase II consisted of two sets of model slabs being monotonically tested upon a stiff subgrade of compacted 'A-base' limestone. Six slabs were tested in Phase II, each slab containing the same number and materials of dowels as in Phase I. Phase III consisted of model slabs being cyclically loaded upon a stiff subgrade, with static tests being conducted periodically. Each slab was carried to one million cycles of maximum service load.

Material testing of the dowels consisting of direct double shear tests was conducted at an early stage of the investigation. It was found that the shear resistance of the steel dowels was approximately four times that of the Glasform dowels and over five times that of the FiberDowels. It should be mentioned again that the GFRP dowels were 38.1 mm (1.5 in) in diameter compared to the 25.4 mm (1 in) steel dowels.

The emphasis of this research was directed towards the behaviour of the joint deflection under load. The deflections provided a measure of joint effectiveness and allowed for comparison of the joint effectiveness between the materials used in the three phases.

7.2 Conclusions

This investigation of the behaviour of GFRP dowels has shown that GFRP dowels can be used in place of the standard steel dowels. Not only do the GFRP dowels transfer sufficient load to an adjacent slab, but do so over the service life of a highway pavement.

Three materials were tested within this investigation. The top performing material was the Glasform dowels followed by the epoxy-coated steel dowels, and finally the FiberDowel product. All doweled joints performed above the 75 percent joint effectiveness acceptance level while the Glasform consistently performed above 90 percent .

The diameter of the GFRP dowels was 38 mm (1.5 in) compared to 32 mm (1.25 in) for the standard epoxy coated steel dowels. The larger diameter provided two advantages, higher shear stiffness of the dowel and lower bearing stresses on the concrete. These features are the reason for the improved performance of the GFRP dowels despite their low shear strength.

The use of deicing salts creates a harsh corrosive environment which deteriorates steel dowels. Epoxy coated dowels are relatively protected, however, dents and cracks in the epoxy layer provide entry points for corrosion. GFRPs are a corrosion resistant material which will require no maintenance during the life span of the pavement. With continued support from the City of Winnipeg and the Department of Highways and Transportation, full utilization of corrosion resistant load transfer mechanisms could soon be standard practice in the pavement construction industry.

7.3 Recommendations

The future use of GFRP dowels for load transfer devices is dependent on the continued study of their behaviour in highway pavements. A long term study has been initiated with this investigation and it is this author's wish that continuing inspections and evaluations are to be conducted on the Bishop Grandin site over the next five to ten years.

One of the materials used in the site application at Bishop Grandin Boulevard was not involved in the extensive testing of this investigation. Creative Pultrusion dowels were utilized for the site application but the were not available at the time of the other tests. There are many other GFRP Dowel producers in the marketplace, some of which produce the dowels as a by-product of the pultrusion processes. Each manufacturer will produce a slightly different product depending upon the fiber content or type of matrix. Further laboratory testing of the Creative Pultrusion dowels as well as other manufacturers' dowels is warranted.

Cooperation with a manufacturer of dowels to develop a product that has a higher resistance to the shearing force could improve the load transfer effectiveness. An attempt at increasing the shearing strength is to twist the fibers during the pultrusion process. This would activate the tensile strength of the fibers during the shearing action, possibly providing a higher shearing strength.

Chapter 8 References

1. Selvadurai, A.P.S., "Elastic Analysis of Soil-Foundation Interaction" in Developments in Geotechnical Engineering, Elsevier Scientific Publishing Company, Vol. 17, p. 1-29, 407- 425, Amsterdam, 1979.

2. Winterkorn, Hans F., and Fang, Hsai-Yang, "Foundation Engineering Handbook," Van Nostrand Reinhold Company, New York, p. 111-114, 132-135, 142-143, 244-249, 516-519, Year Unknown.

3. AASHTO, American Association of State Highway and Transportation Officials, Guide for Design of Pavement Structures, p. I-21 - I-22, II-12 - I-13, II-25 - II-28, II-37 - II-62, 1993.

4. Brown, V. L., and Bartholomew, C. L., "FRP Dowel Bars in Reinforced Concrete Pavements", Widener University in Chester, Pa , SP 138-48, p. 813-829, Year Unknown.

5. Friberg, Bengt F., "Design of Dowels in Transverse Joints of Concrete Pavements", from Proceedings of the ASCE, Vol. 64, pt. 2, p. 1809-1828, 1938.

6. Ioannides, Anastasios M., and Korovesis, George T., "Analysis and Design of Doweled Slab-on-Grade Pavement Systems", Journal of Transportation Engineering, Vol. 118, No. 6, p. 745-768, November/ December, 1992.

7. Marcus, Henri, "Load Carrying Capacity of Dowels at Transverse Pavement Joints", Proceedings of American Concrete Institute, Vol. 48, p. 169-184, 1952, and Journal of the American Concrete Institute, Vol. 23, Oct 1951.

8. Hofbeck, J. A., Ibrahim, I. O., and Mattock, Alan H., "Shear Transfer in Reinforced Concrete", from the American Concrete Institute Journal, p. 119-128, February 1969.

9. Park, R., and Paulay, T., "Reinforced Concrete Structures", p. 321-345, John Wiley and Sons Inc., New York, New York, 1975.

10. Taylor, D. A., Mailvaganam, N. P., Rahman, A. H., Guenter, D., and M. S. Cheung, "Evaluation of Fibre-Reinforced Plastic Reinforcing Bars for Structural Application in Concrete", Proceedings of the 1994 CSCE Annual Conference, Winnipeg, Manitoba, Vol. 2, pp. 573-582, June 1-4, 1994.

11. Porter, Max, Hughes, B. W., Barnes, B. A., and Viswanath, K. P., "Non-Corrosive Tie Reinforcing and Dowel Bars for Highway Pavement Slabs", Report to the Highway Division of the Iowa Department of Transportation and Iowa Highway Research Board, 1993.

12. ACPA, American Concrete Pavement Association, "Design and Construction of Joints for Concrete Streets," Concrete Information, Portland Cement Association, 1992.

13. ACPA, American Concrete Pavement Association, and PCA, Portland Cement Association, "Design and Construction Joints for Concrete Highways",(ISO60-01P), Concrete Paving Technology, Portland Cement Association,, Stokie, Illinois, 1991.

14. Dulacska, Helen, "Dowel Action of Reinforcement Crossing Cracks in Concrete", American Concrete Institute Journal, December 1972, Vol. 69, No. 12, p. 754-757.

15. Paulay, T., Park, R., and Phillips, M. H., "Horizontal Construction Joints in Cast-in-Place Reinforced Concrete", Shear in Reinforced Concrete, Vol. 2, p. 599-616, American Concrete Institute Special Publication Sp.42, Detroit Michigan, 1974.

16. Dei Poli, S., Di Prisco, M., and Gambarova, P. G., "Shear Response, Deformations, and Subgrade Stiffness of a Dowel Bar Embedded in Concrete", American Concrete Institute Structural Journal, 89-S63 1992, p. 665-675.

17. Soroushian, Parviz, Obaseki, Kienuwa, Rojas, Maximo C. and Sim, Jongsung, "Analysis of Dowel Bars Acting Against Concrete Core", American Concrete Institute Structural Journal, 1986, p. 642-649.

18. Timoshenko, S., and Lessells, J. M., "Applied Elasticity: Chapter VI - Bending of Bars on Elastic foundation," Westinghouse Night School Press, East Pittsburgh, PA, 1925.

19. Hsu, Thomas T. C., Mau, S. T., and Chen, Bin, "Theory of Shear Transfer Strength of Reinforced Concrete", from American Concrete Institute Structural Journal, 84-S16, 1987, p. 149-159.

20. Walraven, Joost C., "Fundamental Analysis of Aggregate Interlock," Journal of Structural Division, Proceedings of the American Society of Civil Engineers, Vol. 107, No. ST11, November, 1981.

21. Birkeland, Philip W., and Birkeland, Halvard W., "Connections in Precast Concrete Construction", Journal of the American Concrete Institute: Proceedings, Vol. 63, No. 3, 1966, p. 345-367.

22. Terzaghi, Karl. "Evaluation of Coefficients of Subgrade Reaction", Geotechnique, Volume V, p. 297-325, 1955.

23. Grieef, S. L., "GFRP Dowel Bars for concrete Pavement", Masters Thesis at the University of Manitoba, 1996.

24. Lay, M. G., "Handbook of Road Technology (Volume 1): Planning and Pavements", Gordon and Breach Science Publishers, 1986.

25. Yoder, E. J. and Witczak, M. W., " Principles of Pavement Design: Second Edition", John Wiley & Sons Inc., 1975.

26. Oglesby, C. H., and Hicks, R. G., "Highway Engineering: Fourth Edition", John Wiley & Sons, Inc., 1982.

27. Nilson, A. H., and Winter, G., " Design of Concrete Structures: Eleventh Edition", McGraw-Hill, Inc., 1991.

28. Huang, Yang H., "Pavement Analysis and Design", Prentice Hall, Englewood Cliffs, New Jersey, 1993.

29. Hilderman, S., Department of Highways and Transportation of Manitoba, personal correspondence, 1997.

30. Ambroz, J., Seiler, W. J., and Darter, M. I., ERES Consultants Incorporated, "A State of the Art Report: Load Transfer Design and Benefits for Portland Cement Concrete Pavements", Report #96-128-E1, 1998.

Appendix A. Soil Tests for Phase 2

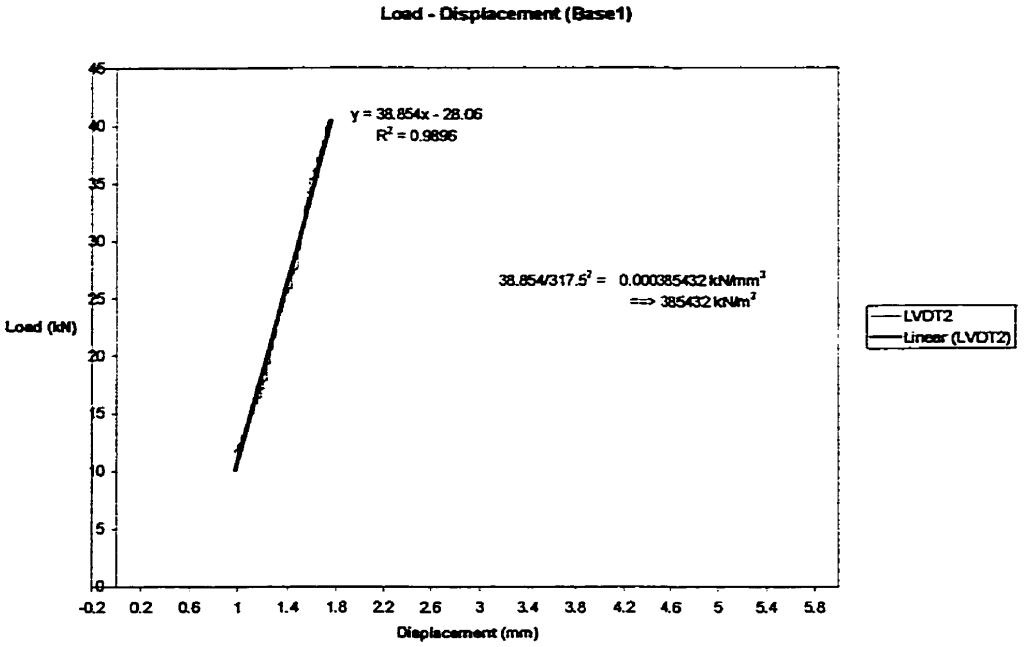

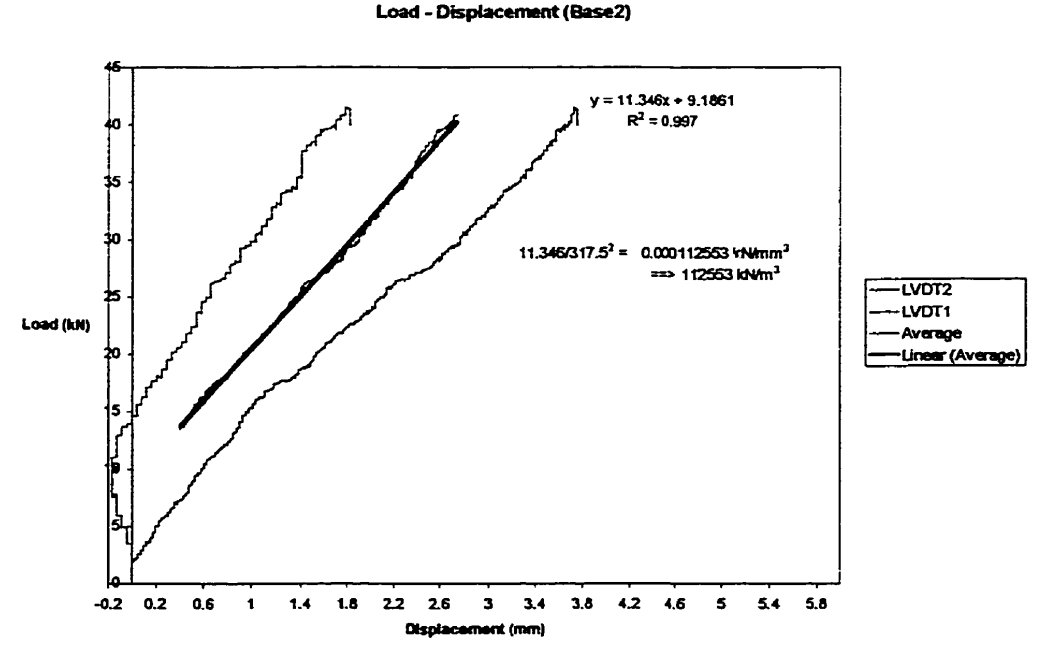

Load - Displacement (Base3a)

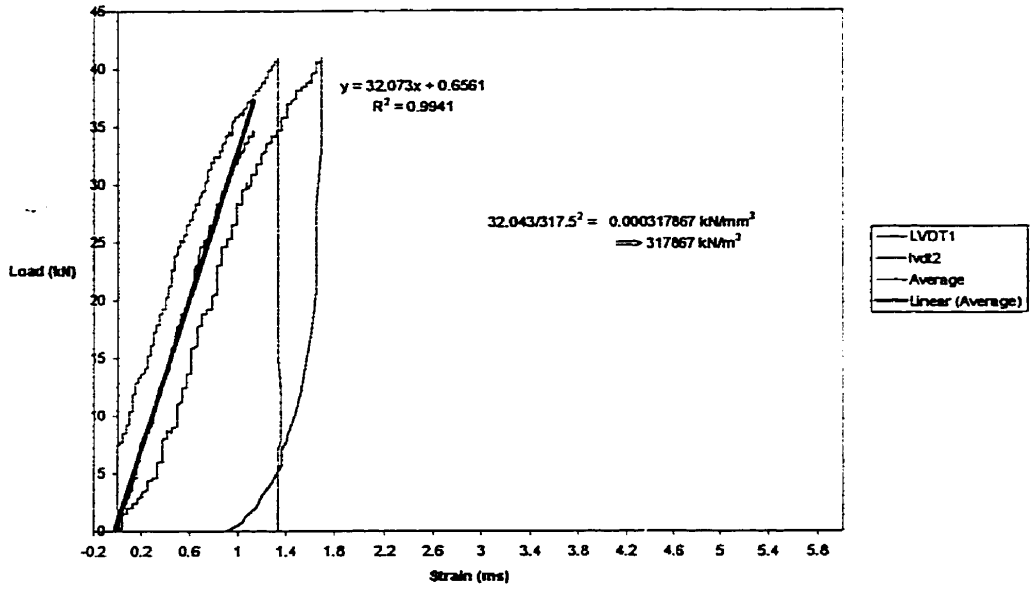

Load - Displacement (Base3b)

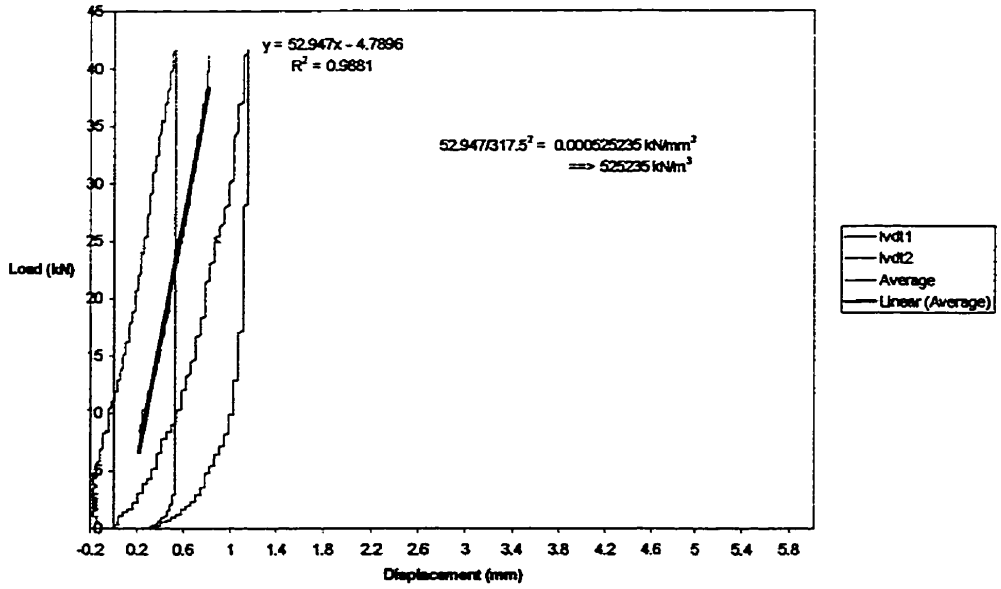

Base Test Between Steel and FiberDowel Tests

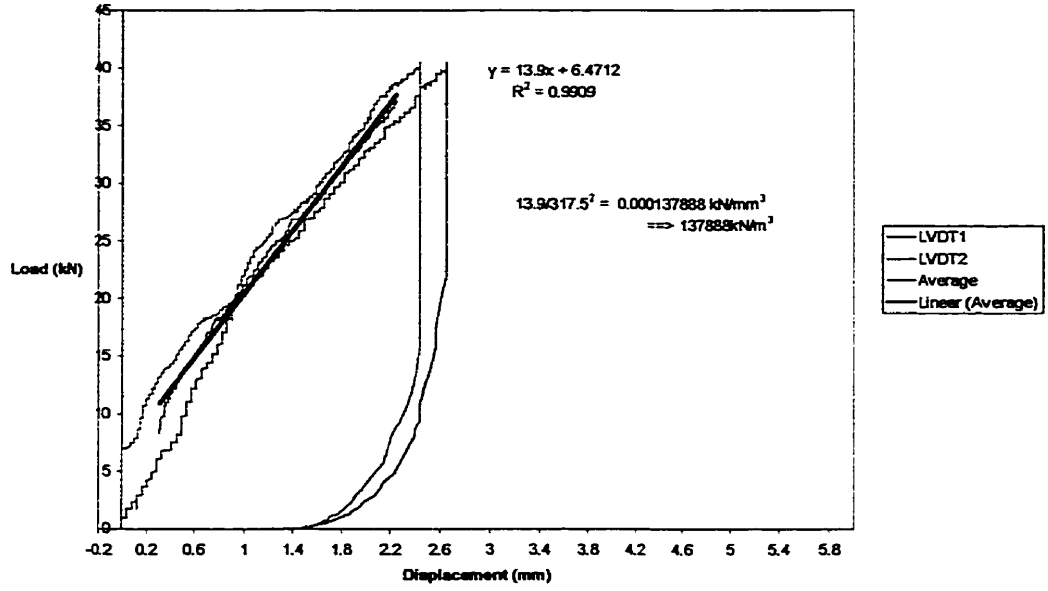

Base Test Between FiberDowel and Glassform Tests

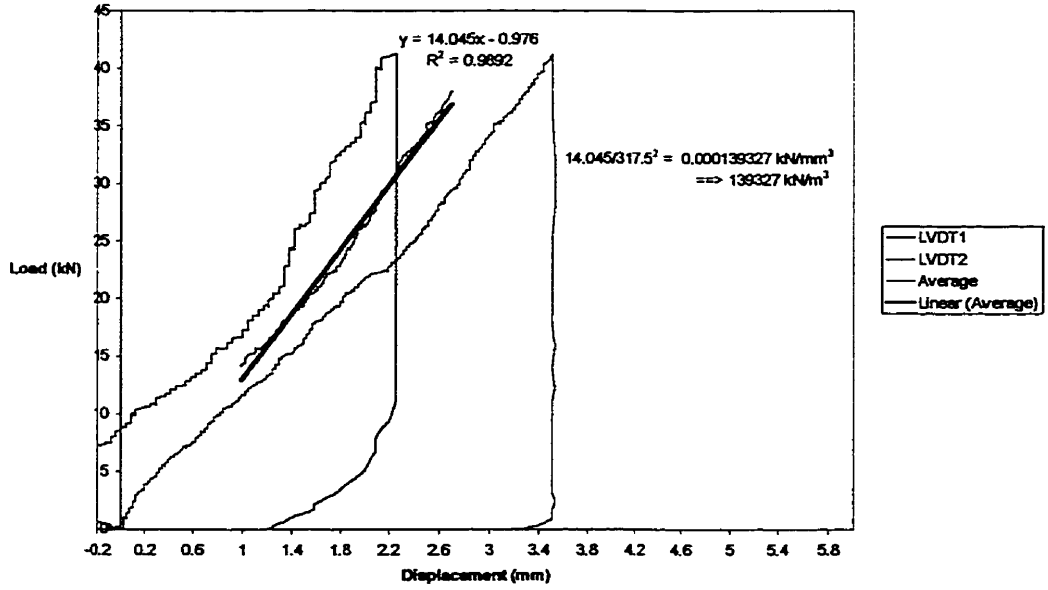

Load vs Deflection of Base Following Glassform Slab Test